

**UNIVERSITÉ DU QUÉBEC À CHICOUTIMI**

**MÉMOIRE PRÉSENTÉ À L'UNIVERSITÉ DU QUÉBEC À  
CHICOUTIMI COMME EXIGENCE PARTIELLE DE LA MAITRISE  
EN SCIENCES DE LA TERRE**

**PAR  
PATRICIA L. CORCORAN**

**IMPLICATIONS OF AN ARCHEAN STRIKE-SLIP BASIN: THE  
CLASTIC BEAULIEU RAPIDS FORMATION, NORTHWEST  
TERRITORIES, CANADA**

**NOVEMBRE, 1996**



### Mise en garde/Advice

Afin de rendre accessible au plus grand nombre le résultat des travaux de recherche menés par ses étudiants gradués et dans l'esprit des règles qui régissent le dépôt et la diffusion des mémoires et thèses produits dans cette Institution, **l'Université du Québec à Chicoutimi (UQAC)** est fière de rendre accessible une version complète et gratuite de cette œuvre.

Motivated by a desire to make the results of its graduate students' research accessible to all, and in accordance with the rules governing the acceptance and diffusion of dissertations and theses in this Institution, the **Université du Québec à Chicoutimi (UQAC)** is proud to make a complete version of this work available at no cost to the reader.

L'auteur conserve néanmoins la propriété du droit d'auteur qui protège ce mémoire ou cette thèse. Ni le mémoire ou la thèse ni des extraits substantiels de ceux-ci ne peuvent être imprimés ou autrement reproduits sans son autorisation.

The author retains ownership of the copyright of this dissertation or thesis. Neither the dissertation or thesis, nor substantial extracts from it, may be printed or otherwise reproduced without the author's permission.

## RÉSUMÉ

La formation de Beaulieu Rapids est une séquence sédimentaire de 0,2 à 1 km d'épaisseur située au centre-sud de la Province structurale de l'Esclave. La formation représente un bassin en décrochement archéen qui s'est développé le long d'une faille majeure de direction NS. Des petits plutons de porphyres quartzo-feldspathiques à hornblende sont localisés le long de la zone de faille. Des datations U-Pb sur zircons donnent un âge approximatif de 2.6 Ga pour ces plutons. La présence de fragments de porphyres dans les conglomérats indique que la formation de Beaulieu Rapids doit conséquemment être plus jeune que cet âge. La marge ouest du bassin est caractérisée par une discordance que sépare la ceinture volcanique de Rivière Beaulieu de la succession sédimentaire. Des failles NE tardives sont présentes sur les bordures nord et sud du bassin.

Structuralement, la formation est caractérisée par une foliation pénétrative NNE et par des plis en échelons dont l'orientation dominante est aussi NNE. Les plis se présentent sous la forme d'une alternance d'anticlinaux et de synclinaux localisés majoritairement dans la partie nord du bassin. Dans ce secteur, la direction de la polarité change rapidement alors que dans la partie sud du bassin les lits sont de direction nord avec une polarité généralement vers l'est. Quelques lits sont renversés mais les lits normaux sont plus communs.

Les roches sédimentaires du bassin de Beaulieu Rapids montrent deux cycles positifs qui indiquent un contrôle tectonique sur la sédimentation. Le premier cycle est représenté par l'association de faciès du conglomérat I (CFA-I: *Conglomerate facies association I*) et le faciès de siltstone-grès sus-jacent (SSFA: *Siltstone-sandstone facies association*). L'association de faciès du conglomérat II (CFA-II: *Conglomerate facies association II*) et l'association de faciès de grès riche en quartz (QSFA: *Quartz-rich sandstone facies association*) qui se trouve juste au-dessus forment ensemble le second cycle de dépôt. Le CFA-I regroupe un conglomérat à cailloux et galets massif à stratifié et un conglomérat à support de matrice. Le premier est caractérisé par des conglomérats massifs à faiblement stratifiés (faciès Gm) et à lits entrecroisés en forme de fosse (Gt) à support de fragments, des conglomérats massifs à support de matrice (Gms), une unité mineure de grès à stratifications horizontales (faciès Sh) et entrecroisées (faciès St, Sp) et une argilite (F1). Localement, les galets deviennent imbriqués et montrent une composante d'écoulement NE prononcée. Le conglomérat massif à stratifié à cailloux et galets se compose des faciès Gm, Gt, Gp, St, Sh et Sp. Le CFA-I a été déposé par coulées de débris (Gms), courants de traction (Gm-Gt-St-Sp-Sh) et coulées en feuillets respectivement sur les portions proximale, médiale et distale du cône alluvionnaire. L'association de faciès du siltstone-grès contient une sous-unité dominée par des grès et caractérisée par les faciès Sp, St, Sh et F1 qui se sont formés en raison de la migration des dunes et dépôts de levée dans un environnement de plaine sableuse avec des étangs locaux. Trente-six mesures de lits entrecroisés en forme de fosse provenant de la partie sud de la région ont été prises pour l'analyse de paléocourants. Ces mesures indiquent que l'écoulement, de façon générale, a été unimodal et parallèle au bassin. Une sous-unité dominée par le siltstone contient des exemples bien préservés de rides de vagues asymétriques (F1), de lits granoclassés et de structures d'échappement d'eau. Ces structures sédimentaires se sont développées pendant une sédimentation de sable dans un environnement lacustre. Le soulèvement résultant d'une reprise de l'activité tectonique est responsable du CFA-II qui comprend les faciès Gm, Gt, St et Sh. Cette unité faciès est interprétée comme s'étant formée en bancs longitudinaux pendant l'activité de traction de fond avec la migration prononcée des dunes dans un environnement proximal de rivières tressées. Les structures sédimentaires du faciès d'association de grès riches en quartz

(QSFA) le plus élevé dans la séquence incluent les faciès St, Sh, Sp et F1 en plus des surfaces d'érosion (Ss) et des lits de cailloux (Gm). Ces caractéristiques suggèrent une migration des dunes prononcée, un dépôt mineur de lamines de boue et un remplissage des surfaces chenalisées dans un environnement de rivières tressées à gradient faible mais à haute énergie. Trente-trois mesures de lits entrecroisés en auge pour l'analyse de paléocourant montrent que l'écoulement était unimodal vers le Nord et donc parallèle au bassin.

Le comptage de points de grès effectués sur les associations SSFA et QSFA révèle que le quartz est le minéral terrigène dominant, représentant 73% des composants. Le plagioclase et le feldspath potassique combinés et les fragments lithiques représentent respectivement 14% et 13%. Le quartz est majoritairement polycristallin, ce qui signifie que le roche source était proximale au bassin sédimentaire puisque le quartz polycristallin est diminué plus rapidement que les autres variétés. De plus, les grès ne sont pas d'origine multicyclique car le quartz monocristallin devient dominant avec les cycles sédimentaires successifs. Les roches plutoniques fournissent typiquement des proportions considérables de quartz polycristallin aux sédiments. Le plagioclase est beaucoup plus commun que le feldspath potassique et les fragments lithiques sont représentés de façon importante par des grains plutoniques et de façon mineure par des membres sédimentaires et volcaniques. Les grès de la formation de Beaulieu Rapids se retrouvent dans le champ d'orogénèse recyclée dans les diagrammes ternaires QmFLt et QFL, ce qui est typique des bassins tardifs. La prédominance des fragments lithiques sur le diagramme QmFLt résulte de la catégorisation du quartz polycristallin en tant que fragment de roche. Un influx rapide et élevé de sédiments dû au tectonisme, un taux de sédimentation élevé causant un enfouissement rapide ainsi qu'une distance de transport limitée sont les facteurs responsables du haut pourcentage de fragments lithiques dans les grès. Le quartz polycristallin est regroupé avec le quartz monocristallin dans le pourcentage total de quartz (Q) sur le diagramme QFL ce qui résulte en un pourcentage faible des fragments lithiques. Ceci suggère que la formation a été déposée dans des conditions climatiques humides parce que les minéraux labiles dans Lv et Ls sont soustraits préférentiellement par l'érosion dans les climats humides contrairement aux climats arides.

Le comptage de fragments des CFA-I et CFA-II présentent des résultats similaires à ceux obtenus à partir du procédé de comptage de point. Les fragments plutoniques et volcaniques mafiques dominent avec 38% et 42.5% respectivement alors que les volcaniques felsiques (<11%), le quartz (<8%) et les fragments sédimentaires (<0,5%) sont des composants mineurs. La région source des roches sédimentaires de la formation de Beaulieu Rapids regroupe le Complexe Gneisso-Plutonique de Sleepy Dragon, les roches volcaniques de Rivière Beaulieu, les plutons de porphyre en marge du bassin et la succession sédimentaire elle-même. La présence de fragments de roches sédimentaires dans le faciès d'association du cycle II implique le cannibalisme des sédiments du cycle I lors de la reprise de l'activité tectonique. Le bassin de Beaulieu Rapids est comparable aux bassins de décrochement modernes qui se forment le long des zones de faille majeures en terme de géométrie du bassin, des contacts de faille et de discordance, des unités lithologiques et enfin, de la succession et de l'organisation des faciès sédimentaires. Des exemples modernes de bassin de décrochement sont: (1) le bassin Hanmer, faille de Hope, Nouvelle-Zélande, (2) le Hazard Lake, faille d'East Anatolian, Turquie, (3) le bassin Ridge, faille de San Andreas, États-Unis, (4) le bassin Nadi, faille de Sovi, Fiji, (5) le bassin Kuji, faille de Taro, Japon et (6) le bassin Little Sulfur Creek, faille de Maacama, États-Unis.

La faille majeure (>300 km de long) le long de laquelle le bassin de décrochement de Beaulieu Rapids s'est développé est aussi caractérisée par une autre séquence sédimentaire qui démontre des caractéristiques lithologiques et structurales semblables. La formation de Keskarrah, située approximativement 300 km au nord de la formation de Beaulieu Rapids a récemment été interprétée comme représentant un bassin en décrochement. Plusieurs autres successions sédimentaires localisées le long du linéament NS incluent les formations de Jackson Lake (<2605Ma), le Conglomérat Kaycee (<2600Ma) et le Conglomérat James Falls (<2600Ma). Ces bassins contemporains tardi-orogéniques sont indicatifs d'un mouvement de plaque horizontal attribué parfois à des processus reliés à la subduction. Des bassins de molasse de cette nature se développent habituellement pendant la dernière phase d'accrétion des terranes et peuvent ainsi représenter des mouvements tardifs sur une zone de suture archéenne.

## TABLE DES MATIÈRES

	p.
RÉSUMÉ	ii
REMERCIEMENTS (ACKNOWLEDGMENTS)	v
TABLE DES MATIÈRES	vii
LISTE DES FIGURES (EN ANGLAIS)	vii
LISTE DES TABLEAUX (EN ANGLAIS)	xii
CHAPITRE I INTRODUCTION	1
1.1 La problématique	1
1.2 La présentation de la thèse	3
1.3 Localisation et géomorphologie	3
1.4 Travaux antérieurs	4
1.5 Étude actuelle	4
CHAPITRE II LE MANUSCRIT	6
Abstract	7
Introduction	9
Slave stratigraphy and setting	10
Problematic	10
Yellowknife volcanic belt	11
Local geology and characteristics	14
Basin geometry and structure	14
Sedimentology	16
Facies associations of the Beaulieu Rapids Formation	16
Conglomerate facies association-I (CFA-I)	16
Hydrodynamic processes of the CFA-I	18
Siltstone-sandstone facies association (SSFA)	19

Hydrodynamic processes of the SSFA	21
Conglomerate facies association-II (CFA-II)	23
Hydrodynamic processes of the CFA-II	24
Quartz-rich sandstone facies association (QSFA)	24
Hydrodynamic processes of the QSFA	25
Provenance	27
Sandstone petrography	27
Methods, constraints and characteristics	27
Results	29
Conglomerate composition	30
Methods and constraints	30
Results	30
Discussion	31
General basin characteristics	31
Basin architecture and depositional environment	33
Tectonic influence on sedimentation	36
Significance of source areas and climatic influence	36
Significance and modern counterparts	39
Conclusion	40
Acknowledgments	42
References cited	43
Tables and figures	57
CHAPITRE III CONCLUSION	83

## LISTE DES FIGURES

- |          |  |          |
|----------|--|----------|
| Figure 1 | Lithological map of the Slave Structural Province showing the location of the various late-stage sedimentary and volcano-sedimentary successions. The N-trending Beniah Lake fault can be traced intermittently for at least 300km along strike. Note that the Beaulieu Rapids (BRF) and Keskarrah (KF) Formations are located adjacent to this major structure. The Anialik River (ARB), High Lake (HLB), Hood River (HRB), Cameron River (CRB), and Beaulieu River (BRB) volcanic belts, the Jackson Lake Formation (JLF), and the Beniah Lake Quartz Arenite (BLQ) are referred to in the text. Modified from Padgham and Fyson (1992). | p.<br>63 |
| Figure 2 | Stratigraphy of the Yellowknife volcanic belt, Slave Structural Province (modified from Helmstaedt and Padgham, 1986; MacLachlan and Helmstaedt, 1995) and lateral pan-Slave correlations of the youngest formations. References for age dates: 1) Isachsen and others, 1991; Isachsen and Bowring, 1994, 2) Lambert and others, 1992, 3) van Breeman and others, 1994, 4) Villeneuve and others, 1993 and 5) Relf and others, 1994. BW, Burwash Formation; CL, Clan Lake felsic volcanic complex; CT, Contwoyto Formation; IN, Ingraham Formation; PL, Prosperous Lake Formation; W, Walsh Lake Formation.                                | 64       |
| Figure 3 | Location of the Beaulieu Rapids Formation (outlined) in the Beaulieu River volcanic belt (BRB) and its proximity to the 2800-2900Ma plutono-gneissic Sleepy Dragon complex (SDC). Note sinistral strike-slip fault on the eastern side of the SDC. CRB, Cameron River volcanic belt; TLR, Turnback Lake Rhyolite; BF, Burwash Formation; BLQ, Beniah Lake Quartz arenite. Modified from Lambert and others, 1992.  | 65       |



- Figure 4A      Structural elements of the Beaulieu Rapids Basin. Arrows indicate sinistral strike-slip motion. Western basin margin characterized by an unconformity and a N-trending fault truncates the formation on the east. A series of NNE-trending en echelon folds in the north are evident. Structural elements  $S_0$  (bedding),  $S_1$  and  $S_2$  in stereonet support strike-slip interpretation. On bedding (north) stereonet, crosses and circles represent the bedding measurements to the west and east of depositional synform ( $F_0$ ), respectively. 66
- Figure 4B      Facies associations in the Beaulieu Rapids Basin. Porphyry dykes/stocks were emplaced along the eastern fault margin in the north. Twelve stratigraphic sections and three detailed sections are indicated in roman numerals and by small rectangles, respectively. The encircled capital letters A-G designate clast count localities. Paleocurrent rose diagrams indicate prominent basin parallel, unidirectional flow in the south of the basin. 67
- Figure 5      Characteristics of the volcanic rocks and porphyry stocks adjacent to the Beaulieu Rapids Basin. (A) Unconformable contact ( $U$ ) between the massive pebbly sandstone of the Figure 3: Location of the Beaulieu Rapids Formation (outlined) in the Beaulieu River volcanic belt (BRB) and its proximity to the 2800-2900Ma plutonogneissic Sleepy Dragon complex (SDC). Note sinistral strike-slip fault on the eastern side of the SDC. CRB, Cameron River volcanic belt; TLR, Turnback Lake Rhyolite; BF, Burwash Formation; BLQ, Beniah Lake Quartz arenite. Modified from Lambert and others, 1992. 68
- Figure 6A      Stratigraphic columns through the Beaulieu Rapids Basin (see Figure 4b). Clast count localities are indicated by circled letters. (A) Sections I-VII from the southern region of the basin show the lateral discontinuity of the CFA-I, the unconformity between the volcanic and the sedimentary rocks, and the presence of two well-defined fining-upward sequences (IV). 69

- Figure 6B Sections VIII-XI from the northern region of the basin with quartz-feldspar porphyries (sections VIII-IX) at the base of the sections. Rapid lateral and vertical facies changes are evident in figures A and B. 70
- Figure 7 Outcrop sketch of the clast-supported conglomerate of the CFA-I (S<sub>0</sub> 181/88) composed of plane-bedded coarse-grained sandstone (*Sh*), trough crossbedded pebbly to coarse-grained sandstone (*St*), and massive, clast-supported conglomerate beds (*Gm*; locality DS1 in Figure 4b). 71
- Figure 8 Characteristics of the CFA-I. Younging directions are indicated by large arrows. (A) Dominant clast constituents of the clast-supported conglomerate: plutonic clasts (*P*) and mafic volcanic clasts (*Mv*). Scale, pencil 13cm. (B) Large plutonic boulders (*P*) in the clast-supported conglomerate. Scale, hammer 34cm. (C) Trough crossbedded (*St*) sandstone interbeds truncated by matrix-supported conglomerate. Small arrows mark erosional surface. Scale, knife 9cm. (D) Laminated argillite (*Fl*) interbed in matrix-supported conglomerate recording pervasive NNE-trending foliation (*F*). Scale, knife 9cm. (E) Truncating sets of trough crossbeds (*St*; arrows) in the pebble-conglomerate subunit. Scale, pencil 13cm and indicating north. (F) Three fining-upward cycles (*arrows*) including stratified conglomerate (*Gm*) capped by argillite (*Fl*) in the pebble-cobble conglomerate subunit. Scale, hammer 50cm. 72
- Figure 9 Outcrop sketch of the sandstone-dominated subunit of the SSFA (S<sub>0</sub> 008/86) composed of truncating trough crossbeds (*St*), argillite (clay) beds (*Fl*), argillite rip-ups, and argillite drapes on foresets (locality DS2 in Figure 4b). 73
- Figure 10 Characteristics of the SSFA. Younging direction is indicated by large arrow. (A) Trough crossbedded sandstone (*St*) with argillite 74

between bedforms and draped on foresets (*Fl*) in the sandstone-dominated subunit. Scale, knife 9cm. (B) Horizontal bedding (*Sh*) and planar crossbedding (*Sp*) in the sandstone-dominated subunit. Scale, pencil 13cm (arrow) and indicating north. (C) Pebble trains (*Gm*) overlain by trough crossbedding (*St*) in the sandstone-dominated subunit. Scale, pencil 13cm and indicating north. (D) Asymmetrical wave ripples (*Sr*) in the siltstone-dominated subunit. Scale, pencil 13cm. (E) Abundant water escape structures as indicated by clastic dykes (*CD*) and dish structures (*DS*) in the siltstone-dominated subunit. Local graded beds (*GB*) are observed. Scale, pencil 13cm. (F) Close-up of dish (*DS*) and pillar (*PS*) structures and graded bedding (*GB*) in the siltstone-dominated subunit. Scale, pencil 13cm.

- Figure. 11 Characteristics of the CFA-II, the QSFA, and clast components of the Beaulieu Rapids Formation. Large arrow indicates younging direction. (A) Clast-supported CFA-II with plutonic (*P*), mafic volcanic (*M*), felsic volcanic (*F*), and quartz (*Q*) clasts. Scale, lens cap 5cm in diameter. (B) Large-scale, high-angle laterally accreting sets of trough crossbeds (*St*) in the QSFA. Scale, knife 9cm (arrow). (C) Composite, up to 10m-long channel (arrows indicate base) of the QSFA. Scale, hammer (arrow) 34cm. (D) Truncating trough crossbeds (*St*) with pebbles on foresets (*Pb*) in the QSFA. Scale, pencil 13cm. (E) Medium-to coarse-grained plutonic clasts with local 0.2-1cm large quartz phenocrysts (arrows). Sample derived from the CFA-II (see Table 2 for point count). Scale, coin 2cm in diameter. (F) Magmatic breccia clast (*Mb*) in the CFA-I. Scale, coin 2cm in diameter. 75
- Figure 12 Stratigraphic column of the QSFA composed of low-angle planar beds (*Sh*), trough crossbeds (*St*), and pebbles on foresets (*Pb*) (locality DS3 in Figure 4b). 76
- Figure 13 Ternary diagrams illustrating the compositions of sandstones and conglomerates of the Beaulieu Rapids Formation. Average 77

compositions indicated by crosses. (A) QFL diagram (Dickinson and others, 1983) illustrating a recycled orogenic provenance.

(B) QmFLt diagram after Dickinson and others (1983) showing the same recycled provenance as in 13A. (C) LpLvLs diagram comparing rock fragments in sandstones with seven clast counts. Plutonic fragments decrease from the CFA-I to the CFA-II. Sedimentary fragments are restricted to the QSFA.

- Figure 14 Results of 4597 clast counts from four different localities in the CFA-I and three different localities in the CFA-II. Clasts were derived predominantly from the gneisso-plutonic Sleepy Dragon Complex and the mafic volcanic Beaulieu River volcanic belt. Clast count localities are indicated in Figure 4b. 78
- Figure 15 Paleogeographic models illustrating the evolution of the Beaulieu Rapids Basin during two depositional phases. (A) First depositional phase includes the uplift of the gneisso-plutonic terrane. Erosion of the younger mafic volcanic belt and the plutonic rocks caused rapid infilling of the basin. Coarse clastic detritus accumulated as alluvial fans and fan deltas along basin margins that prograded onto a small braidplain and into standing bodies of water. (B) The second phase provided additional material into the basin. Small lakes and ponds disappear due to continued basin aggradation. The basin is controlled by a large parallel sandy braided stream system. Porphyry stocks are exposed along the fault. 79

## LISTE DES TABLEAUX

		p.
Table 1	Sedimentary facies associations in the Beaulieu Rapids Basin.	80
Table 2	Composition of quartz-feldspar (QFP) and hornblende (HP) porphyries and the gneisso-plutonic Sleepy Dragon Complex (SDC). Recalculated quartz, potassium feldspar, and plagioclase percentages represented by Q%, K%, and P%, respectively.	81
Table 3	Recalculated point counting results from thirty-two samples derived from the SSFA and QSFA in the Beaulieu Rapids Formation. Grain parameters include: $Q=Q_m+Q_p$ where $Q_m$ is monocrystalline quartz and $Q_p$ is polycrystalline quartz; $F=P+K$ where P is plagioclase feldspar and K is potassium feldspar; $L=L_s+L_p+L_v$ where $L_s$ are sedimentary lithic fragments, $L_p$ are plutonic lithic fragments, and $L_v$ are volcanic lithic fragments; and $L_t=L+Q_p$ .	82

# CHAPITRE I

## INTRODUCTION

### 1.1 La Problématique

Les analyses de faciès, les études pétrographiques, ainsi que la cartographie lithologique des séquences sédimentaires dans les bassins Archéens de la Province de l'Esclave n'ont jamais été étudiées en détail.

Cette étude est importante parce que des processus tectoniques fournissent les débris qui s'accumulent dans les bassins Archéens. De ce fait, ceux-ci enregistrent l'histoire de l'évolution de la terre. De nombreuses études des grès dans des séquences modernes et anciennes ont été employées pour déterminer la provenance et l'environnement tectonique (Dickinson et Suzcek, 1979; Dickinson et al., 1983). En outre, des analyses de faciès des successions sédimentaires ou volcano-sédimentaires sont nécessaires pour déterminer les environnements de dépôt (e.g. Walker et James, 1992). Les patrons de plissement interne et la géométrie des failles sont des éléments structuraux qui enregistrent la déformation synchrone à la formation du bassin. Ces éléments, en association avec les analyses de faciès détaillées et les études de provenance sont essentiels pour déterminer l'évolution des systèmes sédimentaires anciens.

La reconstruction des bassins sédimentaires dans les séquences supracrustales Archéennes (>2.5 Ga) est problématique à cause de la rareté des affleurements, de la complexité des éléments structuraux, du grade métamorphique, et du caractère relique de la séquence stratigraphique. Malgré l'existence de ces contraintes, il est tout de même possible d'identifier des structures sédimentaires qui fournissent une bonne interprétation paléo-

environnementale (e.g. Eriksson et al., 1988). Mueller et Donaldson (1992), par exemple, ont reconnu quatre événements formant des bassins distincts dans la ceinture de roches vertes Archéenne de l'Abitibi. La preuve de ces événements se trouve dans les analyses détaillées de faciès sédimentaires (e.g. Dimroth et al., 1982; Mueller et al., 1991), dans la détermination des âges en utilisant la méthode U-Pb (e.g. Corfu et al., 1989; Mortensen, 1993), et dans les études structurales (e.g. Daigneault et al., 1990). Les événements formant les bassins de la ceinture de l'Abitibi s'échelonnent sur 55 Ma (2730-2675 Ma). Ils sont divisés entre des dépôts de flysch et molasse reliés à la formation de l'arc et à l'érosion des plutons synvolcaniques dans le premier cas et à la collision arc-arc et la fragmentation de l'arc dans le second (Mueller et al., 1996). Des bassins de décrochement tardi-orogéniques de direction est bien documentés et localisés le long des failles majeures sont reliés à la phase terminale de la fragmentation de l'arc. Ces réservoirs sédimentaires sont associés avec une abondance de porphyres intrabassinaux (Mueller et al., 1991) et le volcanisme alcalin contemporain (Cooke et Moorhouse, 1969; Mueller et al., 1994).

Par contraste avec les roches de la ceinture de l'Abitibi, intensivement étudiées, bien peu d'attention a été portée sur les roches sédimentaires de la Province structurale de l'Esclave. Les points d'intérêt principaux de cette étude sont de placer la formation de Beaulieu Rapids dans un contexte géodynamique et de montrer l'importance des bassins de décrochement archéens. Le dernier point est pertinent parce que la tectonique des plaques pendant cette époque, reste énigmatique (e.g. Hamilton, 1995). La combinaison des analyses de faciès sédimentaires, de la caractérisation de la provenance des grès et des conglomérats, d'une analyse structurale de bassin et de la détermination d'âge va permettre d'élucider la formation et l'évolution du bassin. Des études complémentaires de cette nature sont nécessaires pour la compréhension des événements tardifs de la consolidation de la croûte.

## 1.2 La présentation de la thèse

Un manuscrit a été écrit et soumis pour publication dans le journal de "Geological Society of America Bulletin" à cause de l'importance du projet pour la compréhension de l'évolution de la Province de l'Esclave. L'information normalement fournie dans une thèse classique est présentée ici sous forme d'article. La thèse est composée de trois chapitres: 1) une introduction écrite en français, 2) un article rédigé en anglais, et 3) une conclusion écrite en français. Toutes les références se trouvent à la fin de l'article au lieu d'être mises à la fin de la conclusion dans le troisième chapitre.

## 1.3 Localisation et géomorphologie

La formation archéenne de Beaulieu Rapids est située entre les latitudes 63°05'N et 63°00'05"N et les longitudes 112°26'W et 112°23'W, approximativement à 120 km à l'ENE de Yellowknife, TNO. Géomorphologiquement, le terrain d'étude est relativement plat et longe le système anastomosé nord-sud de la rivière Beaulieu. La formation est entourée d'une topographie ondulante. La rivière et trois lacs contigus traversent le centre de la formation au nord. La marge du plus grand lac suit une faille majeure NS dans la partie sud de la formation. La direction que la rivière emprunte est contrôlée par l'orientation des cisaillements et plissements présents dans le substrat rocheux. L'accessibilité du terrain de la formation de Beaulieu Rapids n'est possible que par hydravion.



#### 1.4 Travaux antérieurs

La formation de Beaulieu Rapids de la Province structurale de l'Esclave a été initialement cartographiée par M. Stublely à l'échelle 1:50 000 en 1988 (Stublely, 1989). Plus tard, la formation a été nommée par Roscoe et al. (1989) en se basant sur la proximité du système de la rivière Beaulieu. Le but de leurs études était d'examiner des lentilles uranifères et aurifères dans les conglomérats ainsi que d'expliquer les caractéristiques structurales et sédimentaires observées sur le terrain. Malheureusement, la cartographie à grande échelle a laissé certaines caractéristiques de la formation plutôt méconnues. La description des unités et l'interprétation des environnements de dépôt possibles n'ont pas été discutées. Ces aspects ont été considérés plus tard par Rice et al. (1990) mais le temps limité sur le terrain ne leur a pas permis de faire des interprétations détaillées de chaque association de faciès. Leurs études ont suggéré que le dépôt des sédiments s'est produit sur un cône alluvionnaire sub-aérien et dans un système fluvial sableux. Cette interprétation était basée sur seulement deux des quatre associations de faciès qui se trouvent dans la formation. L'information trop restreinte des études précédentes a justifié une analyse détaillée de la Formation de Beaulieu Rapids.

#### 1.5 Étude actuelle

La cartographie de la Formation de Beaulieu Rapids a été effectuée pendant les étés 1994 et 1995. Le projet a été supporté par le ministère des Affaires Indiennes et du Nord du Canada (DIAND) à Yellowknife, TNO, et par l'Université du Québec à Chicoutimi. Vingt-huit sections stratigraphiques aux échelles 1:2000, 1:1000, 1:200, et 1:100 et quatre croquis d'affleurements détaillés à l'échelle de 1:25 ont été compilés pour cette étude. Le travail a été effectué par le présent auteur, le Dr. Wulf Mueller et une assistante au cours de l'été 1994, et

deux assistants et le présent auteur ont complété la cartographie en 1995. Quatre résumés et un rapport d'EGS ont été publiés (Corcoran et al., 1994; Corcoran et al., 1995a; Corcoran et al., 1995b; Corcoran and Mueller, 1995a; Corcoran and Mueller, 1995b).

**CHAPITRE II****IMPLICATIONS OF AN ARCHEAN STRIKE-  
SLIP BASIN IN THE SLAVE PROVINCE:  
THE CLASTIC BEAULIEU RAPIDS  
FORMATION,  
NORTHWEST TERRITORIES, CANADA**

**Corcoran, P.L., Mueller, W.U.:** Sciences de la terre, Université du  
Québec à Chicoutimi, Québec, Canada, G7H 2B1

**Padgham, W.A. :** Indian and Northern Affairs Canada, Geology Division,  
Yellowknife, N.W.T., Canada, X1A 2R3

The 0.2-1km-thick Beaulieu Rapids Formation, located in the south-central Slave Structural Province, is a late-orogenic strike-slip basin that resulted from horizontal plate motion during the Archean. The formation overlies the Beaulieu River volcanic belt unconformably on the west and is bordered by a major N-trending fault on the east, along which 2.6Ga quartz-feldspar and hornblende porphyry stocks were emplaced. NNE-trending en echelon folds and a pervasive NNE-trending foliation are prominent structural features of this strike-slip basin.

Sedimentary rocks of the Beaulieu Rapids Basin display two fining-upward sequences that indicate a tectonic control on sedimentation. The first sequence (maximum thickness of 375m) is represented by conglomerate facies association I and the overlying siltstone-sandstone facies association, whereas conglomerate facies association II coupled with the overlying quartz-rich sandstone facies association constitute the second depositional sequence (maximum thickness of 300m). The marginal conglomerate facies association I is characterized by debris flow, traction current, and sheetflood deposits that accumulated on the proximal, medial, and distal portions of alluvial fans or fan deltas, respectively. The siltstone-sandstone facies association contains a sandstone-dominated subunit that formed due to megaripple migration and overbank deposition in a sandy braidplain setting with local ponds. A siltstone-dominated subunit represents lacustrine deposition. Recurrent tectonic activity and consequent uplift produced conglomerate facies association II, producing longitudinal bars during streamflow activity in a proximal braided stream setting. The sedimentary structures of the uppermost quartz-rich sandstone facies association are suggestive of pronounced megaripple migration and minor drape deposition in a low-gradient but high-energy braided river environment.

Provenance studies reveal that the dominant source areas of the Beaulieu Rapids sedimentary rocks include the >2.8Ga gneisso-plutonic Sleepy Dragon Complex, the Beaulieu River volcanics, and the fault-controlled porphyry stocks. The characteristics of mineral and rock fragment components reflect rapid deposition, high sediment influx, short transport distances, and a humid climate. Sedimentary rock fragments in the cycle II facies associations imply cannibalism of cycle one sediments during renewed tectonic activity.

The Beaulieu Rapids Basin is similar to modern strike-slip basins that form along major fault zones in terms of basin geometry, faulted and unconformable contacts, lithological units, and sedimentary facies stacking and organization. Successor basins of this nature commonly develop during the last increment of terrane docking and may reflect late movement on an Archean suture zone.

## INTRODUCTION

The early evolutionary history of the earth is commonly recorded in sedimentary basins because they receive detritus generated by tectonic processes. Sandstone constituents of modern and ancient sedimentary successions have been employed in numerous studies to determine provenance and tectonic setting (Dickinson and Suzcek, 1979; Dickinson and others, 1983), whereas facies analyses of sedimentary or volcano-sedimentary successions are necessary to establish depositional environments (e.g. Walker and James, 1992). Internal folding patterns and fault geometry are structural elements that record synbasinal deformation, and in conjunction with detailed facies analyses and provenance studies, are essential in determining the evolution of ancient sedimentary systems.

The reconstruction of sedimentary basins in Archean supracrustal sequences (> 2.5Ga) has been problematic because of limited outcrop exposure, structural complexities, metamorphic grade, and the remnant nature of the stratigraphic sequence. In spite of these constraints, it is still possible to discern the sedimentary structures that provide a sound paleoenvironmental interpretation (e.g. Eriksson and others, 1988). Mueller and Donaldson (1992), for example, recognized 4 distinct basin-forming events in the Archean Abitibi greenstone belt, based on detailed sedimentary facies (e.g. Dimroth and others, 1982; Mueller and others, 1991), precise U-Pb age determinations (e.g. Corfu and others, 1989; Mortensen, 1993), and structural studies (e.g. Daigneault and others, 1990). The basin-forming events, spanning 55Ma (2730-2675Ma), were divided into flysch- and molasse-type deposits related to arc-formation, arc-unroofing, arc-arc collision, and arc fragmentation, respectively (Mueller and others, 1996). Well-documented, late-orogenic, strike-slip basins located along major E-trending faults were related to the terminal arc fragmentation phase.

In contrast to the sedimentary rocks of the well-known Abitibi belt, those of the Archean Slave Structural Province (SSP) have received scant attention (Fig. 1). The principal focus of this study is to place the Beaulieu Rapids Formation into an overall geodynamic context and to show the importance of Archean strike-slip basins because plate tectonic processes during this epoch remain controversial (e.g. Hamilton, 1995). The combination of modern sedimentary facies analyses, provenance characterization of the sandstones and conglomerates, a structural basin analysis, and preliminary U-Pb zircon age determinations will elucidate basin formation and evolution. Complementary studies of this nature are required to comprehend the late stages of Archean cratonization.

## **SLAVE STRATIGRAPHY AND SETTING**

### **Problematic**

The 510km x 710km large SSP (Fig. 1; ca. 213 000 km<sup>2</sup>), in contrast to most Archean greenstone belts, is characterized by (i) a greater abundance of sedimentary than volcanic rocks, (ii) a higher felsic/mafic ratio in the volcanic regimes, (iii) abundant evidence for a sialic basement, and (iv) more evolved potassium-rich granites (Henderson, 1981; Padgham and Fyson, 1992). Are these characteristics an artifact of deformation and rock preservation, or is the SSP a distinct type of Archean craton as advocated by Padgham and Fyson (1992)? The Slave craton spans a 1.4Ga period from 4.0-2.6Ga (Isachsen and Bowring, 1994) and contains the Acasta gneisses, the oldest known rocks in the world (Bowring and others., 1989). This extensive timeframe makes a pan-Slave stratigraphy problematic as at least 3 supercontinental cycles may be represented. The notion of mega- and supercycles has already been suggested for the time-equivalent Pilbara Block in

Australia (Krapez, 1993). Consequently, adjacent stratigraphic successions with similar sedimentary facies, lava flow morphology, and geochemical signatures may be significantly different in age. Correlations of volcano-sedimentary sequences without adequate time constraints are problematic in Archean supracrustal successions. Recent U-Pb age determinations (e.g. Isachsen and Bowring, 1994) in conjunction with detailed mapping of critical areas along regional N-trending fault zones (e.g. Mueller and Donaldson, 1994; Corcoran and Mueller, 1995a) indicate that late-orogenic sedimentary sequences with local volcanism and porphyry intrusions occurred throughout the SSP at 2600Ma (Fig. 2).

### **Yellowknife Volcanic Belt**

The Yellowknife volcanic belt (Henderson, 1970; Fig. 1) is representative of Archean supracrustal successions of the SSP. Mapping by the Geological Survey of Canada (e.g. Lambert and others, 1992) and the Geology Division of Indian and Northern Affairs, Northwest Territories (e.g. Jackson and others, 1985), in addition to radiometric age determinations (Bowring and others, 1989; Isachsen and others, 1991; van Breeman and others, 1992), allowed Padgham and Fyson (1992) to establish three distinct supracrustal assemblages. Similarly, Isachsen and Bowring (1994) contended that the Yellowknife belt was not a product of a single magmatic and tectonic event, but rather a continuum of episodic volcanism and sedimentation spanning 200 m.y.

The 2722-2658Ma Yellowknife volcanic belt (Isachsen and others, 1991; van Breemen and others, 1992; Isachsen and Bowring, 1994) is time-transgressive with the Cameron and Beaulieu River volcanic belts (2663 + 7/-5Ma; Henderson and others, 1987), the High Lake greenstone belt (2700-2662Ma; Henderson and others, 1995), the Anialik River volcanic belt (2687-2678Ma; Relf and others, 1994), and the Hood River volcanic belt (2668±4; van



Breemen and others, 1994; Fig. 1). The Kam, Banting and Duncan Lake Groups comprise the stratigraphy of the Yellowknife volcanic belt (Helmstaedt and Padgham, 1986; Fig. 2). The Kam Group (2722-2688Ma), an inferred 10-15km thick tholeiitic basaltic succession, is composed of massive, pillowed and brecciated flows, intruded by multiple gabbro dikes and sills (MacLachlan and Helmstaedt, 1995) and has local metre-thick (silicified) volcanoclastic units. The lowermost formations represent an ancient analogue of modern ocean floor deposits. Small felsic volcanic edifices developed locally on this Archean ocean floor. The 20m.y.(2722-2702Ma) time period for the development of a subaqueous basalt plain with scattered volcanic edifices is common for Archean sequences (cf. Chown and others, 1992) and is here referred to as volcanic cycle I.

Continuous subaqueous, mafic-dominated volcanism is characterized by an increase of interflow, wave-influenced, quartz-rich, volcanoclastic sediments (Padgham, 1987) and reworked felsic pyroclastic debris up-section (Bode Tuff;  $2688\pm 3$ , Isachsen and others, 1991) in the Yellowknife Bay Formation (2702-2688Ma). The abundance of volcanoclastic sediments is consistent with the breaching of composite volcanic islands. Collectively, these characteristics, possibly indicative of a second volcanic cycle, compare favourably with the development of a broad shield volcano upon which dispersed emergent felsic cones formed (e.g. Ayres, 1982; Mueller and others, 1989).

The Banting and Duncan Lake Groups (2664-2658Ma; Mortensen and others, 1992; Isachsen and Bowring, 1994) are inferred to overlie the Kam Group unconformably (MacLachlan and Helmstaedt, 1995) with a hiatus of 20m.y. They represent an evolved segment of an arc-backarc setting, in correlation with other time-transgressive volcano-sedimentary terranes (e.g. Cameron and Beaulieu River volcanic belts; Fig. 3). Arc evolution is indicated by the calc-alkaline signature of the mafic to felsic lava flows (Cunningham and Lambert, 1989) and the significant volcanoclastic deposits. Volcanic

islands must have emerged intermittently as there is an abundance of locally wave-reworked mass flow volcanoclastic deposits and pyroclastic deposits with fiamme (Padgham, 1980). The turbiditic sedimentary rocks of the Burwash Formation (Duncan Lake Group) are time-equivalent with the felsic volcanic centres at Clan (ca.  $2661 \pm 2$ ; Mortensen and others, 1992) and Turnback Lakes ( $2663 \pm 7/-5$ Ma; Henderson and others, 1987). This indicates the complex interdigitation of volcanic islands and sedimentary basins. The Vanuatu arc, New Hebrides is a modern analogue (Green and Wong, 1988). Shoaling and emerging arc islands of the Banting Group shed detritus into an extensive, diachronously evolving, continental arc (backarc? intra-arc?) basin as represented by the Burwash Formation. A major unconformity lies between the clastic Raquette Lake Formation (Henderson, 1985), the proximal-equivalent Burwash Formation to the east and the older plutono-gneissic rocks of the  $>2800$ - $2900$ Ma Sleepy Dragon Complex (Henderson, 1985; Kusky, 1990).

An apparent 50m.y. hiatus occurs between the volcanics of the Yellowknife belt and the unconformably overlying, N-trending, clastic Jackson Lake Formation ( $< 2605$ Ma; Isachsen and others, 1991). Turbidite (flysch) sequences in other segments of the SSP are as young as 2616-2612Ma (Isachsen and Bowring, 1994), hence, the inferred hiatus between the Burwash and Jackson Lake sedimentary rocks may be particular to the Yellowknife volcanic belt. The 300-500m-thick Jackson Lake Formation (Figs. 1, 2), initially recognized by Henderson and Brown (1966) and described by Henderson (1975), represents the youngest depositional event in the SSP. The formation, exposed intermittently for 35km along strike in the Yellowknife area, represents an alluvial-fluvial sequence (Henderson, 1975) that grades abruptly into a lacustrine/marine sequence (Mueller and Donaldson, 1994). Recent U-Pb age determinations indicate that basins of this type are dispersed throughout the SSP (Fig 1). A detailed study of one of these basins will place significant constraints on the late-stage evolution of the Slave craton. The Beaulieu Rapids

Formation (BRF; lat. 63°05'-63°00'/long. 112°25'-112°23'), herein referred to as the Beaulieu Rapids Basin, was selected because it is the first unequivocal example of an Archean strike-slip basin recognized in the SSP.

### **Local Geology and Characteristics**

The clastic sedimentary BRF (Roscoe and others, 1989; Stubbley, 1989; Rice and others, 1990) of the Beaulieu River volcanic belt, is located in the south-central part of the SSP (Fig. 3). The western margin of the basin is characterized by an unconformity (Figs. 4a, 5a), intermittently traceable for at least 5 km along strike. It separates the mafic massive, brecciated (Fig. 5b), pillowed and hyaloclastite flows (Fig. 5c) with abundant scoria (Fig. 5d) from the sedimentary rocks of the BRF (Corcoran and Mueller, 1995a). Quartz-feldspar porphyry stocks (Fig. 5e) with 1-2mm-large quartz phenocrysts (Fig. 5f) as well as hornblende-feldspar phyrlic, syenitic stocks were emplaced along the faulted northern part of the eastern margin of the Beaulieu Rapids Basin (Figs. 4b).

### **Basin Geometry and Structure**

The Beaulieu Rapids Basin is approximately 9.5km long and has a maximum width of 2km (Fig. 4a). A major >300km long, N-trending fault constrains the basin on the east (Figs. 1, 3) while the northern and southern extremities are truncated by late, NE-trending faults. A prominent, steeply-dipping NNE-trending S<sub>1</sub> foliation (mean of 025/89; Fig. 4a) is locally transected by a NNW-trending S<sub>2</sub> foliation (mean of 347/88; Fig. 4a). Ubiquitous NNE-trending F<sub>1</sub> folds associated with the axial planar S<sub>1</sub> foliation are organized in a multiple left-stepping en echelon array (Fig. 4a) and occur as alternating anticlines and

synclines. Fold wavelength, approaching 450m, is consistent with basin size and geometry. The en echelon  $F_1$  fold pattern is reflected in the change of younging directions in the north (Fig. 4a), where the best-fit great circle of the poles to bedding planes produces a mean fold axial plane of 029/84, strikingly similar to the mean of the  $S_1$  foliation. The southern part of the study area contains relatively constant bedding orientations, producing a mean strike and dip value of 013/85. The beds are commonly upright but are locally overturned.

Reversals in structural facing directions imply that a synformal structure preceded the deformational phase that created the en echelon fold pattern (Fig. 4a). These reversals can be used to trace the location of the initial fold axis (cf. Kehlenbeck, 1984) or may simply mark the presence of an original, depositional synform ( $F_0$ ). It is common to find margin-derived sediments deposited toward the centres of basins fringed by mountains or uplifted blocks in modern settings (cf. Damanti, 1993; ) as well as in ancient environments (cf. Krapez and Barley, 1987; Heubeck and Lowe, 1994). The sediments need not have originated from only one basin margin. Therefore, the axial trace of the syncline traversing the centre of the BRF throughout its length could mark the confluence of detritus derived from opposing sides of the depositional basin. This  $F_0$ -axial trace appears to extend to the east in the southern region where it is truncated by a fault splay from the major north-trending fault, locally referred to as the Beniah Lake Fault (Padgham, 1992).

## **SEDIMENTOLOGY**

### **Facies Associations of the Beaulieu Rapids Formation**

The stratigraphic sequence of the Beaulieu Rapids Formation provides an excellent example of syntectonic deposition within a fault-controlled basin. Mappable lithological units, defined as facies associations, were identified on the basis of grain size, clast composition, sedimentary structures, and stratigraphic position. The BRF is composed of (i) a conglomerate facies association I, (ii) a siltstone-sandstone facies association, (iii) a conglomerate facies association II, and (iv) a quartz-rich sandstone facies association (Table 1). Basin-wide mapping at a scale of 1:2000 accompanied by 12 detailed 150-540m stratigraphic sections (Figs. 6a, b) mapped at scales of 1:20 to 1:800 was effected to constrain the lateral and vertical distribution of individual facies associations (Fig. 4b).

**Conglomerate Facies Association-I (CFA-I).** The 20-320m-thick basal conglomerate facies association I (CFA-I; Figs. 6a, b) constitutes 32% of the sedimentary succession. Two mutually interstratified subunits were identified along strike: (1) a matrix-to clast-supported conglomerate and (2) a massive to stratified pebble-cobble conglomerate. The two subunits were distinguished by principal clast size, sedimentary structures, and sandstone component which is 10% in the former and up to 30% in the latter. Matrix-to clast-supported conglomerate predominates in the south, whereas massive to stratified pebble-cobble conglomerate is characteristic in the north. The CFA-I is found mainly in unconformable contact with the mafic pillowed volcanic rocks of the Beaulieu River greenstone belt but it also occupies the heart of the basin in the north (Fig. 4b).

The matrix- to clast-supported conglomerate has a maximum thickness of 120m and is locally composed of a basal massive pebbly to very coarse-grained sandstone (Fig. 5a) which grades vertically and laterally into a 5-20m-thick matrix-supported conglomerate with the matrix component ranging from 40-50%. Sandstone beds at the unconformity (Fig. 5a), although in direct contact with the mafic volcanic rocks, are locally rich in quartz and plutonic grains. Internal stratification is characteristically absent. The matrix-supported conglomerates grade into clast-supported equivalents that have a matrix percentage ranging from 20-30%. Conglomerate up to 20m-thick is amalgamated as indicated by a change in clast size, clast population, or discontinuous interstratified sandstone beds (Fig. 7). The clast-supported conglomerate, composed of various clast compositions (Fig. 8a), overlies sandstone beds with sharp erosive contacts while diffuse contacts occur where sandstone fills the voids between individual clasts at the conglomerate-sandstone interface. Angular to subrounded clasts in both types of conglomerates are generally cobble-size although boulder-size clasts > 25 cm are not uncommon. The largest clasts, up to 85cm in diameter, are plutonic in composition (Fig. 8b).

Coarse-grained to granule size, 10-100cm-thick, sandstone interbeds are laterally discontinuous and are eroded by conglomerates (Fig. 8c). Cosets of 10-50cm-thick planar and low-angle beds locally cap cosets of trough crossbeds (Fig. 8c). The foreset laminae are tangential and concave in shape and characteristically contain pebbles and small cobbles along their lee sides. Lenticular laminated argillite, 1-30cm-thick, is locally interstratified with the clast-supported conglomerates (Fig. 8d). The sandstone and argillite components constitute < 10% of this facies association.

The 50-200m-thick pebble-cobble conglomerate subunit is characterized by massive to stratified conglomerates and conglomerate-filled channels. Metre-thick, clast-supported, cobble-size conglomerates are amalgamated as shown by the lateral interstratification of

lenticular, coarse- and very coarse-grained, planar to trough crossbedded sandstone beds (Fig. 8e) in addition to the presence of local sandstone lenses.

A high sandstone and argillite content is characteristic of this subunit (Fig. 8f). Truncating trough crossbeds commonly underlie planar beds within the 10-100cm-thick sandstone interbeds. Small-scale fining-upward cycles, up to 2m thick, locally characterize the association of conglomerate-sandstone-argillite (Fig. 8f). Wavy bedding, trough crossbedding, and rare flaser-type bedding is developed within the coarse sand- to granule-sized beds.

**Hydrodynamic Processes of the CFA-I.** The basal CFA-I is dominated by an abundance of traction flow deposits that are inherent to coarse clastic fluvial dispersal systems (e.g. Miall, 1978; Rust, 1984) or streamflow-dominated alluvial fans (Galloway and Hobday, 1983; Ballance, 1984). Amalgamated massive to poorly stratified conglomerates in both subunits may represent ancient, coalescing sheet gravels (Wells, 1984), longitudinal gravel bars (Galloway and Hobday, 1983), in-channel mass flows (Middleton and Trujillo, 1984), sheetflood deposits (Nocita and Lowe, 1990) or hyperconcentrated flood flows (Brierley and others, 1993). The first two interpretations are favoured because of the associated facies and stacking (Table 1), and are characterized as facies Gm (facies code of Miall, 1978). Low-angle scours or channel-fill conglomerates are confined stream channel deposits (facies Gt), whereas subordinate, well-stratified pebble conglomerates with low-angle bedding of the pebble-cobble subunit are interpreted as linguoid bars (facies Gp) that developed during fluctuating sheetflood events. Rapidly fluctuating flow energy and transport conditions are substantiated by the presence of sandstone interbeds. Both subunits of the CSF-1 feature truncating sets of trough crossbeds (facies St) and parallel-laminated sandstones (facies Sh), representing migrating in-channel

lunate megaripples and bar top sands, respectively (Eriksson, 1978). Alternatively, trough crossbeds developed while transverse bars propagated during high-energy flow stages (Dreyer, 1993). Low-angle planar beds (Facies S1) represent upper flow regime bar top sands (Best and Bridge, 1992) deposited on the lee-sides of gravel bars. Minor planar crossbeds (facies Sp), indicative of linguoid sandbars or straight-crested dunes (Reineck and Singh, 1980), are consistent with diminishing flow energy conditions. The interrelation of conglomerate and argillite indicate abrupt fluctuations in flow-energy conditions involving bedload transport and suspension sedimentation. The local preservation of laminated argillite (siltstone-mudstone; facies Fl), derived from the rapid breakdown of the mafic volcanics, is interpreted as overbank or rapidly waning flood deposits on alluvial fans (Miall, 1978; Horton and Schmitt, 1996). The thicker argillite units with flaser-type structures in the pebble-cobble conglomerate are representative of small ephemeral ponds or crevasse splays associated with braided streams (Eriksson, 1978; Rust and Koster, 1984).

The massive pebbly sandstone (facies Sma; Mueller and others, 1994) at the base of the sequence may be a hyperconcentrated flood or sheetflow deposit (Flint and others, 1986; Smith, 1986; Horton and Schmitt, 1996). Matrix-supported conglomerates (facies Gms) with subangular to subrounded clasts are typical of debris flow deposits (Schulz, 1984; Mack and Rasmussen, 1984). The matrix-supported character of the conglomerate in association with a disorganized clast fabric is typical of cohesive mass flows (Nemec and Postma, 1993). This cohesive nature enables debris flows to transport boulder-size material, well-demonstrated in the BRF, where the largest clasts are found in the matrix-supported conglomerate.

**Siltstone-Sandstone Facies Association (SSFA).** The SSFA, constituting 18% of the BRF, conformably overlies the basal conglomerate in most of the Beaulieu



Rapids Basin save for in the northern part where it is eroded by or interstratified with the CFA-I (Figs. 6a, b). The SSFA, divided into a sandstone-dominated and a siltstone-dominated subunit, is in erosional contact with the conglomerate facies association-II and the quartz-rich sandstone facies association. The sandstone-dominated subunit (Fig. 9), which has a maximum thickness of 305m (Fig. 6a, Section Va), is composed of alternating bedsets of sandstone, siltstone and minor argillite and pebble lags. It is characterized by abundant trough crossbeds that range between 5 and 50cm in thickness (Fig. 9). Foreset laminae of crossbeds are angular and tangential in shape (Fig. 10a). Subordinate plane-bedded and planar crossbedded sandstones and siltstones (Fig. 10b) occur in 20-80cm-thick sets and are associated with up to 10m-thick stacks of tangential trough crossbeds. Internal truncation and reactivation surfaces as well as argillite-to fine-grained sandstone drapes between bedforms are common. Discontinuous argillite layers (1 to 75cm-thick) which constitute <5% of this facies association, occur along bedding surfaces and on bedforms (Figs. 9, 10a) and the thicker layers display small-scale cross-lamination and planar laminae. The contacts between the argillite and the overlying crossbeds is sharp and erosive, thus accounting for the local presence of argillite rip-up clasts in the neighbouring sandstone and siltstone beds. Well-sorted, clast-supported, scour based, 5-15cm-thick pebble trains are common in the southern part of the basin (Fig. 10c). Trough crossbeds were measured for paleocurrent flow direction in an east-facing homoclinal succession in the southern part of the basin (Fig. 4b). The flow, parallel to the elongation of the basin was predominantly unimodal to the north with a minor southward-flow component.

The siltstone-dominated subunit, 10-40m thick, is restricted to the centre of the basin but occurs locally along the northwest margin. Typical sequences include 1-5cm-thick siltstone beds alternating with 1-8cm-thick fine-grained sandstone beds. Sedimentary structures found within the siltstone beds include asymmetrical, bifurcated wave ripples, 0.5

cm in height and <4 cm in width (Fig. 10d), graded bedding composed of siltstone-mudstone couplets and normal graded beds (Figs. 10e, f), small clastic dykes (Fig. 10e), curled-up mud chips and domal structures (Fig. 10f). Contacts between the alternating beds are abrupt and generally non-erosional. Small-scale trough crossbeds, planar-bedded sandstones, and Ta-sandstone beds, characterize the sandstone component of the siltstone dominated subunit.

**Hydrodynamic Processes of the SSFA.** The SSFA is the down-slope, lower flow-regime equivalent of the alluvial CFA-I as indicated by the prevalent sandstone component and stratigraphic position. Low-energy bedload- and suspension-sedimentation governed the transport and depositional processes. Minor high-energy traction current processes are indicated by the pebble lags.

The rapid transition with the CFA-I as well as a slightly variable N-S flow component depict either a sandy braidplain (e.g. Plint and Browne, 1994; Wood and others, 1994) or a subaerial to subaqueous, fluvial-influenced fan or braid delta (eg. Hempton and others, 1983; McPherson and others, 1987). Aggradational sets of truncating trough crossbeds or lateral accretional surfaces of tangential trough crossbeds with mudstone drapes are interpreted as migrating shallow-water lunate megaripples (Clifton and others, 1971) or fluvial-dominated braid deltas (Hempton and others, 1983). Mudstone and siltstone drapes between crossbeds and on foresets of bedforms in the sandstone-dominated subunit indicate highly fluctuating flow-energy conditions and waning water stages found in large sandy rivers (Walker and Cant, 1984; Røe and Hermansen, 1993) or rapidly changing wave-energy conditions common to a transitional shoreface environment (Reinson, 1984; Davidson-Arnott and Greenwood, 1987). Trough crossbeds without argillite laminae are considered to be the subaerial, fluvial counterpart, described as in-channel dunes (facies St

of Miall, 1978). Downstream migration of dunes is indicated by vertical stacking of truncating trough crossbeds. In contrast, lateral accretion surfaces display small upward-fining cycles and abundant reactivation surfaces that are consistent with gradual channel abandonment (Willis, 1993). The planar-bedded and planar crossbedded structures represent upper flow regime sands (facies Sh) and linguoid or transverse bars (facies Sp), respectively. In a shallow-water setting, planar crossbeds are indicative of wave-generated, straight-crested dunes (Reineck and Singh, 1980). Thicker argillite beds with ripples possibly formed during extensive overbank flooding in a large pond or small lake. The rapidly changing flow conditions are suggestive of an abundance of flooding that accounts for the observed grain-size distribution and sedimentary structures. Massive pebble horizons or lags (facies Gm) in the sandstone-dominated subunit attest to flash flooding (Blair, 1987a).

The siltstone-dominated subunit was formed by a combination of suspension sedimentation, wave-induced transport, and storm deposition. The argillite beds with siltstone/mudstone couplets are indicative of suspension deposition and associated ripple horizons are consistent with wave-induced currents (Mueller and Dimroth, 1987) or weak oscillatory wave action affecting bottom sediments (Reinson, 1984). Bifurcating, asymmetrical ripples are suggestive of shallow-water wave ripples in the nearshore zone where waves had a stronger forward than backward motion, thus causing ripple asymmetry (Reineck and Singh, 1980). The sediment was deposited rapidly as suggested by the presence of cm-size clastic dykes or pipes, and dish and pillar structures which formed during dewatering in association with consolidation (Lowe, 1975). Shallow ephemeral lakes or ponds (Mueller and others, 1994) with flash flooding best characterize the siltstone-dominated subunit. Graded sandstone beds are indicative of a periodic influx of high energy conditions commonly attributed to storms (Howard and Reineck, 1981; Kreisa, 1981).

Environments demonstrating rapid deposition of mud and sand commonly contain clastic dykes (Reineck and Singh, 1980).

The overall depositional environment of the SSFA is problematic, however the sedimentary structures, rapidly changing facies associations, and paleocurrent data favour an anastomosing sandy braidplain with numerous small lakes and ponds. The absence of vegetation during the Archean would have facilitated the development of extensive braided patterns and the well-developed flood cycles (Schumm, 1968; Galloway and Hobday, 1983).

**Conglomerate Facies Association-II (CFA-II).** The CFA-II, with a maximum thickness of 120m and a limited lateral extent of 4km, constitutes only 4% of the overall sedimentary succession (Fig. 4b). The CFA-I erosionally overlies the SSFA and is in turn conformably overlain by the quartz-rich sandstone facies association (Fig. 6a). Massive, amalgamated, 10-20m-thick, clast-supported conglomerates dominate in select areas. Shallow conglomerate-filled channels were observed only at one locality. The polymictic character of this facies association is evident on shoreline outcrops (Fig. 11a). Cobbles are subrounded to rounded and imbrication is locally discernable. The results of 28 measurements show the mean a-axes of clasts to be aligned in an ENE-WSW direction, generally oblique and some transverse to the main NNE flow direction determined from the paleocurrent measurements. Clast counts indicate that the percentage of matrix ranges from 25% to 27%.

Trough crossbedded sandstones, 5-30cm-thick, are interstratified with 10-20cm-thick planar beds in 0.20-2m-thick cosets. Truncating sets of trough crossbeds are abundant in the south part of the formation. Sandstone interbeds in thick amalgamated conglomerate successions are generally < 40cm-thick.

**Hydrodynamic Processes of the CFA-II.** Clast-supported amalgamated conglomerates indicative of facies Gm (Miall, 1978), containing rounded to well-rounded clasts and locally displaying prominent imbrication, accord with streamflow deposits on alluvial or proximal braided streams (Middleton and Trujillo, 1984; Rust and Koster, 1984). Conglomerate-filled channels (facies Gt) are suggestive of confined streamflow dominated processes. Truncating sets of trough crossbeds within sandstone interbeds represent in-channel migration of lunate megaripples (facies St) while planar beds (facies Sh) reflect upper flow regime deposition along the flanks or lee sides of gravel bars. This facies association is similar to the clast-supported conglomerates of the CFA-I. Orientation of cobbles normal to flow is suggestive of a low-gradient river setting (Sengupta, 1966). The CFA-II best represents longitudinal gravel bars and confined in-channel gravels associated with flow-dissipating sands in areas with consistent stream flow in which only bedload material was deposited.

**Quartz-Rich Sandstone Facies Association (QSFA).** The QSFA, with a maximum thickness of 320m (Fig. 6a, Section I), is the dominant lithology constituting 46% of the mappable clastic units in the BRF (Figs. 4b, 6a, b). This facies association occupies the heart of the basin. Coarse- to very coarse-grained sandstone predominates, but granular to pebbly sandstone is also present. The principal sedimentary structure is high-angle, large- and small-scale trough crossbeds (Fig. 11b), whereas planar crossbeds, planar beds, and siltstone layers are rare (Fig. 12). Trough crossbeds, 10-30cm-thick, generally occur in vertical truncating or lateral accretion sets between 30-100cm-thick (Fig. 11b) . Large composite troughs range from 1-3m-thick and have a lateral extent exceeding 10m in length (Fig. 11c). Reactivation surfaces are common to these structures. Paleocurrent

measurements (Fig. 4b) of trough crossbeds obtained from the southern, east-facing homoclinal part of the Beaulieu Rapids Basin indicate basin parallel flow with a prominent northerly flow direction.

Tangential foresets are commonly draped by pebbles (Fig. 11d) and granules where the pebble size generally increases toward the base of the laminae, although larger pebbles are sometimes concentrated along the upper zone. Trough crossbedding is very well-preserved in the southern portion of the basin, whereas in more northerly areas, sedimentary structures are difficult to distinguish due to thin laminae and lack of contrast between adjacent bed compositions. Planar crossbeds rarely form sets and only appear sporadically throughout the facies association. Argillite rip-ups are restricted to the northern basin localities. Thin (< 3 mm) argillite laminae exist between bedsets and as drapes on foresets of trough crossbeds.

**Hydrodynamic Processes of the QSFA.** Bedload transport dominated during the deposition of the QSFA, as indicated by the ubiquitous presence of cosets of truncating trough crossbeds. The dominance of these structures can be attributed to the in-channel migration of sinuous-crested megaripples (Mueller and others, 1994), downstream migration of lower point bars (Eriksson, 1978), or a combination of the two where sand bars were covered by sinuous-crested dunes in the deeper parts of channels (Willis, 1993). Large channels are composed of composite bedforms common to fluvial sequences. Reactivation surfaces suggest lateral sandbar migration (Røe and Hermansen, 1993; Willis, 1993) caused by a change in flow direction or periodic flow fluctuations (Rainbird, 1992). Vertical aggradation of truncating cosets of medium- to large-scale trough crossbeds resulted from megaripple progradation along channel bottoms during relatively high and constant flow stages. The crossbeds were developed by avalanching of sediment down the lee sides of

megaripples. Following the development of foresets, the process continued with avalanching of coarser-grained material down lee-slopes as seen in the pebble-laden foresets of troughs.

Straight-crested megaripples represented by planar crossbeds (facies Sp) formed during lower flow regime stages (Miall, 1978) and may be the result of downstream accretion of transverse bars during constant flow. Planar beds (facies Sh), rarely present, are indicative of upper flow regime conditions. Mud drapes (facies Fl) formed in the same manner as those found in the SSFA: low-water stands created megaripples whose troughs were then covered with suspension-deposits. Collectively, these aspects are suggestive of a sandy braidplain with relatively high-energy transport. Basin parallel flow, as indicated by paleocurrent data, supports this interpretation.

The absence of fining-upward cycles common to fluvial processes (Walker and Cant, 1984; Willis, 1993) indicate that rapid flow dissipation allowed the suspended fines to bypass this setting and accumulate downslope. Alternatively, incomplete weathering associated with high-energy transport processes and lack of vegetation which characterized Archean sedimentary systems may have inhibited the prolonged exposure needed to weather source rocks into mud and silt.

## PROVENANCE

Framework modes of terrigenous sandstones and clast compositions of conglomerates define provenance terranes. Detailed petrographic analyses of sandstones in Archean sedimentary or volcano-sedimentary successions have been restricted to a few selected areas such as the Figtree and Moodies Groups of the Barberton greenstone belt (Eriksson and others, 1994), the Lalla Rookh Basin (Eriksson and others, 1994), and the Panorama Formation (DiMarco and Lowe, 1989) of the Pilbara Block. Clast population analyses in conglomerate beds have been employed in the strike-slip basins (Mueller and others, 1991, 1994) and dissected arc basins (Mueller and Dimroth, 1987) of the Archean Abitibi greenstone belt.

### **Sandstone Petrography**

**Methods, constraints and characteristics.** Detailed analyses were made of framework constituents in thirty-two thin sections of the sandstone facies associations of the BRF. Twenty-four of these were taken from the QSFA and eight from the SSFA. Biased results were avoided by obtaining widely-distributed samples throughout the sedimentary basin as the dominant source areas may have changed along strike and vertically in the stratigraphy. Cobaltinitrite staining of sandstones for potassium feldspar and point-counting using the Gazzi-Dickinson method was employed (Ingersoll and others, 1984). Sample grain size, texture and maturity were also evaluated. The quartz-feldspar-phyric and hornblende-feldspar phyric porphyry stocks along the eastern basin-margin (Table 2), the volcanic rocks immediately underlying the formation, and the gneisso-plutonic rocks of granitic and tonalitic composition (Table 2) from the nearby Sleepy Dragon Complex were



sampled to determine possible source areas. Specific framework parameters were employed (Table 3) and the results were plotted on three ternary diagrams used to determine source and tectonic environment. These include: 1) a QFL diagram and 2) a QmFLt diagram, (Dickinson and Suzcek, 1979; Dickinson and others, 1983) as well as a proposed LpLvLs diagram that allows direct comparison with the conglomerate clast population.

The QSFA is dominated by coarse- to very coarse-grained sandstones, but medium- to very fine-grained varieties also occur. Grain size varies according to location in the basin with the coarser sandstone found at the northern extremity of the basin and adjacent to the unconformity. The SSFA is predominantly composed of coarse siltstone to fine-grained sandstone; grain size does not appear to be related to basinal location. Although the QSFA and the SSFA are differentiated by grain size and sedimentary structures, their textures and mineralogy are strikingly similar.

At least 350 points were counted using a spacing interval that allowed for total thin section coverage. Samples containing > 20% matrix were discarded and grains finer than 0.03mm were classified as matrix. All sandstones are immature to submature, based on the textural maturity flow chart of Pettijohn et al. (1973). Combined quartz varieties (Qt), polycrystalline (Qp) and monocrystalline grains (Qm), are subangular to subrounded in form and range between 0.1-1.0 mm in size. Polycrystalline grains typically exhibit sutured boundaries, and commonly contain more than three quartz crystals. Both quartz varieties demonstrate undulatory extinction. The plagioclase (P) to total feldspar (F) ratio of 0.73 indicates that the potassium feldspar (K) content is subordinate in the sandstones. Lithic fragments (Lt) are primarily of plutonic (Lp) derivation as well as of volcanic (Lv) and sedimentary (Ls) origin. Plutonic grains (Lp) are comprised of polymineralic quartz, polymineralic quartz and feldspar, or quartz, feldspar and biotite (c.f. Basu, 1976). Volcanic lithic fragments (Lv) are very fine-grained and are of intermediate-basaltic composition.

Sedimentary grains (Ls) are very fine-grained sandstone or siltstone that are chiefly composed of quartz and feldspar with minor chlorite, biotite, and/or sericite. Quartz, chlorite, actinolite and white mica characteristically constitute the matrix of the sandstones.

**Results.** The sandstones of the two facies associations in the BRF are subfeldsarenites to lithic arkoses (Folk and others, 1970) and in terms of basin and terrane analysis, plot in the recycled orogen provenance of the QFL diagram (Fig. 13a). The QFL diagram emphasizes grain stability and hence, the effects of weathering and basin relief during erosion and transport (Dickinson and Suzcek, 1979). Combined quartz ( $Q_t=Q_m+Q_p$ ), which controls the framework mode, ranges from 58-90% and accounts for 73% of the population, while combined feldspars ( $F=K+P$ ) and rock fragments ( $L_v+L_s$ ) account for 14% and 13%, respectively. Potassium feldspar (K) constitutes <5%, but notably sandstones from the northeastern region of the basin display a slightly higher K-feldspar content of ~10% (samples PLC-94-24,25; PLC-95-34) attributed to the proximity of the quartz-feldspar porphyry stocks. The sedimentary rocks of the Beaulieu Rapids Basin plot in the lithic recycled field of the recycled orogen provenance on the  $Q_mFLt$ -diagram (Fig. 13b). This diagram is a measure of the importance of grain size in the source terrane, emphasizing individual components such as monocrystalline quartz and feldspar with respect to the total lithic repertoire ( $L_t=L_v+L_s+L_p+Q_p$ ). The  $L_pL_vL_s$  ternary diagram (Fig. 13c) permits the direct comparison of rock fragments in the sandstones with the clast population in the conglomerate beds. The conglomerates are dominated by plutonic and volcanic clasts with an almost negligible sedimentary clast component. There is a marked decrease in plutonic clasts from conglomerate I to conglomerate II. Similarly, plutonic rock fragments are typically found in the SSFA as opposed to the QSFA. The parallelism of the two trends suggests that two distinct cycles of deposition occurred, including: 1) the CFA-I and the SSFA and 2) the CFA-II and the QSFA.

## **Conglomerate Composition**

**Methods and constraints.** Conglomerates in tectonically-controlled sedimentary basins display compositional signatures of nearby uplifted source terranes in the form of clasts. Reliable clast-counting methods can aid substantially in identifying sedimentary provenance (Howard, 1993). No other method of determining provenance provides more definitive evidence for possible source formations (Graham and others, 1986).

A total of 4597 clasts were counted (Fig. 14) in seven distinct localities (Fig. 4b). The sample locations were randomly chosen and, where possible, at least 400 clasts were counted in four or more closely-spaced zones to minimize the error (Howard, 1993). Any remaining errors in the true percentage of clast compositions may have resulted from the low potential of including deeply buried clasts or smaller clasts as opposed to larger components (Howard, 1993) and clast survivability. The latter is controlled by climate, diagenesis and tectonic processes (DeCelles, 1988).

**Results.** Clasts counts in the conglomerate beds indicate that the volcanic and plutonic components on average account for 42.5% and 38%, respectively. Quartz (<8%), felsic volcanic (<11%), and sedimentary fragments (<.5%) constitute only a minor proportion. The clast counts indicate a dominance of tonalitic to granodioritic clasts (Fig. 11e), but dioritic, quartz-rich granitic, gneissic, and magmatic breccia clasts (Fig. 11f) were also identified. Porphyry clasts are abundant along the northeast basin margin comprising up to 40% of the clast population in that particular area (visual estimate).

## DISCUSSION

Strike-slip basins are characterized by distinct tectonic signatures that influence sedimentation patterns (Steel and others, 1977; Heward, 1978) with local volcanism (Hempton and Dunne, 1984), commonly of alkaline to calc-alkaline character (Cole and Ridgway, 1993; Mueller and others, 1994). Basins of this nature are products of large-scale horizontal plate motion associated directly or indirectly with subduction-related processes. Several features in the Beaulieu Rapids Basin support a strike-slip genesis, including: (1) the general basin characteristics, (2) the basin architecture and depositional environments and, (3) tectonic influence on sedimentation. Provenance studies reflect tectonic setting and climatic conditions during deposition. This study furnishes a well-documented example of an Archean strike-slip basin. The characteristic features of the Beaulieu Rapids Basin are comparable to those of modern strike-slip basins and are therefore significant in the evolution of the SSP.

### **General Basin Characteristics**

Structural elements and internal basin geometry make possible the interpretation of basin-forming processes in strike-slip basins (Sylvester, 1988; Ringenbach and others, 1993). These fault-bounded basins are generated by a larger spectrum of deformation commonly associated with crustal-scale movements (Christie-Blick and Biddle, 1985; Ringenbach and others, 1993). Major crustal structures influence the location of strike-slip faults and the manner in which basins develop along them (Christie-Blick and Biddle, 1985). The Beaulieu Rapids Basin, the time equivalent inferred sedimentary rocks of the Keskarrah Formation (Corcoran and others, 1996), and the >2.9Ga Beniah Lake quartz-

arenite (Roscoe and others, 1989; Fig. 3) formed along the 300km, N-trending, Beniah Lake Fault (Fig. 1).

Faults along basin margins are typical of sequences that are tectonically-controlled or involved with rapid subsidence (e.g. Krapez and Barley, 1987). Geometrically, the Beaulieu Rapids sedimentary basin is elongate and asymmetrical. Strike-slip basins of the simple pull-apart type produce an aspect ratio (length to width) of at least 3:1 (Aydin and Nur, 1982). A slightly higher ratio of 4.75:1 for the Beaulieu Rapids Basin is suggestive of subsequent basin erosion along the margin and/or continued strike-slip deformation.

Porphyry stock emplacement along the eastern fault margin (Fig. 4b) is synchronous with basin evolution and is consistent with local extension. Clasts derived from the quartz-feldspar- and hornblende-phyric porphyry stocks were observed locally in the adjacent conglomerates, suggestive of emplacement and exhumation of the stocks contemporaneous with strike-slip movement. Preliminary U-Pb geochronology of the porphyry yields complex zircon systematics. Most of the zircons are inherited and suggest a component of pre-3.0Ga basement. Zircons without inheritance are high-uranium and are discordant. A preliminary interpretation of the data is that the porphyry is ca. 2.6Ga with inheritance of a much older component (S. Bowring, personal communication), thus providing a well defined timeframe for the crystallization age of the porphyry stocks in addition to a maximum age for the sedimentary sequence.

En echelon folds form in convergent strike slip regimes (Christie-Blick and Biddle, 1985) or develop during crustal shortening (Sylvester and Smith, 1976). These folds are generally confined to a narrow but persistent zone adjacent to a major fault (Sylvester, 1988). The en echelon anticlines and synclines have a mean axial trace of 029°N, explained by left simple shear. The  $S_1$  axial planar foliation conforms to the sinistral movement. The Beaulieu Rapids Basin geometry, prominent NNE-trending en echelon folds associated with

an axial planar foliation, and porphyry stock emplacement along the basin-forming fault are convincing indicators of a sinistral strike-slip basin formation (Figs. 3; 4a, b). The presence of en echelon folds to the north and a homoclinal less-deformed sequence in the south resembles the modern Hanmer strike slip basin along the Hope Fault in New Zealand. The proposed pattern of deformation includes transpression exemplified by a relay pattern of folds at the eastern end and transtension with extensional normal faults and basin subsidence at the western extremity (Wood and others, 1994). The observed deformation pattern, facies associations and basin geometry of both basins is similar, therefore, Beaulieu Rapids Basin may also have formed in a transpression-transtensional regime.

### **Basin Architecture and Depositional Environment**

The chronological succession of the facies associations within the 0.2-1km thick Beaulieu Rapids Formation is the result of allocyclic events such as tectonism, basin subsidence, or long term climatic changes, while the characteristics of the facies associations represent a succession of sedimentary bedforms that comply to short term autocyclic changes, such as floods. Combined, these factors govern facies distribution and hence, basin configuration.

Sedimentary facies architecture, the result of sequential basin evolution, can be divided into two complementary paleogeographic phases (Figs. 15a, b). The southern part of the Beaulieu Rapids Basin displays two large-scale fining-upward cycles (Fig. 6a, Section IV): (1) the combined 375m-thick CFA-I and the SSFA and (2) the 300-400m-thick CFA-II coupled with the QSFA. The facies sequence  $Gm \pm Gms \pm Gt \pm Sm_a - St - Sh \pm Sp \pm Fl$  of the CFA-I (Table 1) shows a prevalence of confined streamflow processes with minor debris and hyperconcentrated flow deposits all of which are an inherent part of alluvial fans (Mack and

Rasmussen, 1984; Rust and Koster, 1984; Blair, 1987a) or fan deltas (McPherson and others, 1987; Flint and others, 1986; Horton and Schmitt, 1996). Fan-building is commonly characterized by incipient unconfined catastrophic flood events in which braided channels are subsequently incised (e.g. Blair, 1987a). The lateral extent of the basal conglomerate unit along the basin margins represents coalescing fans, common to structurally-controlled basins (Steel and others, 1977; Christie-Blick and Biddle, 1985). Significant relief is a prerequisite for the generation of coarse clastic debris that flowed transverse to the basin axis (Fig. 15a). The rapid and abrupt vertical juxtaposition of the siltstone-sandstone facies association indicates a fundamental change in flow energy conditions and depositional environment. Paleoflow directions, although variable, are predominantly basin parallel. The facies sequence St-Sp-Sh-Fl of the SSFA (Table 1) is characteristic of a sandy fine-grained braidplain setting with numerous ephemeral ponds or small lakes (Fig. 15a). Small sandy braid deltas (McPherson and others, 1987; Plint and Browne, 1994) with an increase in the mudstone-siltstone (argillite) component indicate a transition from fluvial to lacustrine deposits. Thicker beds of argillite in the siltstone-dominated subunit are suggestive of deposition in small lakes (Blair, 1987b; Mueller and others, 1991; Plint and Browne, 1994)

The 120m-thick CFA-II commences the second fining-upward cycle (Fig. 15b). The facies sequence Gm±Gt-St±Sh (Table 1) is characteristic of streamflow-dominated processes that are found on alluvial fans or proximal braidplains (Miall, 1978; Rust and Koster, 1984). The latter is favoured because of the well-rounded clasts, the clast-supported nature of the conglomerates, and the abrupt underlying contact with the SSFA. The limited lateral extent of the cycles is indicative of asymmetric tectonic influence with local uplift prevailing in the mid-southern region of the basin. The facies sequence Ss±Gm-St±Sh±Sp±Fl of the QSFA (Table 1) represents a coarse-grained sandy braidplain characterized by confined flow in shallow high-energy streams. The absence of unconfined

sheetflood deposits support the interpretation of a traction current, braided-stream setting, as indicated by a prominent basin-parallel flow component.

In the northern part of the basin, the CFA-I and the QSFA are the dominant lithological units. The CFA-1 grades directly into the siltstone-dominated subunit of the SSFA, representing a part of a fan delta or a braid delta passing directly into a small lake. Rapid infilling of the lake is characterized by dish and pillar structures (Figs.10e, f). The facies distribution indicates that extensive clastic input diminished the abundance of ponds and small lakes through time. Such rapid basin infilling is characteristic of small tectonically-controlled basins. Further criteria consistent with strike-slip basin formation is the distribution of facies associations: marginal coarse clastic fans or fan deltas (CFA-1) with transverse flow direction prograding into a fine-grained braidplain and/or lake (SSFA, QSFA) that displays basin parallel flow (e.g. Rust and Koster, 1984; Nilsen and McLaughlin, 1985; Blair, 1987b; Wood and others, 1994).

The recognition of porphyry stocks at the basin margin and porphyry clasts within the conglomerate (Corcoran and Mueller, 1995b) is significant as this feature is characteristic of the strike-slip basins in the Wabigoon Subprovince (Kresz, 1984) and in the Abitibi greenstone belt (Mueller and others, 1991, 1994). The fact that the stocks are not restricted to one greenstone belt nor one Archean craton suggests that similar tectono-magmatic processes occurred and that late transcurrent movement may have been a common feature.



## **Tectonic Influence on Sedimentation**

The features indicative of tectonic influence on sedimentation that are evident in the Beaulieu Rapids basin include: (1) rapid vertical and lateral facies changes over tens of metres (e.g. Christie-Blick and Biddle, 1985; Figs. 6a, b), (2) cyclic repetition of similar lithological units over 100's of metres (e.g. Rust and Koster, 1984; Fig. 4b), (3) fining-upward sequences in the coupled conglomerate and sandstone units (e.g. Heward, 1978; Fig. 6a, Section IV), (4) high sediment accumulation rates implying rapid subsidence (e.g. Johnson, 1985), (5) the presence of basin margin unconformities (Fig. 4a) and abundant intrabasinal erosional contacts (e.g. Johnson, 1985; Fig.8c), (6) coarse clastic detritus at the basin margin passing laterally into central shallow-water deposits (e.g. Hempton and others, 1983; Blair, 1987b; Figs. 15a, b), and (7) a thick stratigraphic sequence in comparison with basin size (e.g. Christie-Blick and Biddle, 1985).

Strike-slip movement created local extension as documented in the basin itself as well as the emplacement of porphyry stocks. Uplift, synchronous with basin subsidence, caused significant topographic relief that facilitated alluvial-fan formation at the faulted margin (Figs. 15a, b). The asymmetric distribution of facies associations between the northern and southern regions of the basin further attests to local diachronous tectonism which is a common characteristic of strike-slip basins (Johnson, 1985).

## **Significance of Source Areas and Climatic Influence**

The composition of sandstones and conglomerates are the direct results of source rocks, tectonic influence, and climate. These factors influence the position of the components on QFL, QmFLt, and LpLvLs ternary diagrams. Original source rock compositions are

reflected in the absence or presence of key minerals and/or rock fragments. Additionally, relief propagated by uplift and subsidence, transport distance, and intensity of deposition are all contingent on tectonic influence. The third factor, climate, affects the composition of sedimentary rocks through the degree of weathering.

The BRF sandstones plot in the recycled orogenic provenance on the QFL and QmFLt diagrams (Figs. 13a-c). Folded and faulted sedimentary and metasedimentary rocks are generally considered to be the sources for sandstones of this composition (Dickinson and Suczek, 1979). There are no sedimentary sequences surrounding the BRF and, hence, the classification is not wholly valid. Intermediate to high quartz contents accompanied by low feldspar percentages are alternatively attributed to a gneisso-plutonic source with little or no significant potassium feldspar. Other possible source rocks for recycled orogen detritus include plutonic terranes involved in crustal collision leading to sediment deposition in complex successor, or late-stage basins (Dickinson and Suczek, 1979). The Beaulieu Rapids Basin formed during the latest stages of cratonization of the Slave Province and possesses the significant characteristics of successor basins (c.f. Ingersoll, 1988; Mueller and Donaldson, 1992).

The high percentage of rock fragments on the QmFLt diagram (Fig. 13b) is primarily a function of incorporating Qp with Lt. The prevalence of lithic fragments implies that a high and rapid sediment influx due to tectonism was important and transport distances must have been limited. However, polycrystalline quartz is essentially a monomineralic resistate fragment (Basu, 1976). Therefore, it will not react to transport and subsequent weathering in the same manner as do other lithic fragments. The amount of fragments, with the exception of Qp, then becomes largely a function of climate and source.

Labile minerals in Lv and Ls are preferentially affected by weathering in humid climates as opposed to arid climates (Basu, 1976; Potter, 1978, 1986). Suttner and others (1981),

upon plotting numerous samples derived from both arid and humid regions on a QFL diagram, discovered that there is a marked difference in sandstone composition. The arid samples tend to contain lower percentages of quartz and higher amounts of lithic fragments in contrast to the humid samples. Quartz, a resistant mineral, survives much longer in a humid climate where rock fragments are weathered into individual minerals. The fact that the quartz is predominantly polycrystalline signifies several important factors (Blatt and Christie, 1963). 1) The source rocks were proximal to the sedimentary basin because polycrystalline quartz is destroyed more rapidly than monocrystalline varieties, and 2) the sandstones did not undergo a multicycle origin, as monocrystalline quartz becomes dominant with successive sedimentary cycles. Plutonic rocks typically supply considerable proportions of polycrystalline quartz to sediments (Blatt and Christie, 1963).

The comparative LpLvLs ternary plot (Fig. 13c) shows an abundance of plutonic fragments in both the sandstones and conglomerates. In addition to the two fining-upward sequences in the southern region of the basin, represented by differences in the proportion of plutonic fragments, there is also a change in the percentage of sedimentary fragments. The absence of sedimentary rock surrounding the basin indicates that the influx of sedimentary rock fragments in the QSFA resulted from continuous tectonic uplift and penecontemporaneous erosion of intraformational basin sediments located lower in the stratigraphic sequence. The fragments must have been derived from the SSFA. The fact that sedimentary clasts are absent or minimal in the clast population of the conglomerates supports this hypothesis. Cannibalism of basin sediments is not uncommon in tectonically-controlled basins (Wood and others, 1994; Dart and others, 1995).

The sandstone and conglomerate components signify that there were at least four dominant local source areas for the Beaulieu Rapids detritus: 1) the gneisso-plutonic Sleepy Dragon Complex (Table 2), 2) the mafic-intermediate volcanic rocks of the Beaulieu River

volcanic belt, 3) the porphyry stocks emplaced along the northeastern boundary (Table 2), and 4) the felsic volcanic rocks located southeast of the basin. The presence of quartz clasts reflects the erosion of quartz veins that are common in the Sleepy Dragon Complex and the neighbouring porphyry stocks as well as in the volcanic rocks. Abundant polycrystalline quartz and plutonic fragments, in addition to minor volcanic fragments in the sandstones were also derived from the adjacent quartz-rich, plutono-gneissic rocks and the Beaulieu River volcanic belt.

### **Significance and Modern Counterparts**

Comparisons between ancient and present-day tectonic processes and their products by sedimentary facies analysis allows interpretation of the development of Archean sequences. Modern strike-slip basins develop in island arcs (Hathway, 1993), active continental margins (Crowell, 1974; Christie-Blick and Biddle, 1985), and cratonic settings (Hempton and Dunne, 1984). The occurrence of long strike-slip faults is strong evidence for the existence of rigid plates and deformable plate boundaries (Sleep, 1992). Modern prototypes include: (1) the Hanmer basin, Hope fault, New Zealand (Wood and others, 1994), (2) the Hazar Lake, East Anatolian fault, Turkey (Hempton and others, 1983), (3) the Ridge basin, San Andreas fault, USA (Crowell, 1974), (4) the Nadi basin, Sovi fault, Fiji (Hathway, 1993), (5) the Kuji basin, Taro fault, Japan (Minoura and Yamauchi, 1989), and the Little Sulfur Creek basin, Maacama fault, USA (Nilsen and McLaughlin, 1985).

The Beaulieu Rapids Basin has similar structural, geometrical and sedimentary characteristics of these modern strike-slip basins that are governed by major fault systems. Transcurrent motion occurred at circa 2600Ma, after the SSP had been consolidated and arc terrane accretion had ceased. Most authors agree that Archean plate tectonics were active in a

modified version (e.g., Sleep and Windley, 1982; Abbott and Hoffman, 1984; Taira and others, 1992) possibly due to the presumed higher heat budget (Bickle, 1978; Sleep, 1992). The deformation style of most greenstone belts is comparable to subduction-related Phanerozoic orogenic belts (Kusky and Vearncombe, 1995).

The importance of the N-trending Beniah Lake fault zone is augmented by its recognition as a significant Pb-Pb isotope boundary dividing the SSP into distinct eastern and western segments (Padgham, 1992; Padgham and Fyson, 1992; Thorpe and others, 1992). According to Padgham (1992), the Beniah Lake fault zone may represent the trace of a pre-2.8Ga suture that was reactivated numerous times. Late transcurrent motion with strike-slip basin formation are a logical extension of this hypothesis. Successor basins of this nature commonly develop at terrane boundaries (Ingersoll, 1988). Seismic recognition of an Archean subduction zone to the north of the Abitibi greenstone belt (Calvert et al., 1995) and unequivocal documentation of terrane docking (Mueller et al., 1996) indicate that plate tectonic processes were active during the early evolution of the earth. Whether or not the Beniah Lake Fault defines an Archean collision or suture zone can be tested and resolved using deep seismic profiles of the Slave craton through LITHOPROBE. The Beaulieu Rapids Basin is interpreted as a late-stage product of a subduction-related process.

## CONCLUSIONS

The structural elements, basin geometry, sedimentary facies organization and depositional setting of the BRF compare favourably with modern strike-slip analogues that are principally driven by horizontal movements related to large-scale plate tectonic processes. The major N-trending Beniah Lake fault is a crustal-scale structure that divides the SSP into

an older (> 2.8Ga) continental-type western segment with quartz-arenite successions and a younger arc-type eastern segment (< 2.8Ga; Padgham, 1992).

The facies associations, in addition to their stacking and organization are suggestive of tectonic control on sedimentation, displaying two depositional sequences. Extensive weathering of uplifted source rocks followed by rapid infilling of the basin occurred during depositional cycle I. The coarse clastic detritus concentrated at the basin margins represents first-cycle alluvial fans, proximal braided streams and braid-deltas that prograded into a central sandy braid-plain with local ponds and small lakes. A second phase of tectonic activity contributed accessory material represented by the CFA-II and the QSFA. The high influx of debris during cycle I filled most of the basin, as demonstrated by the absence of lacustrine deposits and the omnipresence of fluvial deposits that accumulated in a large low-gradient braidplain during depositional cycle II. Flow direction in the sandstones is basin parallel, consistent with clast imbrication results obtained from the conglomerates. Local basin extension is further demonstrated by the emplacement and exhumation of the <2.6Ga porphyry stocks.

Individual mineral and rock fragment components in the sandstones and clast components in the conglomerates indicate that the majority of the detritus was derived from a plutonic source terrane during humid climatic conditions. Subordinate source areas appear to have been local. Tectonic provenance diagrams indicate that the Beaulieu Rapids Basin plots in the recycled orogen field, not surprising considering the successor-molasse-type nature of the basin. The BRF, a rare example of an Archean strike-slip basin is of fundamental importance due to its association with >2.5Ma plate tectonic processes.

## ACKNOWLEDGMENTS

This project has been funded by NSERC and LITHOPROBE grants as well as the geology division of Indian Affairs and Northern Development, Northwest Territories, Canada. Many thanks to E. H. Chown, D. W. Roy, and S. Bowring for their critical comments which improved the manuscript. The authors are indebted to C. Dallaire for his drafting skills. We would also like to thank field assistants S. Belley, J. Bucher and F. Savoie for their hard work and incredible patience.

**REFERENCES CITED**

- Abbott, D. A., and Hoffman, S. E. 1984, Archean plate tectonics revisited: Heat flow, spreading rate, and the age of subducting oceanic lithosphere and their effects on the origin and evolution of continents: *Tectonics*, v. 3, p. 429-448.
- Aydin, A., and Nur, A., 1982, Evolution of pull-apart basins and their scale independence: *Tectonics*, v. 1, p. 91-105.
- Ayres, L. D., 1982, Pyroclastic rocks in the geologic record, *in* Ayres, L. D., ed., *Pyroclastic volcanism and deposits of Cenozoic intermediate to felsic volcanic islands with implications for Precambrian greenstone-belt volcanoes: Geological Association of Canada Short Course Notes*, v. 2, p. 1-17.
- Ballance, P., 1984, Sheet-flow dominated gravel forms on the non-marine Middle Cenozoic Simmler Formation, central California. *Sedimentary Geology*, v. 38, p. 337-359.
- Basu, A., 1976, Petrology of Holocene fluvial sand derived from plutonic source rocks: implications to paleoclimate interpretation: *Journal of Sedimentary Petrology*, v. 46, p. 694-709.
- Best, J. and Bridge, J., 1992. The morphology and dynamics of low amplitude bedwaves upon upper stage plane beds and the preservation of planar laminae. *Sedimentology*, 39: 737-752.
- Bickle, M. J. 1978, Heat loss from the earth: A constraint on Archean tectonics from the relation between geothermal gradients and the rate of plate production. *Earth and Planetary Science Letters*, v. 40, p. 301-315.
- Blair, T. C., 1987a, Sedimentary processes, vertical stratification sequences, and geomorphology of the Roaring River alluvial fan, Rocky Mountain National Park, Colorado: *Journal of Sedimentary Petrology*, v. 57, p. 1-18.
- Blair, T. C., 1987b, Tectonic and hydrologic controls on cyclic alluvial fan, fluvial, and lacustrine rift-basin sedimentation, Jurassic-lowermost Cretaceous Todos Santos Formation, Chiapas, Mexico: *Journal of Sedimentary Petrology*, v. 57, p. 845-862.



- Blatt, H., and Christie, J. M., 1963, Undulatory extinction in quartz of igneous and metamorphic rocks and its significance in provenance studies of sedimentary rocks: *Journal of Sedimentary Petrology*, v. 33, p. 559-579.
- Bowring, S. A., Williams, I. S., and Compston, W., 1989, 3.96 Ga gneisses from the Slave Province, Northwest Territories Canada: *Geology*, v. 17, p. 971-975.
- Brierley, G. J., Liu, K., and Crook, K. A. W., 1993, Sedimentology of coarse-grained alluvial fans in the Markham Valley, Papua New Guinea: *Sedimentary Geology*, v. 86, p. 297-324.
- Calvert, A., Sawyer, E. W., Davis, W. J., and Ludden, J. N., 1995, Archaean subduction inferred from seismic images of a mantle suture in the Superior Province: *Nature*, v. 375, p. 670-674.
- Chown, E.H., Daigneault, R., Mueller, W., and Mortensen, J.K., 1992. Tectonic evolution of the northern volcanic zone, Abitibi belt, Quebec. *Canadian Journal of Earth Sciences*, 29, 2211-2225.
- Christie-Blick, N., and Biddle, K. T., 1985, Deformation and basin formation along strike-slip faults, *in* Biddle, K. T., and Christie-Blick, N., eds., *Strike-slip deformation, basin formation, and sedimentation: Society of Economic Paleontologists and Mineralogists Special Publication 37*, p. 1-34.
- Clifton, H.E., Hunter, R.E., and Phillips, R.L., 1971, Depositional structures and processes in the non-barred high-energy nearshore: *Journal of Sedimentary Petrology*, v. 41, p. 651-670.
- Cole, R. B., and Ridgway, K. D., 1993, The influence of volcanism on fluvial depositional systems in a Cenozoic strike-slip basin, Denali fault system, Yukon Territory, Canada: *Journal of Sedimentary Petrology*, v. 63, p. 152-166.
- Corcoran, P. L., and Mueller, W., 1995a, The Beaulieu formation, Slave Province, NWT: a late orogenic molasse basin?: *Indian and Northern Affairs, N.W.T., EGS 1995-13*, 19p.
- Corcoran, P. L., and Mueller, W. U., 1995b, Alluvial-fan and fluvial-dominated deposits in an ancient strike-slip basin: Archean Beaulieu Rapids formation, NWT: *Exploration Overview 1995, Northwest Territories, Indian Affairs and Northern Development, Abstracts*, p. 3-8.

- Corcoran, P. L., Mueller, W. U., Bucher, J., and Savoie, F., 1996, The Keskarrah formation at Cyclops Peninsula: EGS map and marginal notes, (in press).
- Corfu, F., Krogh, T. E., Kwok, Y. Y., and Jensen, L. S., 1989, U-Pb zircon geochronology in the southwestern Abitibi greenstone belt, Superior Province: *Canadian Journal of Earth Sciences*, v. 26, p. 1747-1763.
- Crowell, J.C., 1974, Origin of Cenozoic basins in southern California, *in* Dickinson, W. R., ed., *Tectonics and sedimentation: Society of Economic Paleontologists and Mineralogists Special Publication*.22: p. 190-204.
- Cunningham, M. P., and Lambert, R. St J., 1989, Petrochemistry of the Yellowknife volcanic suite at Yellowknife, N.W.T.: *Canadian Journal of Earth Sciences*, v. 26, p. 1630-1646.
- Daigneault, R., St-Julien, P., and Allard, G. O., 1990, Tectonic evolution of the northeast portion of the Archean Abitibi greenstone belt, Chibougamau area, Quebec: *Canadian Journal of Earth Sciences*, v. 27, p. 1714-1736.
- Damanti, J. F., 1993, Geomorphic and structural controls on facies patterns and sediment composition in a modern foreland basin, *in* Marzo, M., and Puigdefabregas, C., eds., *Alluvial sedimentation: International Association of Sedimentologists Special Publication* 17, p. 221-233.
- Dart, C., Cohen, H. A., Akyüz, H. S., and Barka, A., 1995, Basinward migration of rift-border faults: implications for facies distributions and preservation potential: *Geology*, v. 23, p. 69-72.
- Davidson-Arnott, R. G. D., and Greenwood, B., 1987, Facies relationships on a barred coast, Kouchibouguac Bay, New Brunswick, Canada, *in* *Beach and nearshore sediments and processes: Society of Economic Paleontologists and Mineralogists Special Publication* 24, p. 71-90.
- DeCelles, P. G., 1988, Lithologic provenance modeling applied to the late Cretaceous synorogenic Echo Canyon Conglomerate, Utah: a case of multiple source areas: *Geology*, v. 16, p. 1039-1043.

- Dickinson, W. R., Beard, L. S., Brakenridge, G. R., Erjavec, J. L., Ferguson, R. C., Inman, K. F., Knepp, R. A., Lindberg, F. A., and Ryberg, P. T., 1983, Provenance of North American Phanerozoic sandstones in relation to tectonic setting: *Geological Society of America Bulletin*, v. 94, p. 222-235.
- Dickinson, W. R., and Suczek, C. A., 1979, Plate tectonics and sandstone compositions: *American Association of Petroleum Geologists Bulletin*, v. 63, p. 2164-2182.
- DiMarco, M. J., and Lowe, D. R., 1989, Petrography and provenance of silicified early Archaean volcanoclastic sandstones, eastern Pilbara Block, Western Australia: *Sedimentology*, v. 36, p. 821-836.
- Dimroth, E. I., Imreh, L., Rocheleau, M., and Goulet, N., 1982, Evolution of the south-central part of the Archean Abitibi Belt, Quebec. Part I: Stratigraphy and paleogeographic model: *Canadian Journal of Earth Sciences*, v. 19, p. 1729-1758.
- Dreyer, T., 1993, Quantified fluvial architecture in ephemeral stream deposits of the Esplugafreda Formation (Paleocene), Tremp-Graus Basin, northern Spain, *in* Marzo, M., and Puigdefabregas, C., eds., *Alluvial sedimentation: International Association of Sedimentologists Special Publication 17*, p. 337-362.
- Eriksson, K. A., 1978, Alluvial and destructive beach facies from the Archaean Moodies Group, Barberton Mountain Land, South Africa and Swaziland, *in* Miall, A. D., ed., *Fluvial Sedimentology: Canadian Society of Petroleum Geologists Memoir 5*, p. 287-311.
- Eriksson, K.A., Kidd, W.S.F., and Krapez, B., 1988, Basin analysis in regionally metamorphosed and deformed early Archean terrains: examples from southern Africa and Western Australia, *in* Kleinspehn and Paola, C., eds., *New Perspectives in Basin Analysis: Springer Verlag, Heidelberg*, p. 371-404.
- Eriksson, K. A., Krapez, B., and Fralick, P. W., 1994, Sedimentology of Archean greenstone belts: signatures of tectonic evolution: *Earth-Science Reviews*, v. 37, p. 1-88.

- Folk, R. L., Andrews, P. B., and Lewis, D. W., 1970, Detrital sedimentary rock classification and nomenclature for use in New Zealand: *New Zealand Journal of Geology and Geophysics*, v. 13, p. 937-968.
- Galloway, W.E., and Hobday D.K., 1983, *Terrigenous clastic depositional systems: Heidelberg*, Springer-Verlag, 423p.
- Graham, S. A., and 14 others, 1986, Provenance modelling as a technique for analysing source terrane evolution and controls on foreland sedimentation, in Homewood, P., and Allen, P. A., eds., *Foreland basins: International Association of Sedimentologists Special Publication 8*, p. 425-436.
- Green, H.G.G., and Wong, F.L., 1988, *Geology and offshore resources of Pacific island arcs - Vanuatu region: Circum-Pacific Council for Energy and Mineral Resources Earth Science Series*, v. 8, 442p.
- Hamilton, W. B., 1995, Subduction systems and magmatism, *in* Smellie, J. L., ed., *Volcanism associated with extension at consuming plate margins: Geological Society of London Special Publication*, v. 81, p. 3-28.
- Hathway, B., 1993, The Nadi Basin: Neogene strike-slip faulting and sedimentation in a fragmented arc, western Viti Levu, Fiji: *Journal of the Geological Society of London*, v. 150, p. 563-581.
- Helmstaedt, H., and Padgham, W., 1986, A new look at the stratigraphy of the Yellowknife Supergroup at Yellowknife, N.W.T.--implications for the age of gold-bearing shear zones and Archean basin evolution: *Canadian Journal of Earth Sciences*, v. 23, p. 454-475.
- Hempton, M.R., Dunne, L.A., and Dewey, J.F. 1983, Sedimentation in an active strike-slip basin, southeastern Turkey: *Journal of Geology*, v. 91, p. 401-412.
- Hempton, M. R., and Dunne, L. A., 1984, Sedimentation in pull-apart basins: active examples in eastern Turkey: *Journal of Geology*, v. 92, p. 513-530.
- Henderson, J. B., 1970, Stratigraphy of the Yellowknife Supergroup, Yellowknife Bay-Prosperous Lake area, District of Mackenzie: *Geological Survey of Canada Paper 70-26*, 12p.

- Henderson, J. B., 1975, Sedimentology of the Archean Yellowknife Supergroup at Yellowknife, District of Mackenzie: Geological Survey of Canada Bulletin 246, 62p.
- Henderson, J.B., 1981, Archean basin evolution, *in* Kröner, A., ed., Precambrian plate tectonics, Amsterdam, Elsevier, p.213-235.
- Henderson, J. B., 1985, Geology of the Yellowknife-Hearne Lake area, District of Mackenzie: segment across an Archean Basin: Geological Survey of Canada Memoir 414, 135 p.
- Henderson, J. B., van Breemen, O., and Loveridge, W. D., 1987, Some U-Pb zircon ages from Archean basement, supracrustal and intrusive rocks, Yellowknife-Hearne Lake area, District of Mackenzie, in Radiogenic Age and Isotopic Studies: Report 1, Geological Survey of Canada Paper 87-2, p. 111-121.
- Henderson, J. F., and Brown, I. C., 1966, Geology and structure of the Yellowknife greenstone belt, District of Mackenzie: Geological Survey of Canada Bulletin 141, 87p.
- Henderson, J. R., Kerswill, J. A., Henderson, M. N., Villeneuve, M., Petch, C. A., Dehls, J. F., and O'Keefe, M. D., 1995, Geology, geochronology, and metallogeny of High Lake greenstone belt, Archean Slave Structural Province, Northwest Territories: Current Research 1995-C, Geological Survey of Canada, p. 97-106.
- Heubeck, C., and Lowe, D. R., 1994, Depositional and tectonic setting of the Archean Moodies Group, Barberton greenstone belt, South Africa: Precambrian Research, v. 68, p. 257-290.
- Heward, A. P., 1978, Alluvial fan sequence and megasequence models: with examples from Westphalian D-Stephanian B coalfields, northern Spain, *in* Miall, A. D., ed., Fluvial Sedimentology: Canadian Society of Petroleum Geologists Memoir 5, p. 669-702.
- Horton, B. K., and Schmitt, J., 1996, Sedimentology of a lacustrine fan-delta system, Miocene Horse Camp Formation, Nevada, USA: Sedimentology, v. 43, p. 133-156.
- Howard, J. L., 1993, The statistics of counting clasts in rudites: a review, with examples from the upper Palaeogene of southern California, USA: Sedimentology, v. 40, p. 157-174.

- Howard, R.L., and Reineck, H.E., 1981, Depositional facies of high-energy beach-to-offshore sequence: comparison with low-energy sequence: American Association of Petroleum Geologists Bulletin, v. 65, p. 807-830.
- Ingersoll, R. V., 1988, Tectonics of sedimentary basins: Geological Society of America Bulletin, v. 100, p. 1704-1719.
- Ingersoll, R. V., Bullard, T. F., Ford, R. L., Grimm, J. P., Pickle, J. D., and Sares, S. W., 1984, The effect of grain size on detrital modes: A test of the Gazzi-Dickinson point-counting method: Journal of Sedimentary Petrology, v. 54, p. 103-116.
- Isachsen, C. E., Bowring, S. A., and Padgham, W. A., 1991, U-Pb zircon geochronology of the Yellowknife volcanic belt, NWT, Canada: New constraints on the timing and duration of greenstone belt magmatism: Journal of Geology, v. 99, p. 55-67.
- Isachsen, C. E., and Bowring, S. A., 1994, Evolution of the Slave Craton: Geology, v. 22, p. 917-920.
- Jackson, V. A., Crux, J., Ellis, C. E., Howson, S., Padgham, W. A., and Relf, C., 1985, Geology of the Mistake Lake area, Anialik River greenstone belt: Indian and Northern Affairs, N.W.T., EGS 1985-5.
- Johnson, S. Y., 1985, Eocene strike-slip faulting and non-marine basin formation in Washington, in Biddle, K. T., and Christie-Blick, N., eds., Strike-slip deformation, basin formation, and sedimentation: Society of Economic Paleontologists and Mineralogists Special Publication 37, p. 283-302.
- Kehlenbeck, M. M., 1984, Use of structural facing directions to delineate the geometry of refolded folds, near Thunder Bay, Ontario: Geoscience Canada, v. 11, p. 23-32.
- Krapez, B., 1993, Sequence stratigraphy of the Archaean supracrustal-belts of the Pilbara Block, Western Australia: Precambrian Research, v. 60, p. 1-45.
- Krapez, B., and Barley, M. E., 1987, Archaean strike-slip faulting and related ensialic basins: evidence from the Pilbara Block, Australia: Geological Magazine, v. 124, p. 555-567.

- Kreisa, R.D., 1981, Storm-generated sedimentary structures in subtidal marine facies with examples from the Middle and Upper Ordovician of southwestern Virginia: *Journal of Sedimentary Petrology*, v 51, p. 823-848.
- Kresz, D., 1984, Evolution of an Archean greenstone belt in the Stormy Lake-Kawashagamuk Lake area (stratigraphy, structure and geochemistry), western Wabigoon Subprovince, northwest Ontario. [MSc. thesis]: St Catherines, Brock University, 262p.
- Kusky, T. M., 1990, Evidence for Archean ocean opening and closing in the southern Slave Province: *Tectonics*, v. 9, p. 1533-1563.
- Kusky, T.M. and Vearnecombe, J., 1995, Structure of Archean Greenstone Belts in: de Wit, M. J. and Ashwal, L. D., eds., *Tectonic Evolution of Greenstone Belts: Oxford Monograph on Geology and Geophysics*, p. 95-128.
- Lambert, M. B., Ernst, R. E., and Dudas, F. O. L., 1992, Archean mafic dyke swarms near the Cameron River and Beaulieu river volcanic belts and their implications for tectonic modelling of the Slave Province, Northwest Territories: *Canadian Journal of Earth Sciences*, v. 29, p. 2226-2248.
- Lowe, D. R., 1975, Water-escape structures in coarse-grained sediments: *Sedimentology*, v. 22, p. 157-204.
- Mack, G. H., and Rasmussen, K. A., 1984, Alluvial-fan sedimentation of the Cutler Formation (Permian-Pennsylvanian) near Gateway, Colorado: *Geological Society of America Bulletin*, v. 95, p. 109-116.
- MacLachlan, K., and Helmstaedt, H., 1995, Geology and geochemistry of an Archean mafic dike complex in the Chan Formation: basis for a revised plate-tectonic model of the Yellowknife greenstone belt: *Canadian Journal of Earth Sciences*, v. 32, p. 614-630.
- McPherson, J. G., Shanmugan, G., and Moiola, R. J., 1987, Fan-deltas and braid deltas: varieties of coarse-grained deltas: *Geological Society of America Bulletin*, v. 99, p. 331-340.
- Miall, A. D., 1978, Lithofacies types and vertical profile models in braided river deposits: a summary, in Miall, A. D., ed., *Fluvial Sedimentology: Canadian Society of Petroleum Geologists Memoir 5*, p. 597-604.

- Middleton, L. T., and Trujillo, A. P., 1984, Sedimentology and depositional setting of the upper Proterozoic Scanlan conglomerate, central Arizona, *in* Koster, E. H., and Steel, R. J., eds, Sedimentology of Gravels and conglomerates: Canadian Society of Petroleum Geologists Memoir 10, p. 189-201.
- Minoura, K., and Yamauchi, H., 1989, Upper Cretaceous-Paleogene Kuji Basin of northeast Japan: tectonic controls on strike-slip basin sedimentation, *in* Taira, A., and Masuda, F., eds., Sedimentary Facies in the Active Plate Margin: Terra Scientific Publishing Company, Tokyo, p. 633-658.
- Mortensen, J. K., Henderson, J. B., Jackson, V. A., and Padgham, W. A., 1992, U-Pb geochronology of Yellowknife Supergroup felsic volcanic rocks in the Russell Lake and Clan Lake areas, southwestern Slave Province, N.W.T., *in* Radiogenic age and isotopic studies: Report 5, Geological Survey of Canada Paper 91-2, p. 1-7.
- Mortensen, J. K., 1993, U-Pb geochronology of the eastern Abitibi Subprovince. Part 1: Chibougamau-Matagami-Joutel region: Canadian Journal of Earth Sciences, v. 30, p. 11-28.
- Mueller, W., and Dimroth, E., 1987, A terrestrial-shallow marine transition in the Archean Opemisca Group east of Chapais, Quebec: Precambrian Research, v. 37, p. 29-55.
- Mueller, W., Chown, E.H., Sharma, K.N.M., Tait, L., and Rocheleau, M., 1989, Paleogeographic evolution of a basement-controlled Archean supracrustal sequence, Chibougamau - Caopatina, Quebec: Journal of Geology., v. 97, p. 399-420.
- Mueller, W., Donaldson, J.A., Dufresne, D., and Rocheleau, M., 1991, The Duparquet Formation: sedimentation in a late Archean successor basin, Abitibi greenstone belt, Quebec, Canada: Canadian Journal of Earth Sciences, v. 28, p. 1394-1406.
- Mueller, W., and Donaldson, J.A., 1992, Development of sedimentary basins in the Abitibi belt: an overview: Canadian Journal of Earth Sciences, v. 29, p. 2249-2265.
- Mueller, W., and Donaldson, J. Allan, 1994, Sedimentology of the late-orogenic sedimentary Jackson Lake Formation in the Slave Province: Open file report, NTS 85 J, Indian Affairs and Northern Development, EGS-10-94, 13p.



- Mueller, W., Donaldson, J. A., and Doucet, P., 1994, Volcanic and tectono-plutonic influences on sedimentation in the Archean Kirkland Basin Abitibi greenstone belt, Canada: *Precambrian Research*, v. 68, p. 201-230.
- Mueller, W.U., Daigneault, R., Mortensen, J.K., and Chown, E.H., 1996, Archean terrane docking: Upper crust collision tectonics, Abitibi greenstone belt, Quebec, Canada: *Tectonophysics*, (in press).
- Nemec, W., and Postma, G., 1993, Quaternary alluvial fans in southwestern Crete: sedimentation processes and geomorphic evolution, in Marzo, M., and Puigdefabregas, C., eds., *Alluvial sedimentation: International Association of Sedimentologists Special Publication 17*, p. 235-276.
- Nilsen, T. H., and McLaughlin, J., 1985, Comparison of tectonic framework and depositional patterns of the Hornelen strike-slip basin of Norway and the Ridge and Little Sulphur Creek strike-slip basins of California, in Biddle, K. T., and Christie-Blick, N., eds., *Strike-slip deformation, basin formation, and sedimentation: Society of Economic Paleontologists and Mineralogists Special Publication 37*, p. 79-103.
- Nocita, B. W., and Lowe, D. R., 1990, Fan-delta sequence in the Archean Fig Tree Group, Barberton Greenstone Belt, South Africa: *Precambrian Research*, v. 48, p. 375-393.
- Padgham, W. A., 1980, An Archean ignimbrite at Yellowknife and its relationship to the Kam Formation basalts: *Precambrian Research*, v. 12, p. 99-113.
- Padgham, W. A., 1987, Yellowknife Bay Formations and the Banting Group, in Padgham, W. A., ed., *A guide to the geology of the Yellowknife Volcanic belt and its bordering rocks: Mineral Deposits Division, Geological Association of Canada*, p. 55-79.
- Padgham, 1992, Mineral deposits in the Archean Slave Structural Province; lithological and tectonic setting: *Precambrian Research*, v. 58, p. 1-24.
- Padgham, W. A., and Fyson, W. K., 1992, The Slave Province: a distinct Archean craton: *Canadian Journal of Earth Sciences*, v. 29, p. 2072-2086. ✓

- Pettijohn, F. J., Potter, P. E., and Siever, R., 1973, *Sand and Sandstone*: Heidelberg, Springer-Verlag, 618p.
- Plint, A. G., and Brown, G. H., 1994, Tectonic event stratigraphy in a fluvio-lacustrine, strike-slip setting: the Boss Point Formation (Westphalian A), Cumberland Basin, Maritime Canada: *Journal of Sedimentary Research*, v. B64, p. 341-364.
- Potter, P. E., 1978, Petrology and chemistry of modern big river sands: *Journal of Geology*, v. 86, p. 423-449.
- Potter, P. E., 1986, South America and a few grains of sand: Part 1--beach sands: *Journal of Geology*, v. 94, p. 301-319.
- Rainbird, R. H., 1992, Anatomy of a large-scale braid-plain quartzarenite from the Neoproterozoic Shaler Group, Victoria Island, Northwest Territories, Canada: *Canadian Journal of Earth Sciences*, v. 29, p. 2537-2550.
- Reineck, H. E., and Singh, I. B., 1980, *Depositional Sedimentary environments*: Heidelberg, Springer, 549p.
- Reinson, G. E., 1984, Barrier island systems., *in* Walker, R.G., ed., *Facies models* (2nd edition): Geoscience Canada, Reprint Series 1, p. 119-140.
- Relf, C., Chouinard, A., Sandeman, H., and Villeneuve, M., 1994, Contact relationships between the Anialik River volcanic belt and the Kangguyak gneiss belt, northwestern Slave Province, Northwest Territories: *Current Research 1994-C*, Geological Survey of Canada, p. 49-59.
- Rice, R. J., Long, D. G. F., Fyson, W. K., and Roscoe, S. M., 1990, Sedimentological evaluation of three Archean metaquartzite and conglomerate-bearing sequences in the Slave Province, N.W.T.: *Current research, part C*, Geological Survey of Canada Paper 90-1C, p. 305-322.
- Ringenbach, J. C., Pinet, N., Stéphan, J. F., and Delteil, J., 1993, Structural variety and tectonic evolution of strike-slip basins related to the Philippine fault system, northern Luzon, Philippines: *Tectonics*, v. 12, p. 187-203.

- Røe, S.-L., and Hermansen, M., 1993, Processes and products of large, Late Precambrian sandy rivers in northern Norway, *in* Marzo, M., and Puigdefabregas, C, eds., Alluvial sedimentation: International Association of Sedimentologists Special Publication 17, p. 151-166.
- Roscoe, S. M., Stubbley, M., and Roach, D., 1989, Archean quartz-arenites and pyritic paleoplacers in the Beaulieu River supracrustal belt, Slave Structural Province, N.W.T.: Current research, part C, Geological Survey of Canada Paper 89-1C, p. 199-214.
- Rust, B.R., 1984, Proximal braidplain deposits in the Middle Devonian Malbaie Formation of eastern Gaspé, Canada: *Sedimentology*, v.31, p. 675-695.
- Rust, B.R., and Koster, E.H., 1984, Coarse clastic deposits, *in* Walker, R.G., ed., *Facies models* (2nd edition): Geoscience Canada, Reprint Series 1, p. 53-69.
- Schultz, A. W., 1984, Subaerial debris-flow deposition in the upper Paleozoic Cutler Formation, western Colorado: *Journal of Sedimentary Petrology*, v. 54, p. 759-772.
- Schumm, S.A., 1968, Speculations concerning paleohydrologic controls of terrestrial sedimentation: *Geological Society of America Bulletin*, v. 79, p. 1573-1588.
- Sengupta, S., 1966, Studies on orientation and imbrication of pebbles with respect to cross-stratification: *Journal of Sedimentary Petrology*, v. 36, p. 362-369.
- Sleep, N. H. and Windley, B. F., 1982, Archean plate tectonics: constraints and inferences: *Journal of Geology*, v. 90, p. 363-379.
- Sleep, N. H., 1992, Archean plate tectonics: what can be learned from continental geology?: *Canadian Journal of Earth Sciences*, v. 29, p. 2066-2071.
- Smith, G. A., 1986, Coarse-grained nonmarine volcanoclastic sediment: Terminology and depositional process: *Geological Society of America Bulletin*, v. 97, p.1-10.
- Steel, R.J., Maehle, S., Nielsen, H., Roe, S.L., and Spinnagr, A., 1977, Coarsening-upward cycles in the alluvium of Hornelen Basin (Devonian), Norway: sedimentary response to tectonic events: *Geological Society of America Bulletin*, v. 88, p 1124-1134.

- Stublely, M., 1989, Geology of the Spencer Lake area; parts of NTS 85 P/1,2: Indian and Northern Affairs, N.W.T.: EGS 1989-12, scale 1:50 000.
- Suttner, L. J., Basu, A., and Mack, G. H., 1981, Climate and origin of quartz arenites: *Journal of Sedimentary Petrology*, v. 51, p. 1235-1246.
- Sylvester, A. G., 1988, Strike-slip faults: *Geological Society of America Bulletin*, v. 100, p. 1666-1703.
- Sylvester, A. G., and Smith, R. R., 1976, Tectonic transpression and basement-controlled deformation in San Andreas fault zone, Salton Trough, California: *The American Association of Petroleum Geologists Bulletin*, v. 60, p. 173-194.
- Taira, A., Pickering, K. T., Windley, B. F., and Soh, W., 1992, Accretion of Japanese island arcs and implications for the origin of Archean Greenstone Belts: *Tectonics*, v. 11, p. 1224-1244.
- Thorpe, R. I., Cumming, G. L., and Mortensen, J. K., 1992, A major Pb-isotope boundary in the Slave Province and its probable relation to ancient basement in the western Slave, *in* Canada-NWT MDA summary volume: Geological Survey of Canada, Open File 2484, p. 179-184.
- van Breemen, O., Davis, W. J., and King, J. E., 1992, Temporal distribution of granitoid plutonic rocks in the Archean Slave Province, northwest Canadian Shield: *Canadian Journal of Earth Sciences*, v. 20, p. 2186-2199.
- van Breemen, O., Henderson, J. R., Jefferson, C. W., Johnstone, R. M., and Stern, R., 1994, U-Pb age and Sm-Nd isotopic studies in Archean Hood River and Torp Lake supracrustal belts, northern Slave Province, Northwest Territories, in *Radiogenic Age and Isotopic Studies: Report 8*, Geological Survey of Canada 1994-F, p. 1-16.
- Villeneuve, M., Hrabí, B., Jackson, V., and Relf, C., 1993, Geochronology of the supracrustal sequences in the central and northern Slave Province: *Exploration Overview 1993, Northwest Territories, NWT Geology Division, Indian and Northern Affairs Canada*, p.53.
- Walker, R. G., and James, N. P., 1992, Facies Models: Response to sea level change: Geological Association of Canada, 409p.

- Walker, R.G., and Cant, D.J., 1984, Sandy fluvial systems, in Walker, R.G., ed., *Facies models* (2nd edition): Geoscience Canada, Reprint Series 1, p. 71-89.
- Wells, N. A., 1984, Sheet debris flow and sheetflood conglomerates in Cretaceous cool-Maritime alluvial fans, South Orkney Islands, Antarctica, in Koster, E. H., and Steel, R. J., eds, *Sedimentology of Gravels and conglomerates: Canadian Society of Petroleum Geologists Memoir 10*, p. 133-145.
- Willis, B., 1993, Ancient river systems in the Himalayan foredeep, Chinji Village area, northern Pakistan: *Sedimentary Geology*, v. 88, p. 1-76.
- Wood, R. A., Pettinga, J. R., Bannister, S., Lamarche, G., and McMorran, T. J., 1994, Structure of the Hanmer strike-slip basin, Hope fault, New Zealand: *Geological Society of America Bulletin*, v. 11, p. 1459-1473.

## Tables and Figures

Table 1: Sedimentary facies associations in the Beaulieu Rapids Basin.

Table 2: Composition of quartz-feldspar (QFP) and hornblende (HP) porphyries and the gneisso-plutonic Sleepy Dragon Complex (SDC). Recalculated quartz, potassium feldspar, and plagioclase percentages represented by Q%, K%, and P%, respectively.

Table 3: Recalculated point counting results from thirty-two samples derived from the sandstone facies associations in the Beaulieu Rapids Formation. Grain parameters include:  $Q=Q_m+Q_p$  where  $Q_m$  is monocrystalline quartz and  $Q_p$  is polycrystalline quartz;  $F=P+K$  where P is plagioclase feldspar and K is potassium feldspar;  $L=L_s+L_p+L_v$  where  $L_s$  are sedimentary lithic fragments,  $L_p$  are plutonic lithic fragments, and  $L_v$  are volcanic lithic fragments; and  $L_t=L+Q_p$ .

Figure 1: Lithological map of the Slave Structural Province showing the location of the various late-stage sedimentary and volcano-sedimentary successions. The N-trending Beniah Lake fault can be traced intermittently for at least 300km along strike. Note that the Beaulieu Rapids (BRF) and Keskarrah (KF) Formations are located adjacent to this major structure. The Anialik River (ARB), High Lake (HLB), Hood River (HRB), Cameron River (CRB), and Beaulieu River (BRB) volcanic belts, the Jackson Lake Formation (JLF), and the Beniah Lake Quartz arenite (BLQ) are referred to in the text. Modified from Padgham and Fyson (1992).

Figure 2: Stratigraphy of the Yellowknife volcanic belt, Slave Structural Province (modified from Helmstaedt and Padgham, 1986; MacLachlan and Helmstaedt, 1995) and lateral pan-Slave correlations of the youngest formations. References for age dates: 1) Isachsen and others, 1991; Isachsen and Bowring, 1994, 2) Lambert and others, 1992, 3) van Breeman and others, 1994, 4) Villeneuve and others, 1993 and 5) Relf and others, 1994. BW, Burwash Formation; CL, Clan Lake felsic volcanic complex; CT, Contwoyto Formation; IN, Ingraham Formation; PL, Prosperous Lake Formation; W, Walsh Lake Formation.

Figure 3: Location of the Beaulieu Rapids Formation (outlined) in the Beaulieu River volcanic belt (BRB) and its proximity to the 2800-2900Ma plutono-gneissic Sleepy Dragon complex (SDC). Note sinistral strike-slip fault on the eastern side of the SDC. CRB, Cameron River volcanic belt; TLR, Turnback Lake Rhyolite; BF, Burwash Formation. Modified from Lambert and others, 1992.

Figure 4: A) Structural elements of the Beaulieu Rapids Basin. Arrows indicate sinistral strike-slip motion. Western basin margin characterized by an unconformity and a N-trending fault truncates the formation on the east. A series of NNE-trending en echelon folds in the north are evident. Structural elements  $S_0$  (bedding),  $S_1$  and  $S_2$  in stereonet support strike-slip interpretation. On bedding (north) stereonet, crosses and circles represent the bedding measurements to the west and east of depositional synform ( $F_0$ ), respectively.

B) Facies associations in the Beaulieu Rapids Basin. Porphyry stocks were emplaced along the eastern fault margin in the north. Twelve stratigraphic sections and three detailed sections are indicated in Roman numerals and by small rectangles, respectively. The encircled capital letters A-G designate clast count localities. Paleocurrent rose diagrams indicate prominent basin parallel, unidirectional flow in the south of the basin.

Figure 5. Characteristics of the volcanic rocks and porphyry stocks adjacent to the Beaulieu Rapids Basin. (A) Unconformable contact (*U*) between the massive pebbly sandstone of the CFA-I (figure 6a, section IV) and the underlying mafic volcanic rocks of the Beaulieu River volcanic belt (*V*). Scale, pencil 14cm. Large arrow indicates younging direction. (B) Brecciated mafic flow of the Beaulieu River volcanic belt with angular clasts. Scale, knife 9cm. Large arrow indicates younging direction. (C) Stratified hyaloclastite deposit (small arrows) of the Beaulieu River volcanic belt. Scale, knife 9cm. Large arrow indicates younging direction. (D) Photomicrograph of a scoria lapillus (*L*) in a recrystallized vitric matrix from the hyaloclastite deposit. (E) Quartz-feldspar porphyry stock located along the faulted eastern basin margin with <2mm quartz phenocrysts (*Q*). (F) Photomicrograph of quartz-feldspar porphyry showing euhedral, embayed quartz phenocrysts (*Q*) in a quartzofeldspathic matrix.

Figure 6: Stratigraphic columns through the Beaulieu Rapids Basin (see Figure 4b). Clast count localities are indicated by circled letters. (A) Sections I-VII from the southern region of the basin show the lateral discontinuity of the CFA-I, the unconformity between the volcanic and the sedimentary rocks, and the presence of two well-defined fining-upward sequences (IV). (B) Sections VIII-XI from the northern region of the basin with quartz-feldspar porphyries (sections VIII-IX) at the base of the sections. Rapid lateral and vertical facies changes are evident in figures A and B.

Figure 7: Outcrop sketch of the clast-supported conglomerate of the CFA-I (S0 181/88) composed of plane-bedded coarse-grained sandstone (*Sh*), trough crossbedded pebbly to coarse-grained sandstone (*St*), and massive, clast-supported conglomerate beds (*Gm*; locality DS1 in Figure 4b).



Figure 8: Characteristics of the CFA-I. Younging directions are indicated by large arrows

(A) Dominant clast constituents of the clast-supported conglomerate: plutonic clasts (*P*) and mafic volcanic clasts (*Mv*). Scale, pencil 13cm. (B) Large plutonic boulders (*P*) in the clast-supported conglomerate. Scale, hammer 34cm. (C) Trough crossbedded (*St*) sandstone interbeds truncated by matrix-supported conglomerate. Small arrows mark erosional surface. Scale, knife 9cm. (D) Laminated argillite (*Fl*) interbed in matrix-supported conglomerate recording pervasive NNE-trending foliation (*F*). Scale, knife 9cm. (E) Truncating sets of trough crossbeds (*St*; arrows) in the pebble-conglomerate subunit. Scale, pencil 13cm and indicating north. (F) Three fining-upward cycles (*arrows*) including stratified conglomerate (*Gm*) capped by argillite (*Fl*) in the pebble-cobble conglomerate subunit. Scale, hammer 50cm.

Figure 9: Outcrop sketch of the sandstone-dominated subunit of the SSFA (S0 008/86) composed of truncating trough crossbeds (*St*), argillite (clay) beds (*Fl*), argillite rip-ups, and argillite drapes on foresets (locality DS2 in Figure 4b).

Figure 10: Characteristics of the SSFA. Younging direction is indicated by large arrow. (A) Trough crossbedded sandstone (*St*) with argillite between bedforms and draped on foresets (*Fl*) in the sandstone-dominated subunit. Scale, knife 9cm. (B) Horizontal bedding (*Sh*) and planar crossbedding (*Sp*) in the sandstone-dominated subunit. Scale, pencil 13cm (arrow) and indicating north. (C) Pebble trains (*Gm*) overlain by trough crossbedding (*St*) in the sandstone-dominated subunit. Scale, pencil 13cm and indicating north. (D) Asymmetrical wave ripples (*Sr*) in the siltstone-dominated subunit. Scale, pencil 13cm. (E) Abundant water escape structures as indicated by clastic dykes (*CD*) and dish structures (*DS*) in the

siltstone-dominated subunit. Local graded beds (*GB*) are observed. Scale, pencil 13cm. (F) Close-up of dish (*DS*) and pillar (*PS*) structures and graded bedding (*GB*) in the siltstone-dominated subunit. Scale, pencil 13cm.

Figure. 11: Characteristics of the CFA-II, the QSFA, and clast components of the Beaulieu Rapids Formation. Large arrow indicates younging direction. (A) Clast-supported CFA-II with plutonic (*P*), mafic volcanic (*M*), felsic volcanic (*F*), and quartz (*Q*) clasts. Scale, lens cap 5cm in diameter. (B) Large-scale, high-angle laterally accreting sets of trough crossbeds (*St*) in the QSFA. Scale, knife 9cm (arrow). (C) Composite, up to 10m-long channel (arrows indicate base) of the QSFA. Scale, hammer (arrow) 34cm. (D) Truncating trough crossbeds (*St*) with pebbles on foresets (*Pb*) in the QSFA. Scale, pencil 13cm. (E) Medium- to coarse-grained plutonic clasts with local 0.2-1cm large quartz phenocrysts (arrows). Sample derived from the CFA-II (see Table 2 for point count). Scale, coin 2cm in diameter. (F) Magmatic breccia clast (*Mb*) in the CFA-I. Scale, coin 2cm in diameter.

Figure 12: Stratigraphic column of the QSFA composed of low-angle planar beds (*Sh*), trough crossbeds (*St*), and pebbles on foresets (*Pb*) (locality DS3 in Figure 4b).

Figure 13: Ternary diagrams illustrating the compositions of sandstones and conglomerates of the Beaulieu Rapids Formation. Average compositions indicated by crosses. (A) QFL diagram (Dickinson and others, 1983) illustrating a recycled orogenic provenance. (B) QmFLt diagram after Dickinson and others (1983) showing the same recycled provenance as in 13A. (C) LpLvLs diagram comparing rock fragments in sandstones with seven clast counts. Plutonic fragments decrease from the CFA-I to the CFA-II. Sedimentary fragments are common to the QSFA only.

Figure 14: Results of 4597 clast counts from four different localities in the CFA-I and three different localities in the CFA-II. Clasts were derived predominantly from the gneisso-plutonic Sleepy Dragon Complex and the mafic volcanic Beaulieu River volcanic belt. Clast count localities are indicated in Figure 4b.

Figure 15: Paleogeographic models illustrating the evolution of the Beaulieu Rapids Basin during two depositional phases. (A) First depositional phase includes the uplift of the gneisso-plutonic terrane. Erosion of the younger mafic volcanic belt and the plutonic rocks caused rapid infilling of the basin. Coarse clastic detritus accumulated as alluvial fans and fan deltas along basin margins that prograded onto a small braidplain and into standing bodies of water. (B) The second phase provided additional material into the basin. Small lakes and ponds are near-full and the basin is controlled by a large, basin parallel sandy braided stream system. Porphyry stocks are exposed along the fault at the the north end of the basin.

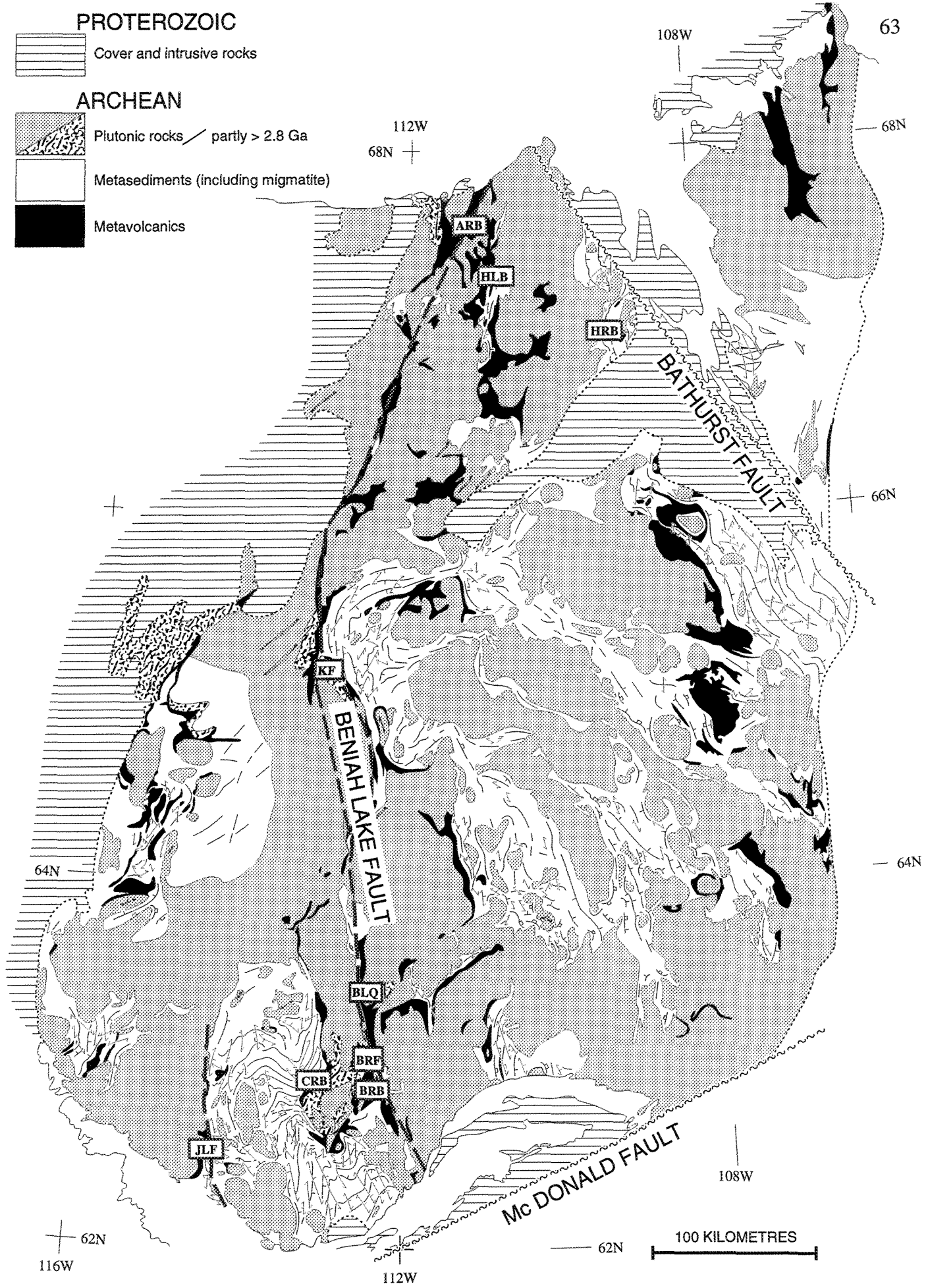


Figure 1

# Slave-wide correlation of late-orogenic molasse-type basins

Yellowknife Volcanic Belt

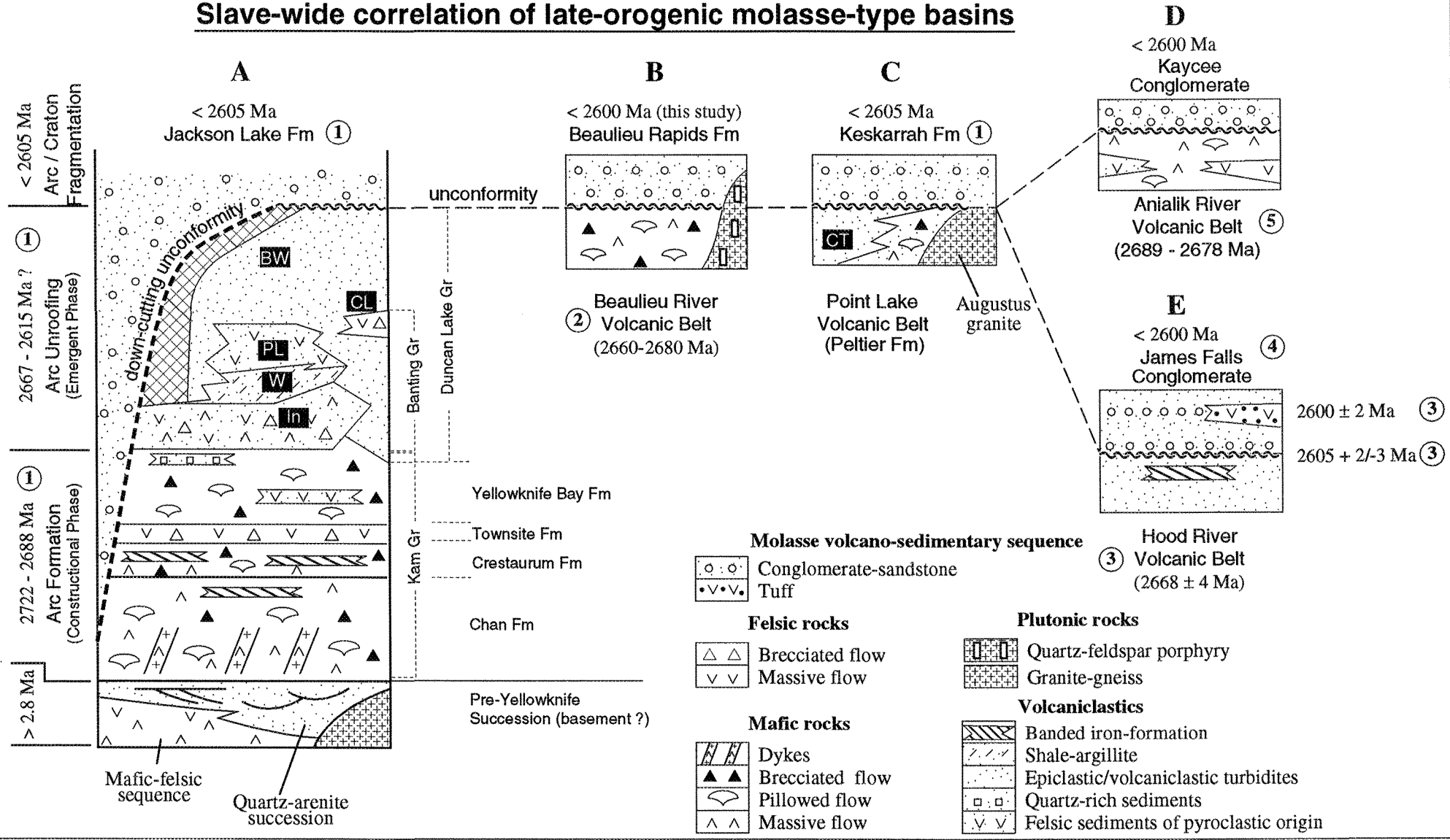


Figure 2

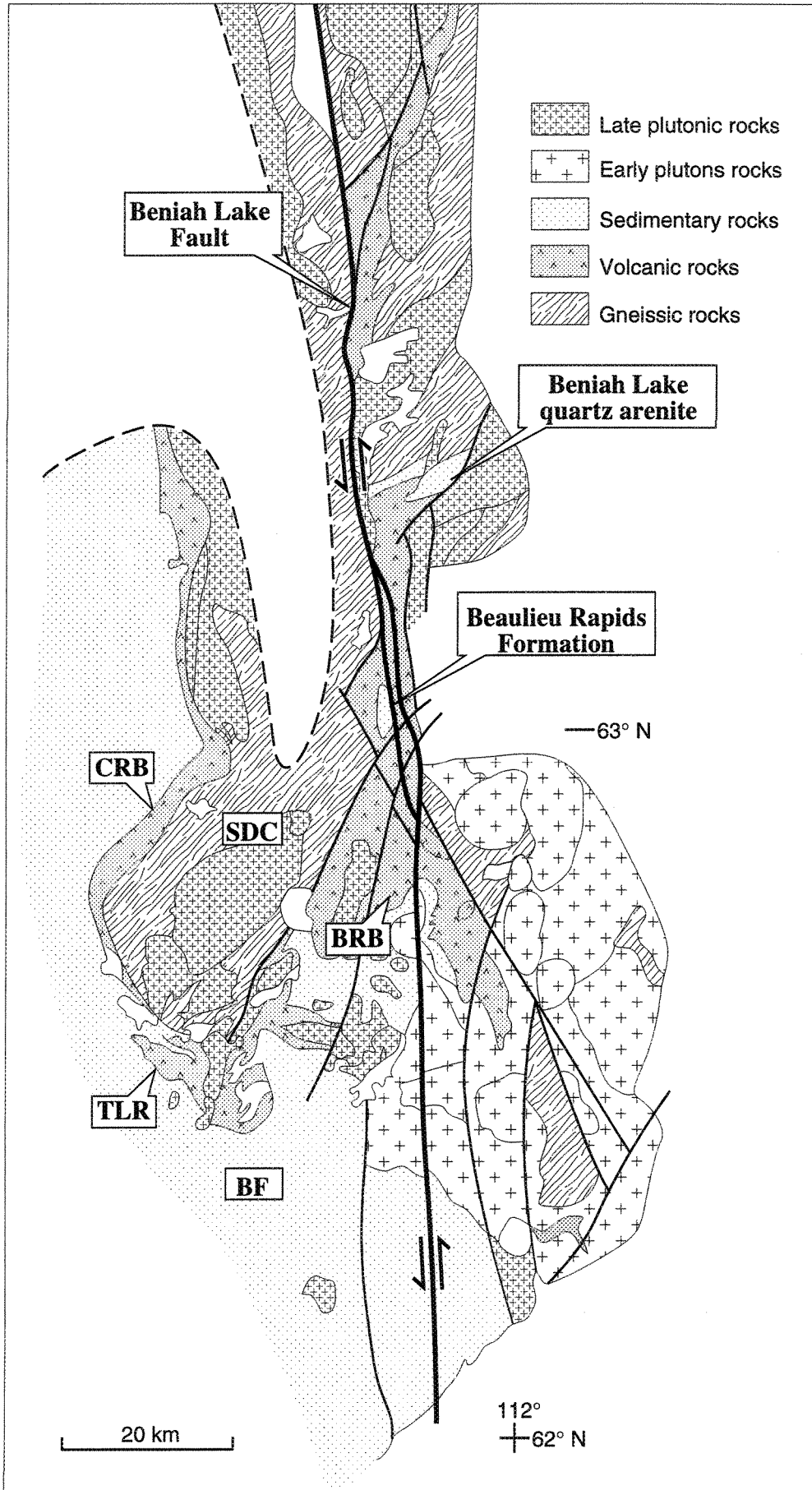
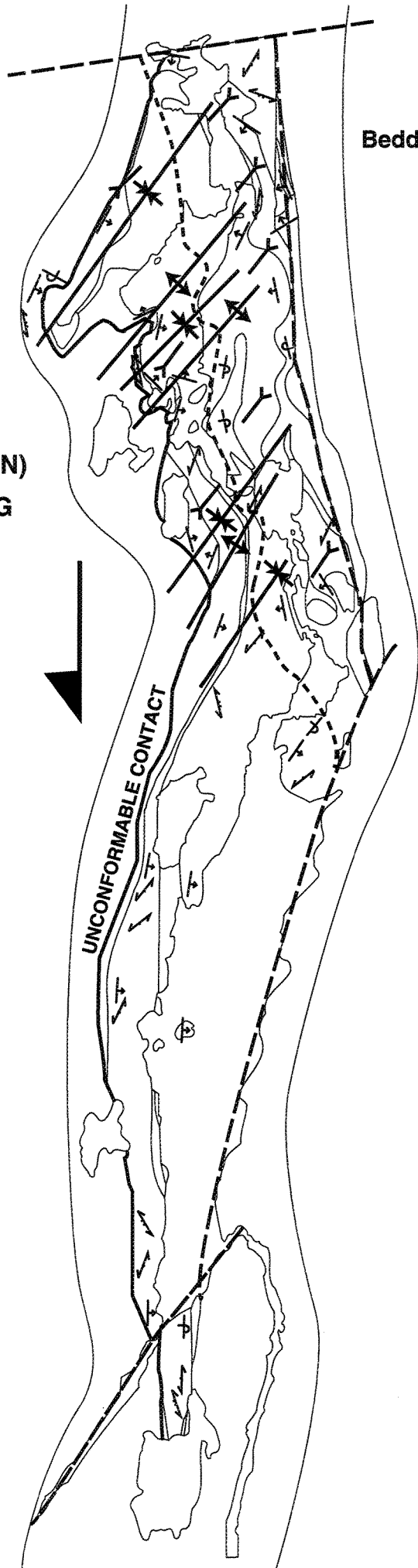


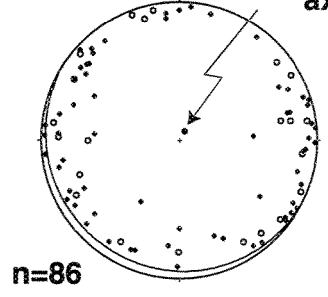
Figure 3

- F<sub>0</sub> SYNFORM
- ↔ ANTICLINE
- \* SYNCLINE
- ↗ FACING DIRECTION
- FAULT
- ↗ S1 FOLIATION
- ↗ S2 FOLIATION
- ↗ BEDDING (TOPS KNOWN)
- ↗ OVERTURNED BEDDING

2 km



Bedding (north) N  
mean deformation axis



• east of synform  
• west of synform

Bedding (south) N

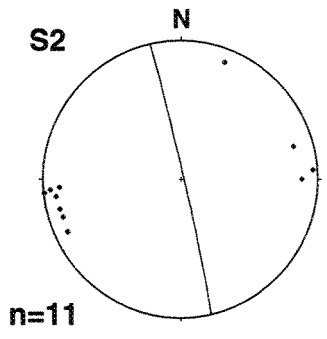
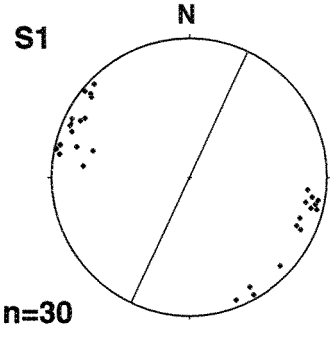
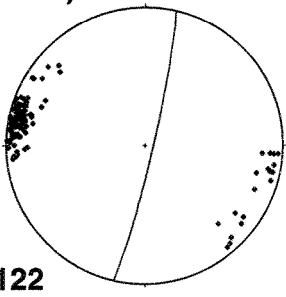
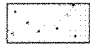

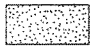



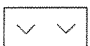

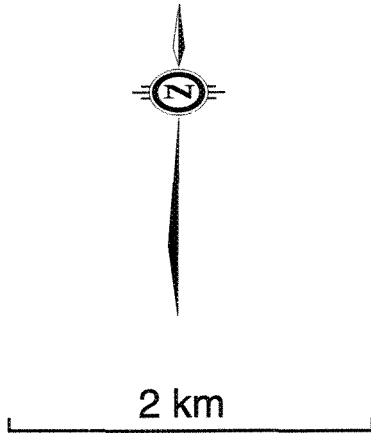
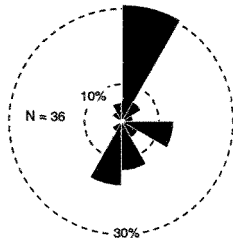


Figure 4A

-  Quartz-rich sandstone facies association
-  Conglomerate facies association II
- Siltstone-sandstone facies association**
-  Sandstone-dominated subunit
-  Siltstone-dominated subunit
-  Conglomerate facies association I
-  Mafic-intermediate volcanic rocks
-  Felsic volcanic rocks
-  Porphyry stocks



SILTSTONE-SANDSTONE FACIES ASSOCIATION



QUARTZ-RICH SANDSTONE FACIES ASSOCIATION

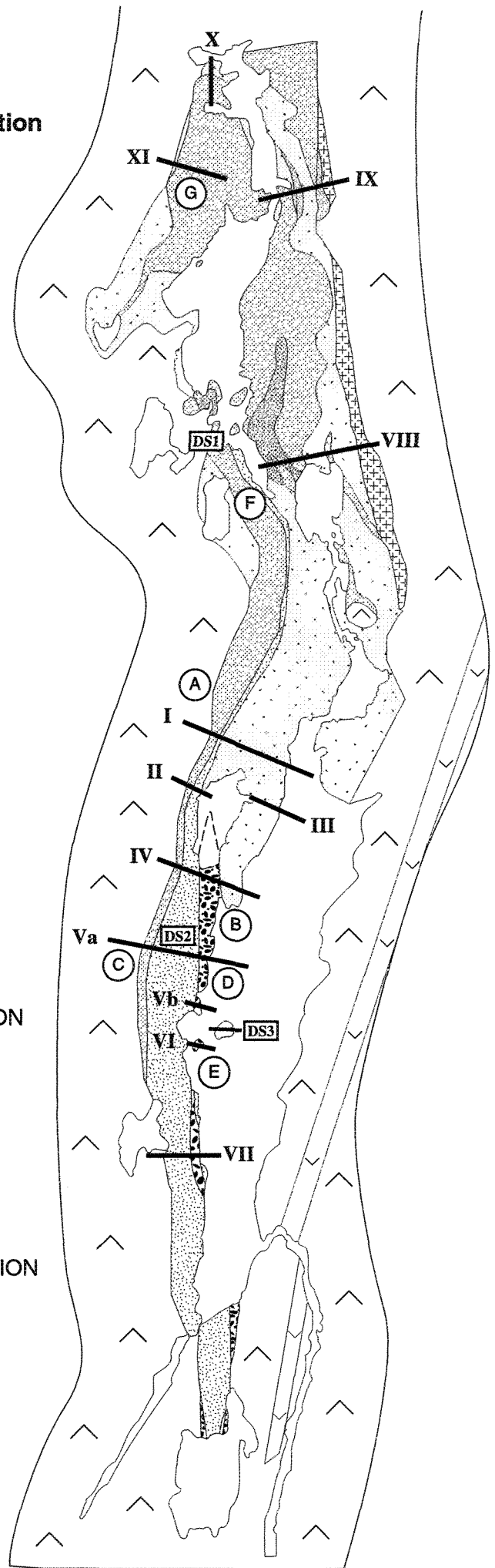
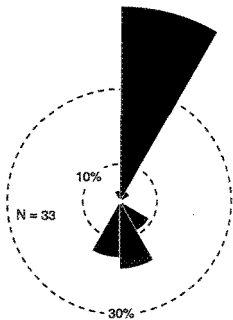


Figure 4B



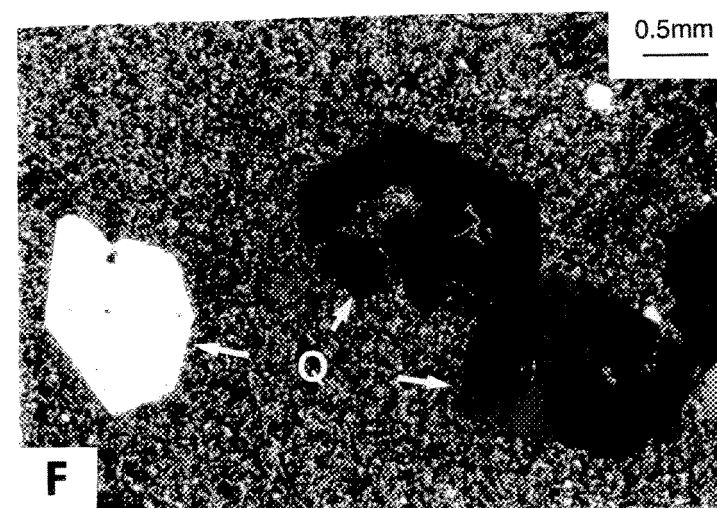
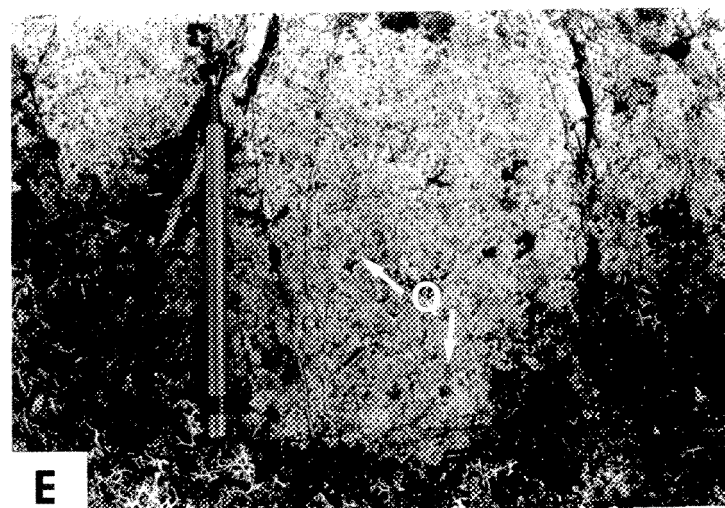
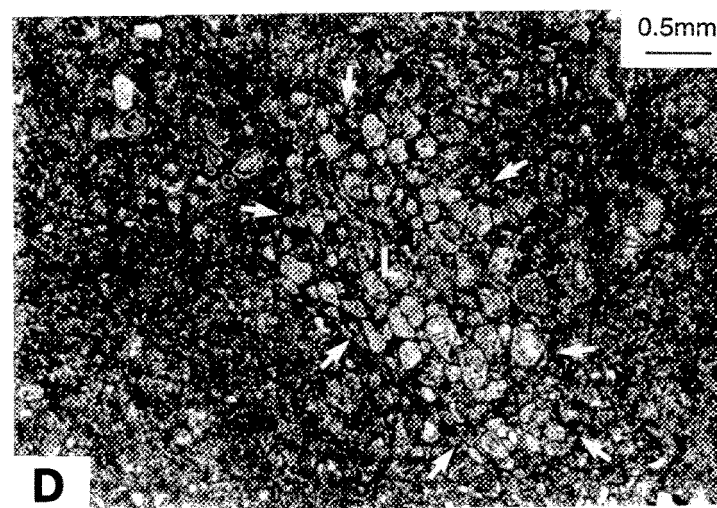
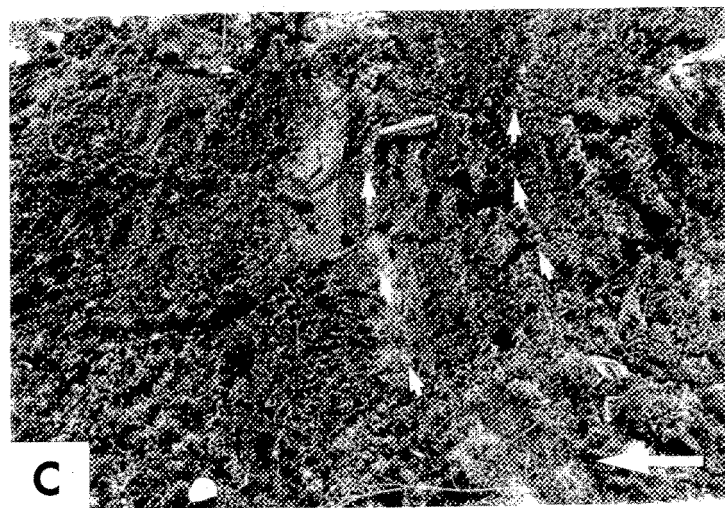
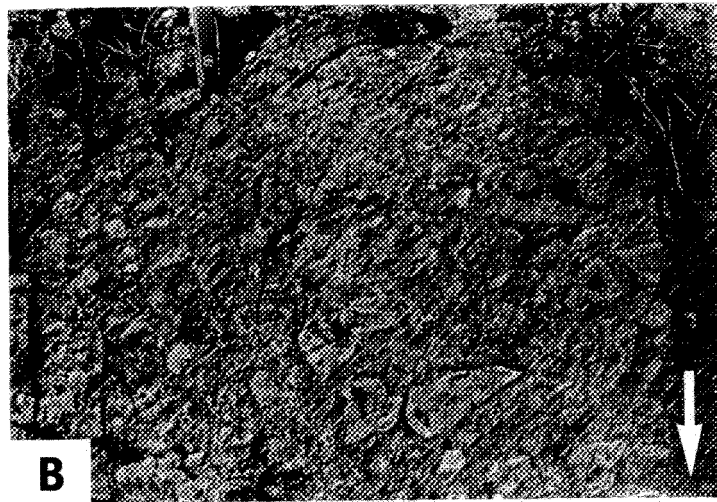
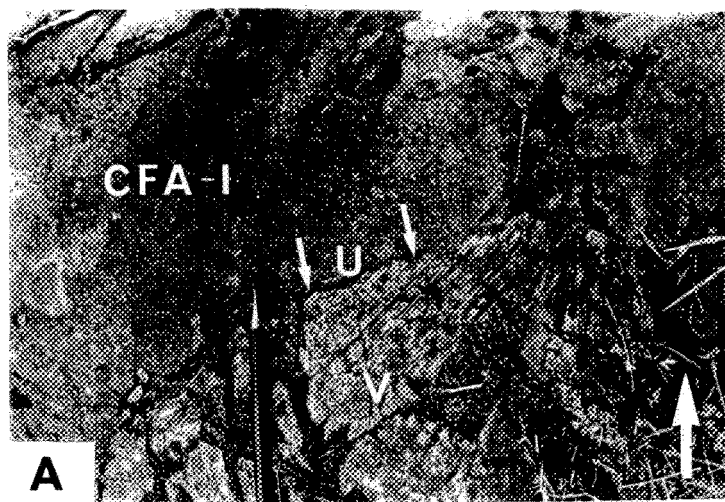


Figure 5

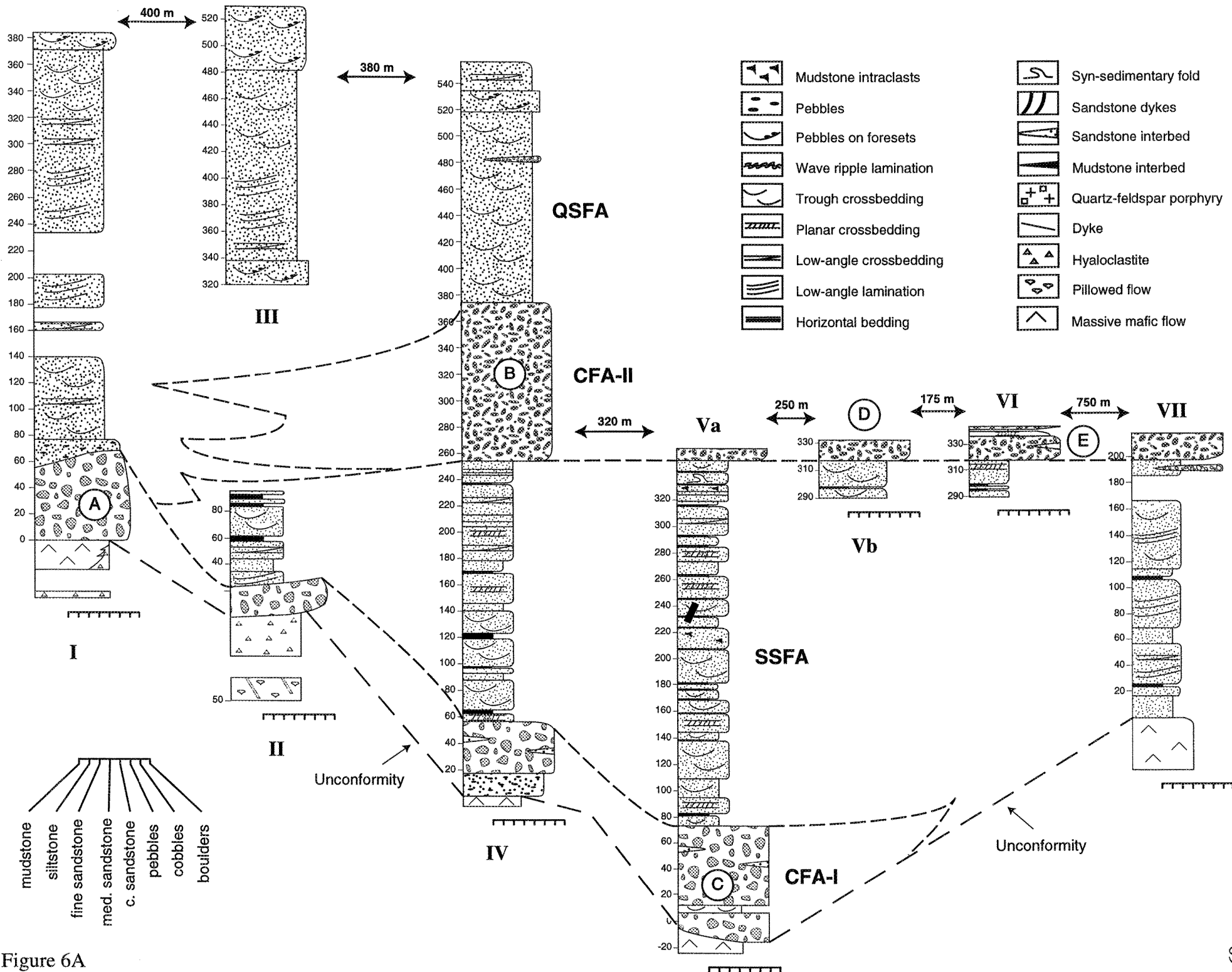


Figure 6A

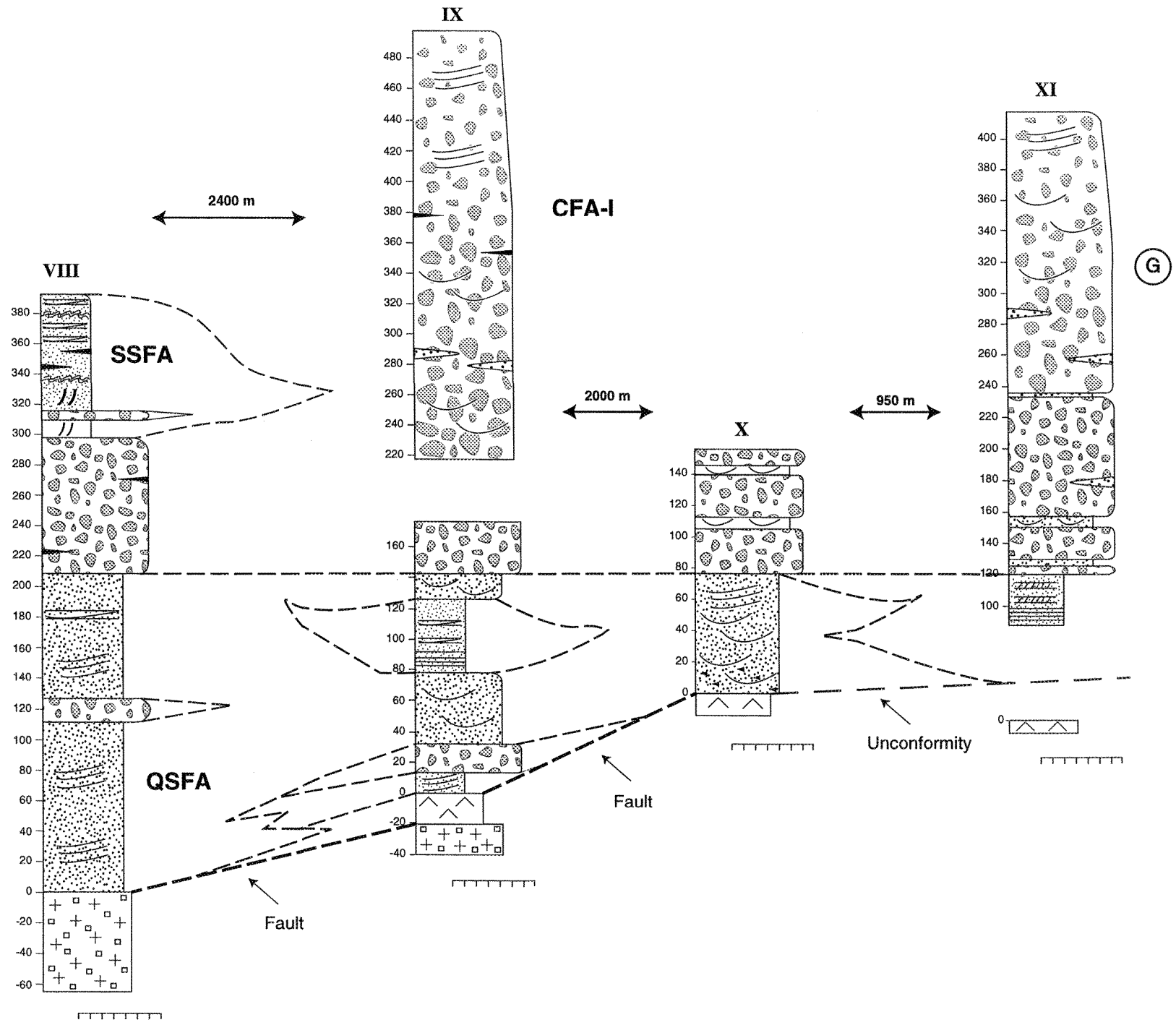


Figure 6B

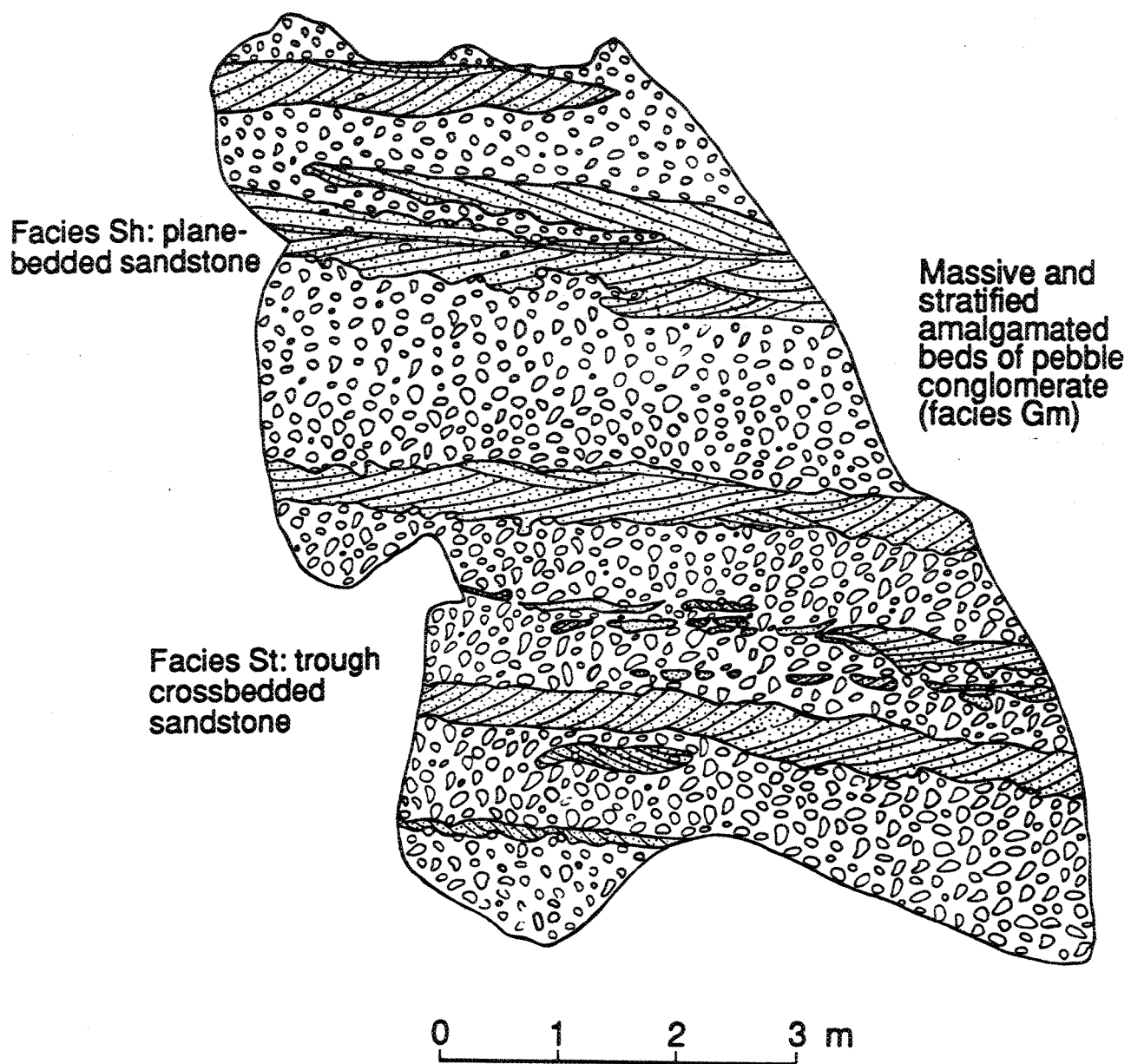


Figure 7

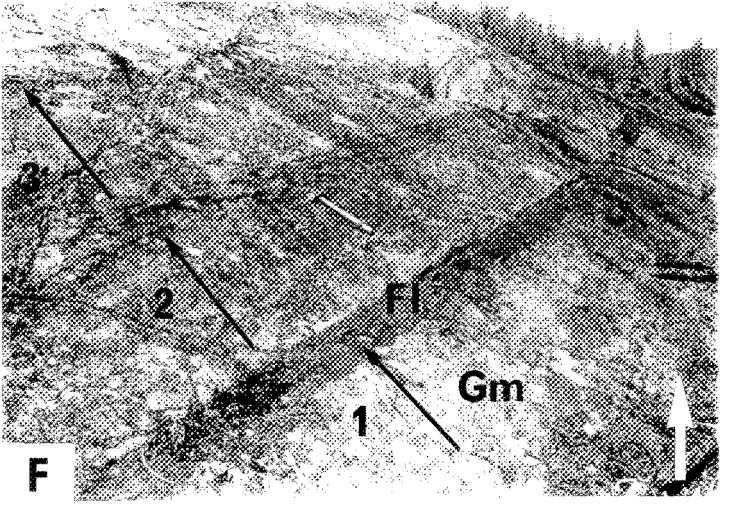
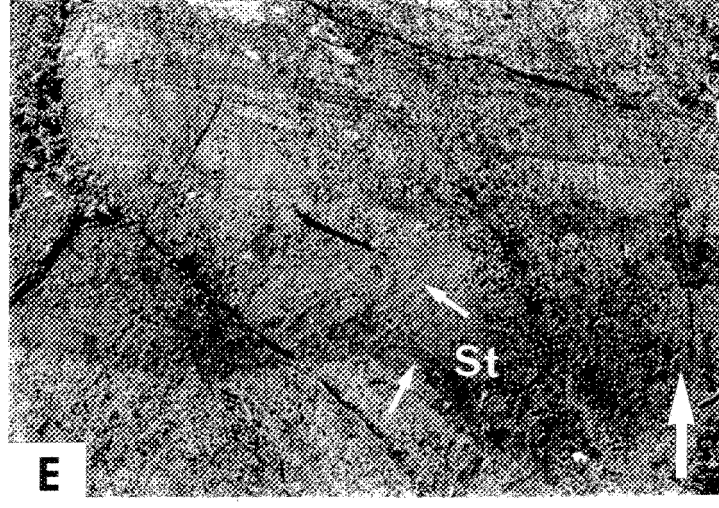
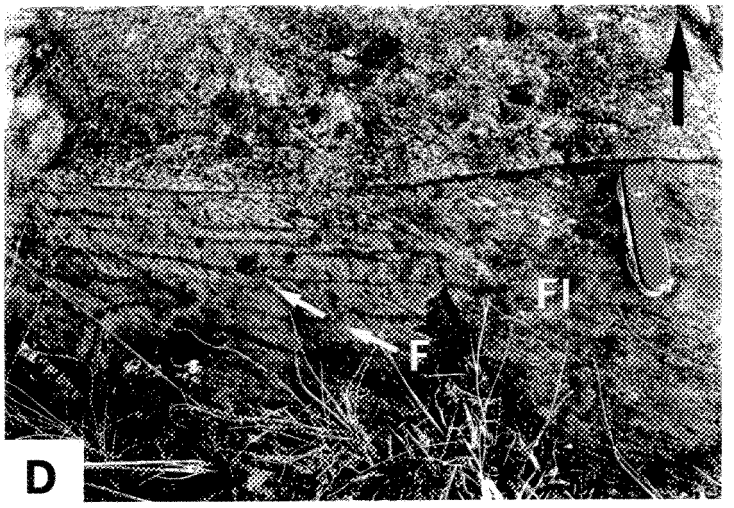
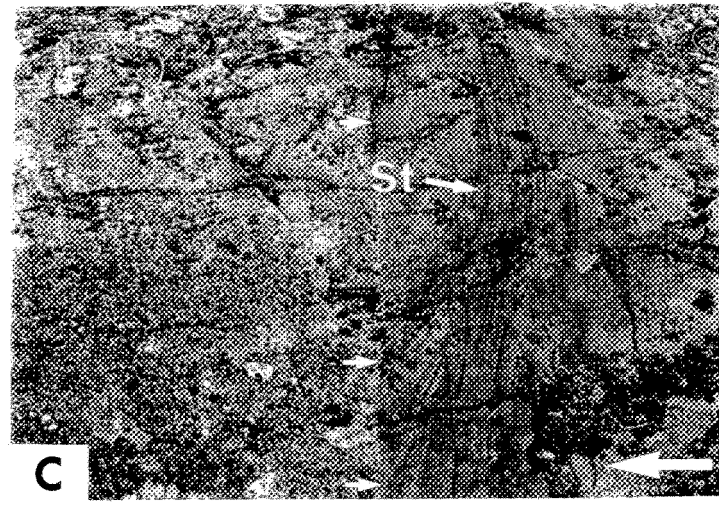
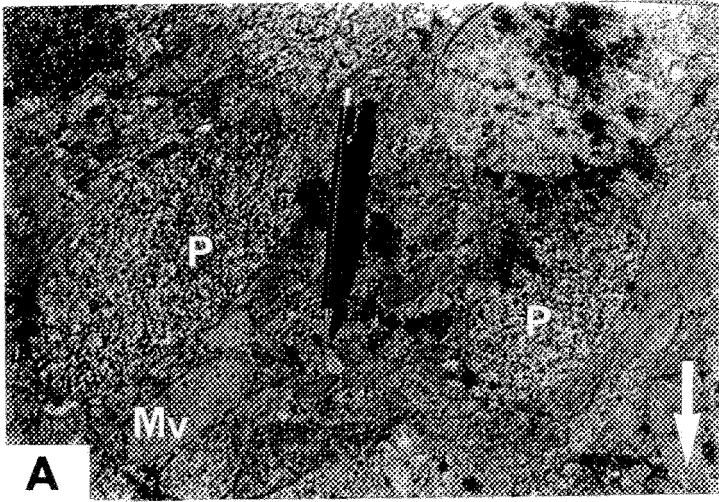
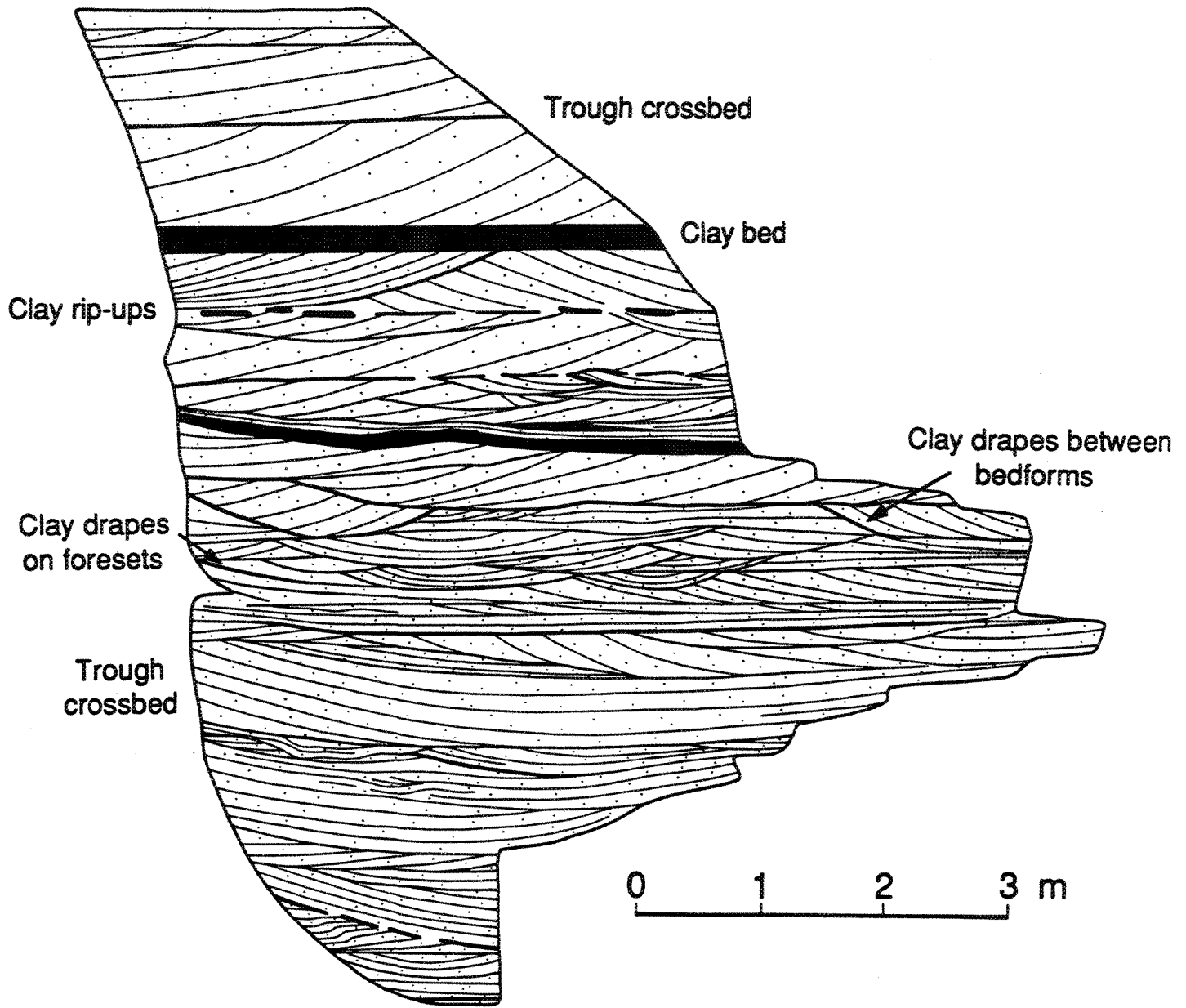


Figure 8



SANDY BRAIDPLAIN WITH SMALL PONDS

Figure 9

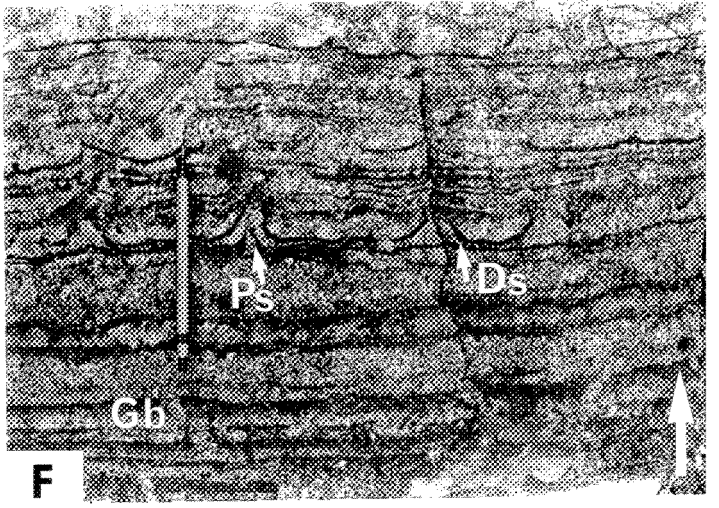
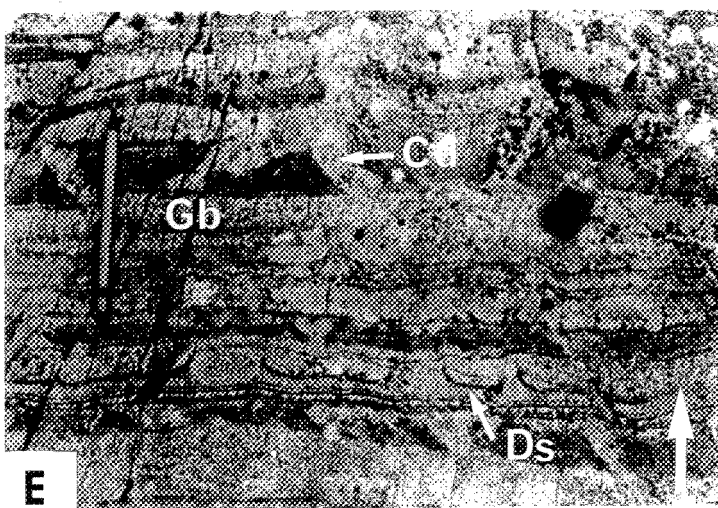
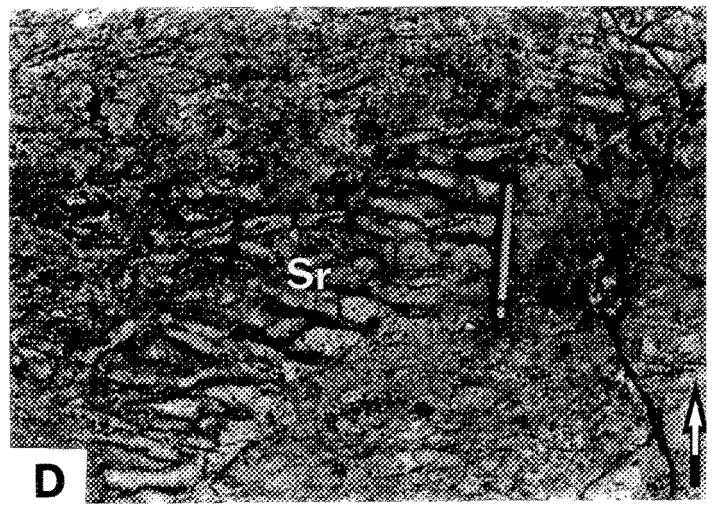
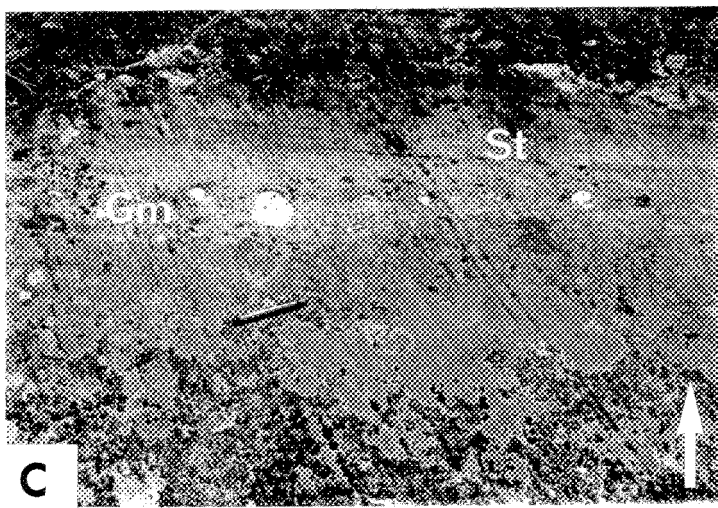
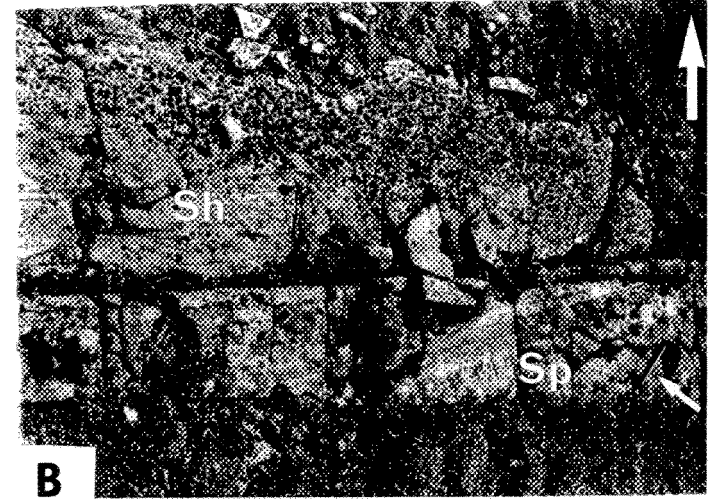
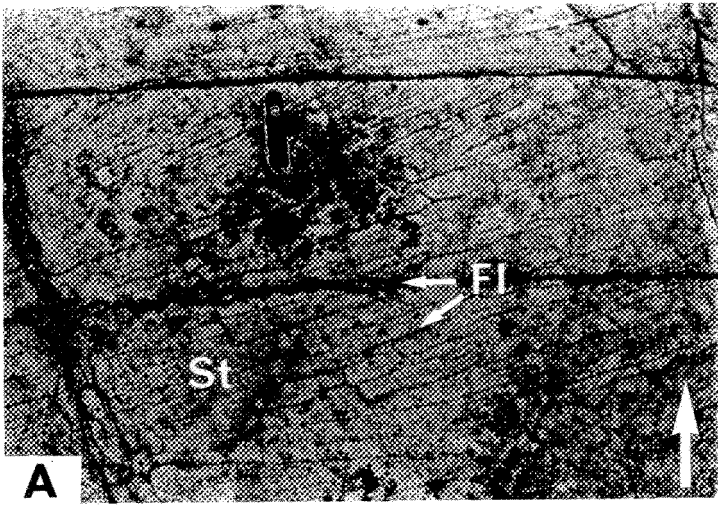


Figure 10

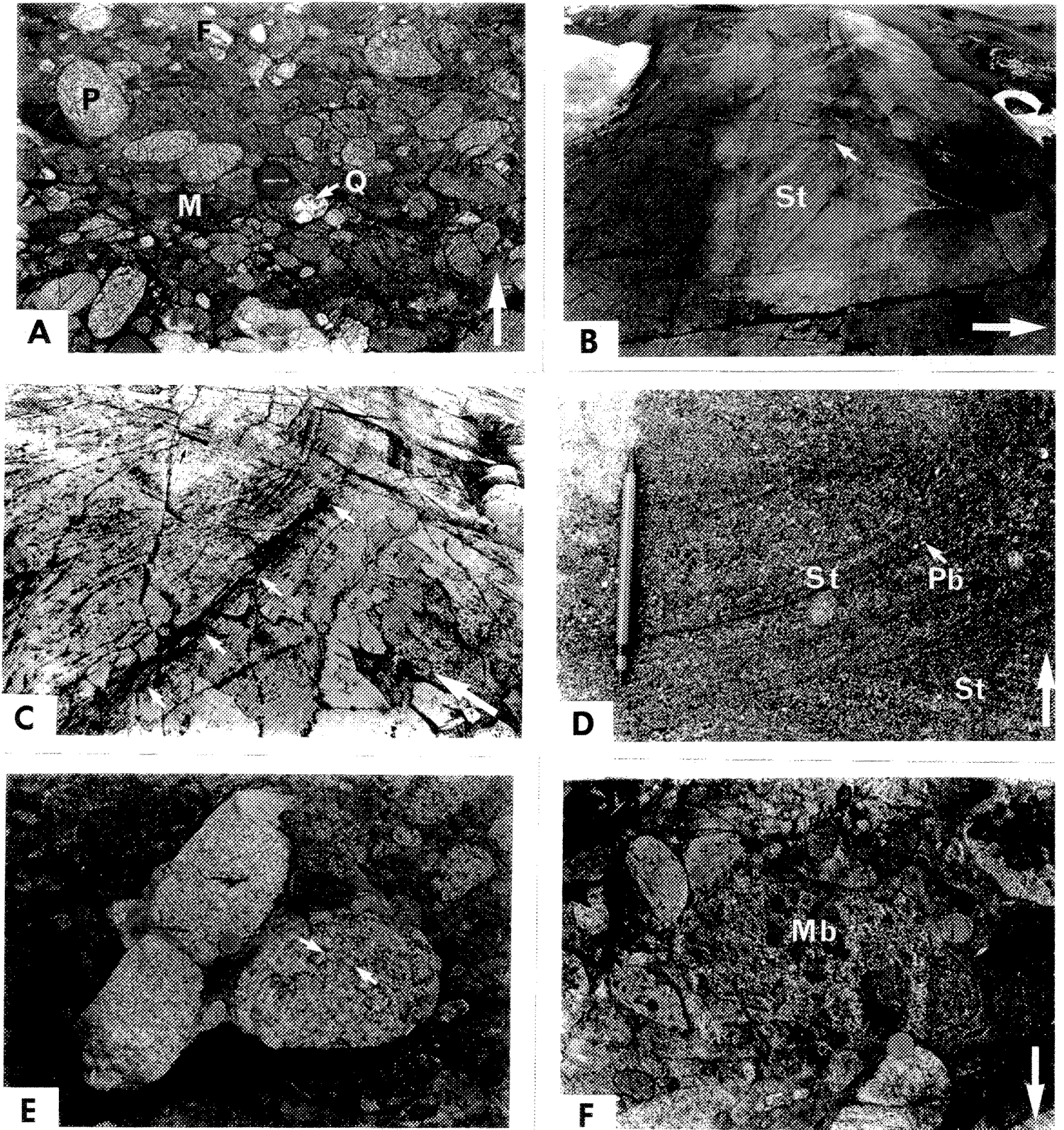


Figure 11



**Quartz-rich sandstone facies association**

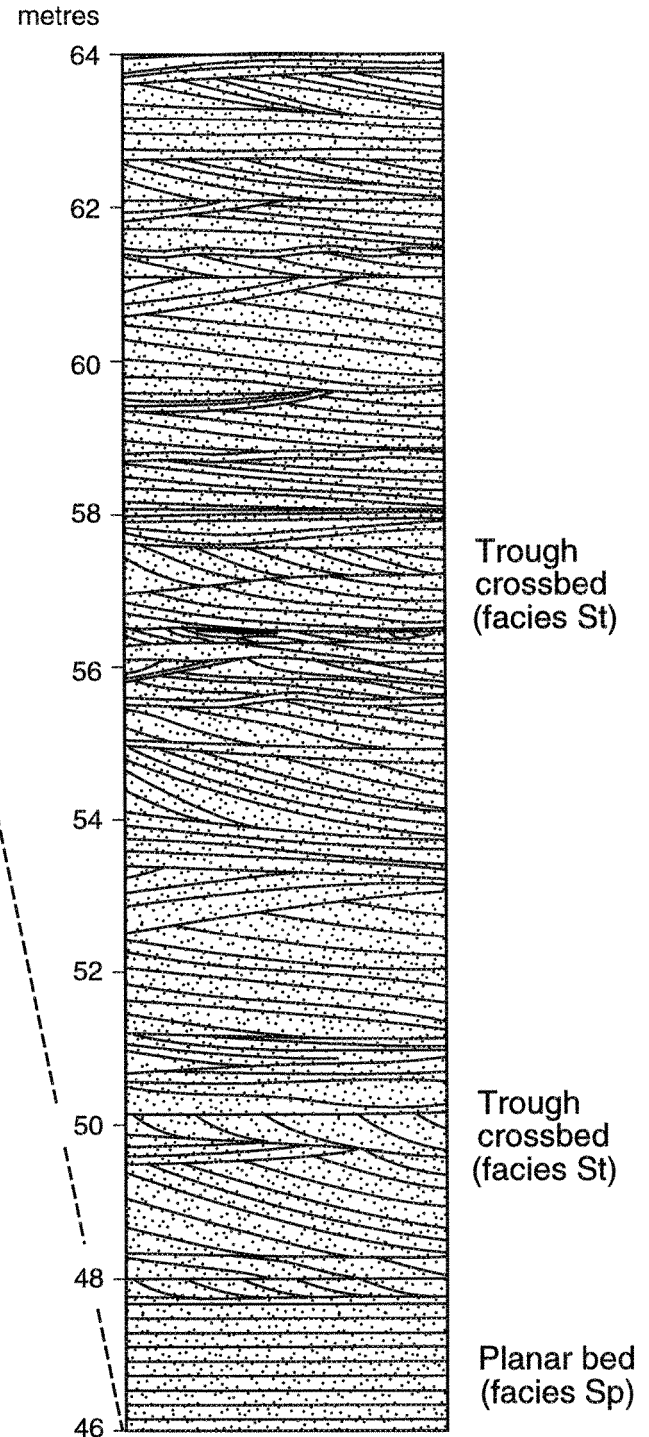
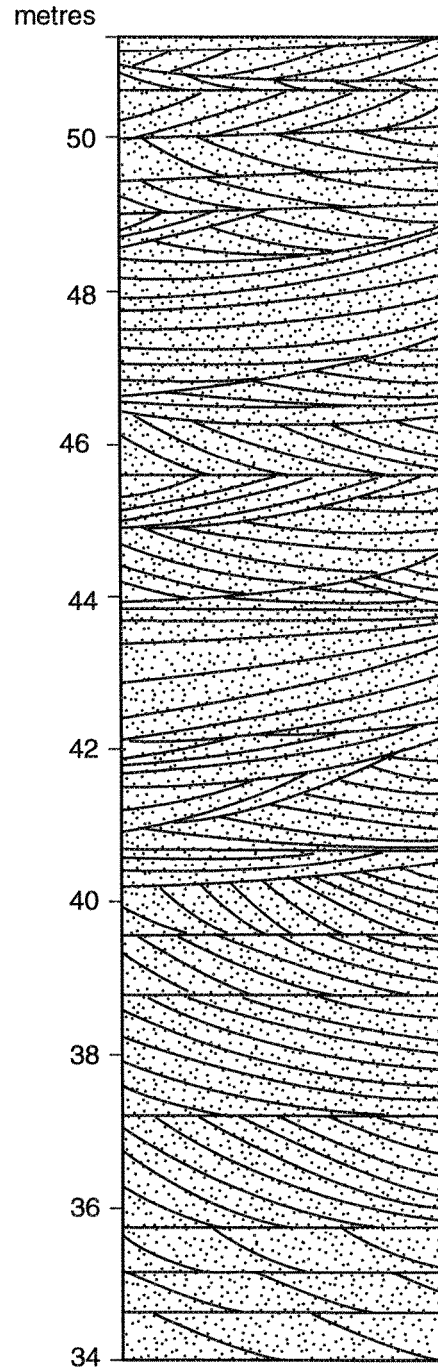
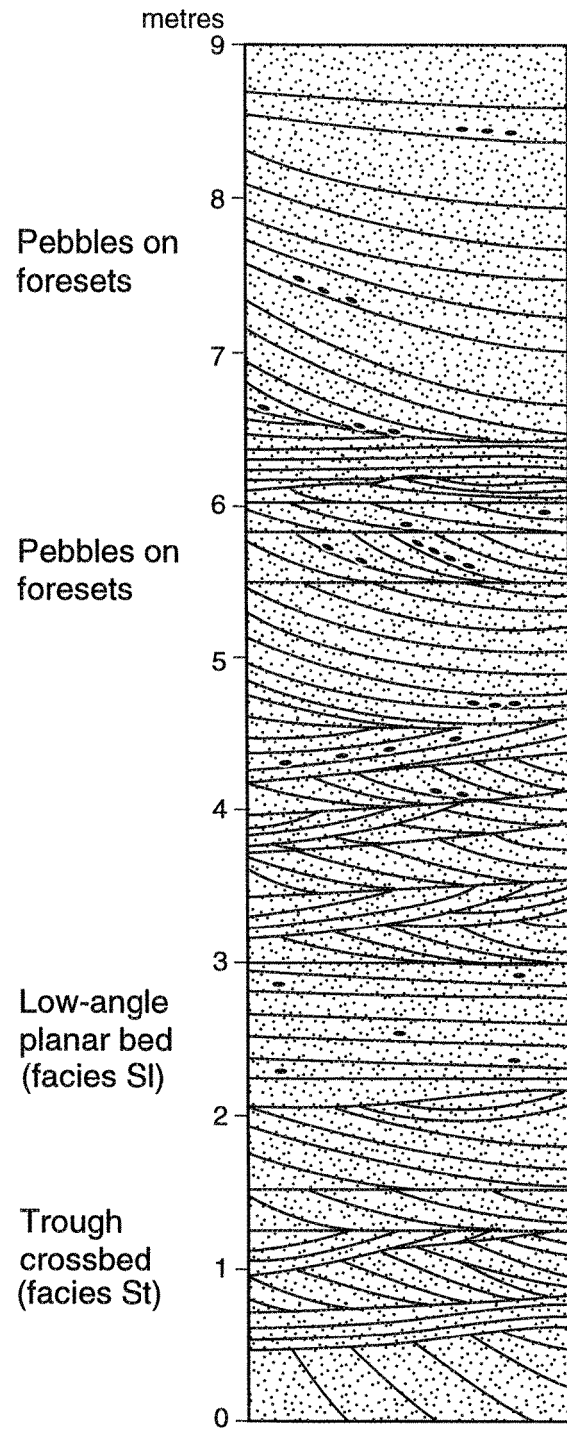
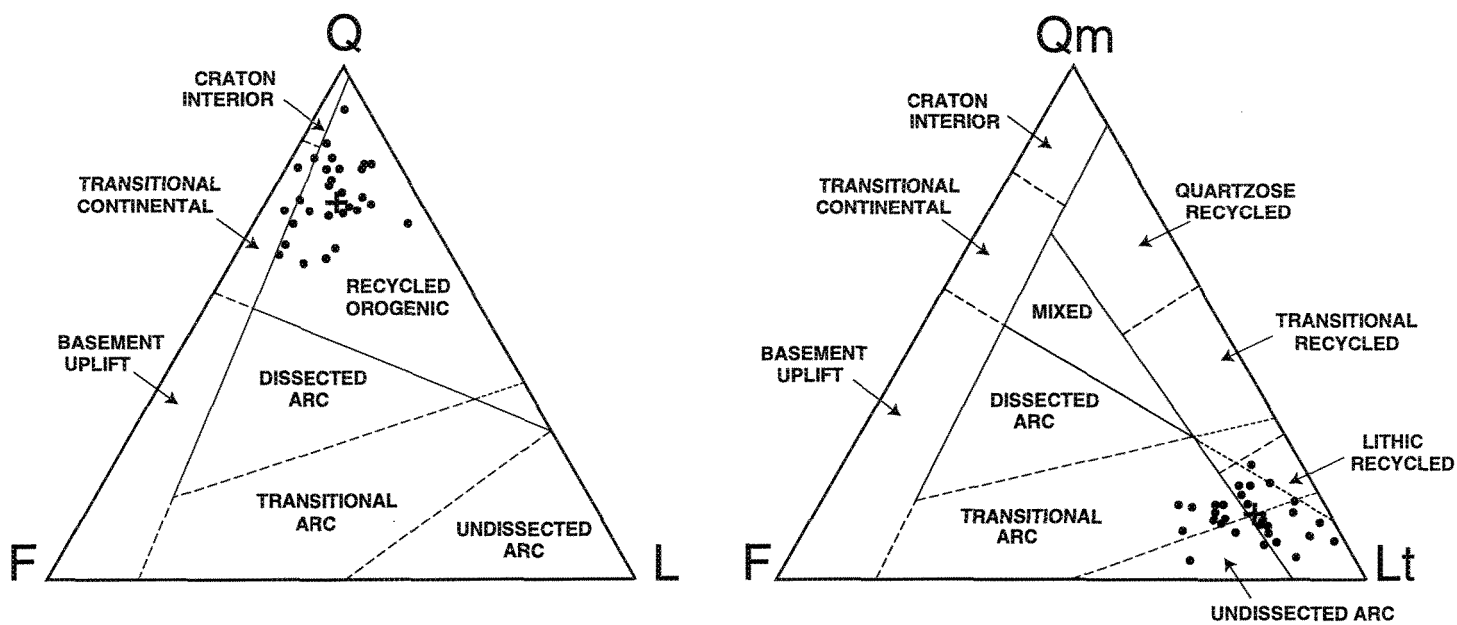
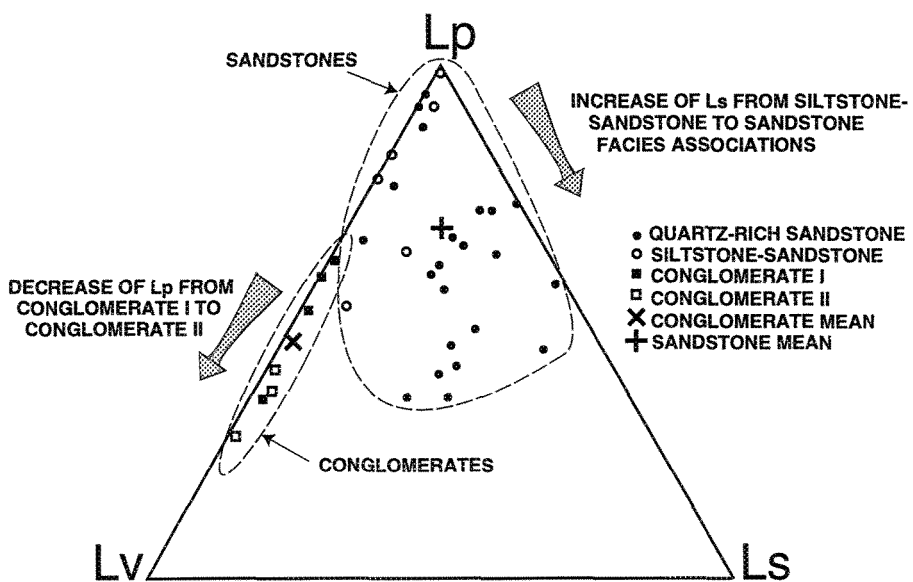


Figure 12



(A)

(B)



(C)

Figure 13

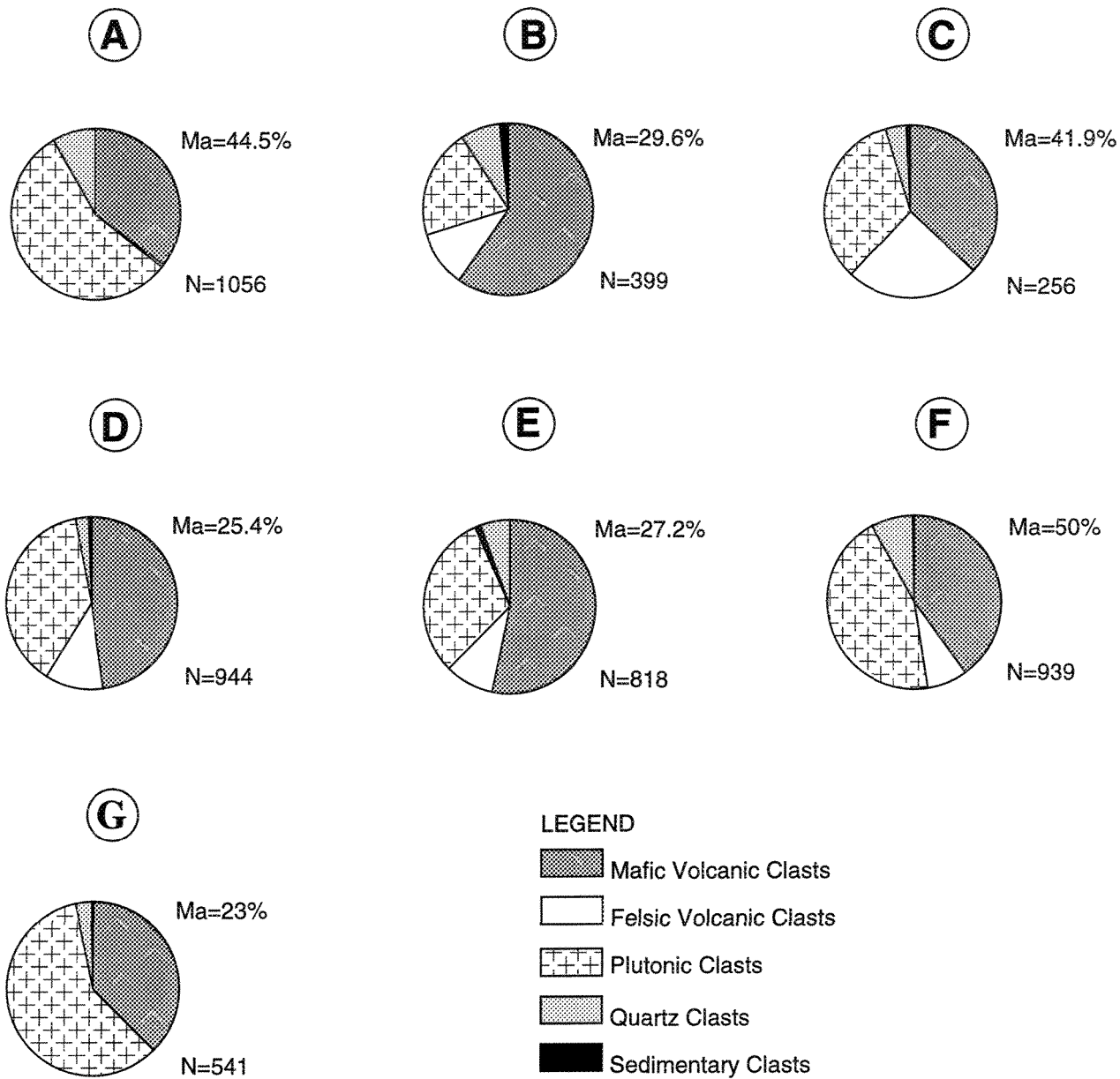


Figure 14

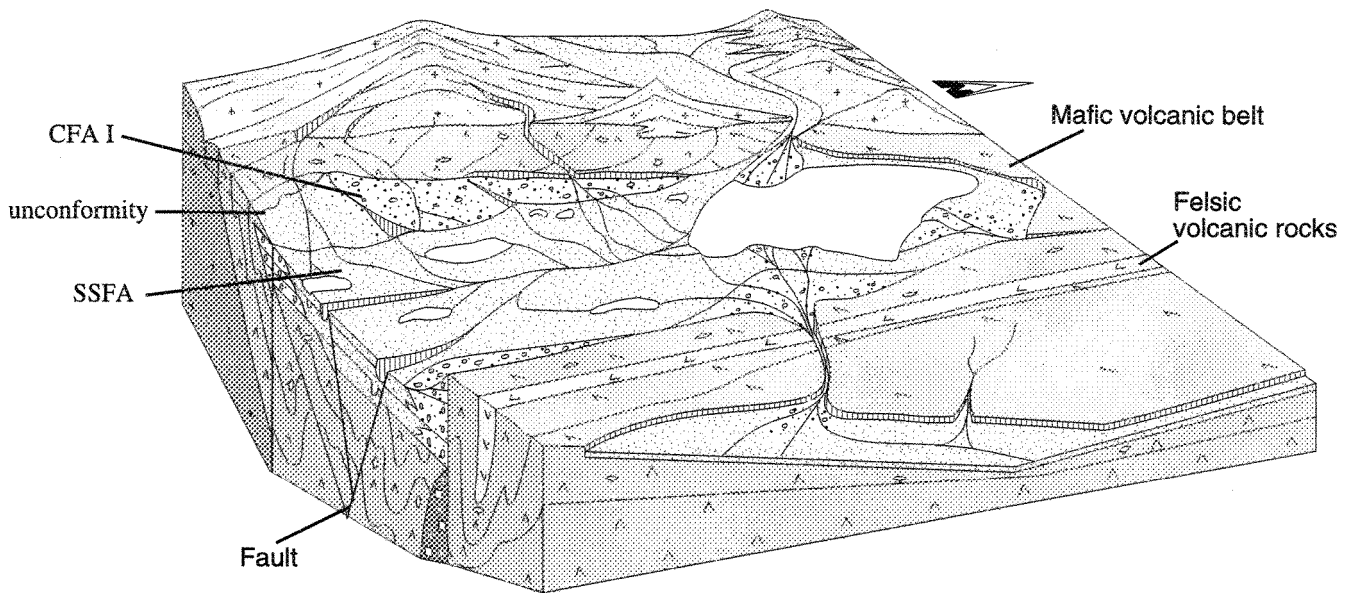
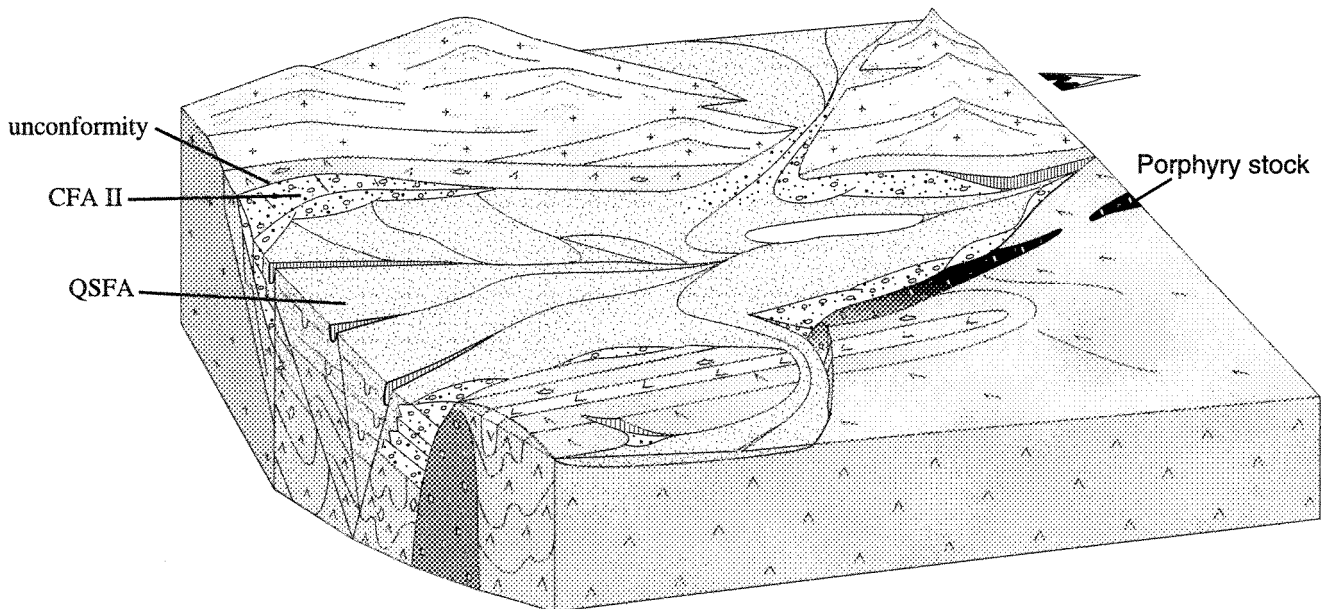
**A) First depositional phase****B) Second depositional phase**

Figure 15

<b>Facies Association</b>	<b>Facies</b>	<b>Process</b>	<b>Setting</b>
<b>Conglomerate Facies Association I (CFA-I)</b> Gm±Gms±Gt±Sm <sub>a</sub> -St-Sh±Sp±Sl±Fl			
(1) Matrix-clast-supported conglomerate Gm±Gms±Gt±Sm <sub>a</sub> -St-Sh±Sl±Fl	(1) Massive-crudely bedded conglomerate (Gm); massive, matrix-supported conglomerate (Gms); trough crossbedded clast-supported conglomerate (Gt); massive pebbly sandstone (Sm <sub>a</sub> ); trough crossbedded sandstone (St); horizontally stratified sandstone (Sh); low-angle planar beds(Sl); mudstone, massive and/or laminated (Fl)	(1) Gm, longitudinal bars; Gms, debris flow; Gt, channel fills; Sm <sub>a</sub> , hyperconcentrated flow or sheetflow; St, megaripple migration; Sh, planar bed flow (upper flow regime); Sl, upper flow regime bar top sands; Fl, overbank or drape deposition	(1) Proximal to medial reaches of alluvial fans adjacent to uplifted volcanics and porphyry stocks, streamflow-dominated alluvial fans with suspended fines
(2) Massive-stratified pebble-cobble conglomerate Gm±Gp±Gt-St-Sh-Sp	(2) St, Sh, Sp; Fl; Gm; Gt; planar crossbedded conglomerate (Gp)	(2) St, megaripple migration; Sh, planar bed flow (upper flow regime); Sp, transverse or linguoid bars; Fl, overbank or drape deposition; Gm, longitudinal bars; Gt, channel fills; Gp, longitudinal bars	(2) Lower reaches of streamflow-dominated alluvial fans
<b>Siltstone-Sandstone Facies Association (SSFA)</b> Ss-St-Sp-Sh-Fl			
(1) Sandstone-dominated subunit Ss±Gm-St-Sp-Sh-Fl	(1) Scour surfaces (Ss); pebble trains (Gm); trough crossbeds (St); planar crossbeds (Sp); horizontal bedding (Sh); mudstone (Fl)	(1) Ss, Gm, flash flooding; St, migration of sinuous-crested megaripples; Sp, migration of straight-crested megaripples; Sh, rare periods of wave activity; Fl, overbank or waning flood deposition	(1) Subaerial to subaqueous, wave- to fluvial-influenced fan-or braid-delta, or sandy braidplain with variable flow directions
(2) Siltstone-dominated subunit Fl	(2) Asymmetrical wave ripples (Fl); graded beds, dish and pillar structures; clastic dykes	(2) Graded beds due to rapid suspension sedimentation; Fl, wave ripples; dish and pillars, clastic dykes during rapid deposition of mud and sand	(2) Shallow ephemeral lakes or ponds, with flash flooding
<b>Conglomerate Facies Association II (CFA-II)</b> Gm±Gt-St±Sh			
	Massive to crudely bedded conglomerate (Gm); trough crossbedded conglomerate (Gt); horizontally-stratified sandstone (Sh); trough crossbedded sandstone (St)	Gm, longitudinal bars; Gt, channel fills; Sh, planar bed flow (upper flow regime); St, megaripple migration	Distal streamflow-dominated regions of alluvial fans or proximal braided stream
<b>Quartz-Rich Sandstone Facies Association (QSFA)</b> St±Sh±Sp±Sl±Fl			
	High-angle trough crossbedding (St); planar beds (Sh); low-angle planar crossbeds (Sp); low-angle planar beds (Sl); mudstone (Fl)	St, migration of sinuous-crested megaripples; Sh, planar bed flow (upper flow regime); Sp, migration of straight-crested megaripples; Sl, upper flow regime bar top sands; Fl, overbank or drape deposits	Braided stream

Table 1

Sample number	Q%	K%	P%
PLC-95-22 (SDC)	82	2	16
PLC-95-24 (SDC)	77	3	20
PLC-95-000 (QFP)	71	8	20
PLC-95-37 (QFP)	72	7	21
PLC-95-45 (HP)	35	11	54

Table 2

Sample number	Q	F	L	Qm	F	Lt	Lp	Lv	Is	P/F
94-03	69	4	27	11	3	86	57	2	41	0.63
94-05	73	12	15	15	12	73	71	5	24	0.67
94-08	75	9	16	5	9	86	43	26	31	0.93
94-09	76	12	12	9	12	79	65	15	20	0.89
94-10	80	13	7	17	13	70	48	19	33	0.77
94-11	71	17	12	13	17	70	62	8	30	0.67
94-13	65	19	16	13	19	68	71	6	23	0.76
94-15	80	7	13	19	7	74	77	23	0	1.0
94-16	75	19	6	14	19	67	53	40	7	0.80
94-17	73	12	15	10	12	78	64	14	22	0.74
94-18	62	26	12	4	28	68	72	0	28	1.0
94-22	63	21	16	12	20	68	100	0	0	0.86
94-23	74	8	18	23	8	69	91	7	2	1.0
94-24	72	12	16	12	12	76	59	22	19	0.65
94-25	81	5	14	14	5	81	36	36	28	0.46
94-26	80	11	9	8	11	81	42	29	29	0.71
94-27	72	14	14	11	13	76	76	21	3	0.82
94-30	69	24	7	15	24	61	81	19	0	0.75
94-31	86	9	5	23	8	69	93	7	0	1.0
94-32	83	13	4	18	13	69	100	0	0	0.97
94-33	83	11	6	18	11	71	92	8	0	0.96
94-38	78	13	9	7	14	79	88	8	4	0.77
94-40	73	23	4	14	23	63	63	25	12	0.87
94-42	64	28	8	15	28	67	100	0	0	0.71
94-43	81	6	13	8	6	86	66	31	3	0.93
94-44	80	18	2	9	18	73	60	20	20	0.76
94-48	77	14	9	7	14	79	46	25	29	0.65
94-49	73	18	9	12	18	70	56	22	22	0.69
95-04	90	5	5	16	4	80	48	19	33	0.75
95-19	86	2	12	8	1	91	45	9	46	0.75
95-34	66	27	7	9	27	64	36	32	32	0.50
Mean	73	14	13	12	14	74	67	16	17	0.78
SD	7	7	5	5	7	7	20	11	14	14

Table 3

## CHAPITRE III

### CONCLUSION

Les éléments structuraux, la géométrie du bassin, l'organisation des faciès sédimentaires, et l'environnement de dépôt de la Formation de Beaulieu Rapids s'accordent favorablement avec les caractéristiques des bassins de décrochement modernes. Ces bassins sont principalement gouvernés par les mouvements horizontaux reliés à la tectonique des plaques. La faille majeure de direction nord de Beniah Lake est une structure à grande échelle qui divise la Province de l'Esclave en deux parties. La partie la plus vieille ( $> 2.8$  Ga) à l'ouest est de type continental et contient des séquences d'arenite quartzique. À l'est, les séquences de type arc sont plus jeunes ( $< 2.8$  Ga). La présence de cette faille associée avec le petit bassin de décrochement de Beaulieu Rapids est importante pour comprendre l'évolution de la Province de l'Esclave.

Les quatre associations de faciès avec leur empilement et organisation suggèrent un contrôle tectonique pendant la sédimentation. Ces associations démontrent deux cycles de dépôt. Une érosion importante des hautes-terres a été suivie par le remplissage rapide du bassin pendant le cycle de dépôt I. Ce premier cycle de dépôt est représenté par l'association de faciès du conglomérat I et par l'association de faciès de siltstone-grès. Les débris grossiers concentrés le long des marges du bassin représentent des cônes alluvionnaires de premier cycle, des rivières tressées proximales, et des deltas tressés. Ces formes de terrain ont progradé vers une plaine tressée caractérisée par des étangs locaux et des petits lacs. La deuxième phase d'activité tectonique a contribué à l'apport des matériaux représentés par



l'association de faciès du conglomérat II et par l'association de faciès du grès riche en quartz. L'apport important de débris pendant le cycle de dépôt I a rempli la majeure partie du bassin, ce qui est souligné par l'absence de dépôts lacustres et l'omniprésence de dépôts fluviatiles. Tous les dépôts de cycle II se sont accumulés dans une grande plaine tressée à faible pente. La direction d'écoulement dans les grès est parallèle au bassin, en accord avec l'imbrication des fragments dans le conglomérat II. L'extension locale du bassin est caractérisée par l'emplacement et l'exhumation des porphyres d'âge <2.6Ga.

L'abondance de quartz polycristallin et de fragments de roches plutoniques dans les grès indique que la majorité des débris sont dérivés d'une source plutonique. Cette hypothèse est soutenue par la présence de nombreux fragments plutoniques dans les conglomérats et de fragments de quartz dérivés des veines de quartz du Complexe de Sleepy Dragon situé à l'ouest du bassin. Des sources secondaires de sédiments proviennent des roches volcaniques qui entourent le bassin et des porphyres situés à la marge est. La nature polycristalline du quartz et la prédominance des dépôts d'écoulement confinés suggèrent un climat humide pendant le dépôt des sédiments. Les diagrammes de provenance tectonique indiquent que le Bassin de Beaulieu Rapids se situe dans le champ d'orogénèse recyclée. Ce résultat n'est pas surprenant vu la nature de type molasse ou "successor" du bassin. Les sédiments se sont déposés rapidement sur une courte distance en raison de l'influence tectonique. La Formation de Beaulieu Rapids, rare exemple d'un bassin de décrochement Archéen, est d'importance fondamentale à cause de son association avec les processus de tectonique des plaques d'âge >2.5 Ma .